

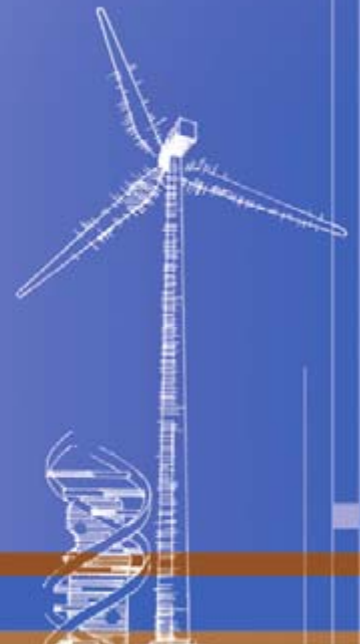
WindPACT Turbine Rotor Design Study

June 2000 — June 2002

D.J. Malcolm
Global Energy Concepts, LLC
Kirkland, Washington

A.C. Hansen
Windward Engineering
Salt Lake City, Utah

Subcontract Report
NREL/SR-500-32495
Revised April 2006



NREL is operated by Midwest Research Institute • Battelle Contract No. DE-AC36-99-GO10337



WindPACT Turbine Rotor Design Study

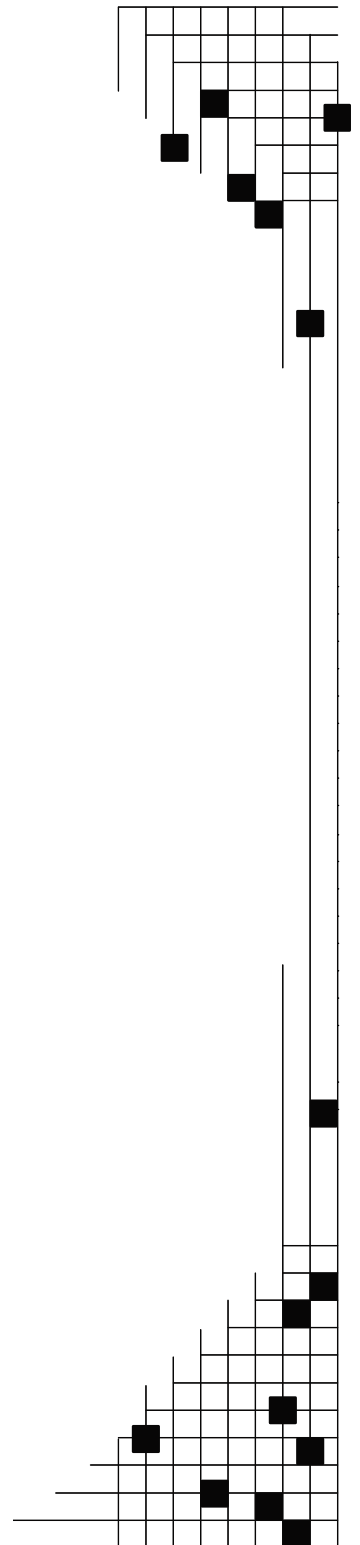
June 2000 — June 2002

D.J. Malcolm
Global Energy Concepts, LLC
Kirkland, Washington

A.C. Hansen
Windward Engineering
Salt Lake City, Utah

NREL Technical Monitor: A. Laxson
Prepared under Subcontract No. YAT-0-30213-01

Subcontract Report
NREL/SR-500-32495
Revised April 2006



National Renewable Energy Laboratory
1617 Cole Boulevard, Golden, Colorado 80401-3393
303-275-3000 • www.nrel.gov

Operated for the U.S. Department of Energy
Office of Energy Efficiency and Renewable Energy
by Midwest Research Institute • Battelle

Contract No. DE-AC36-99-GO10337

NOTICE

This report was prepared as an account of work sponsored by an agency of the United States government. Neither the United States government nor any agency thereof, nor any of their employees, makes any warranty, express or implied, or assumes any legal liability or responsibility for the accuracy, completeness, or usefulness of any information, apparatus, product, or process disclosed, or represents that its use would not infringe privately owned rights. Reference herein to any specific commercial product, process, or service by trade name, trademark, manufacturer, or otherwise does not necessarily constitute or imply its endorsement, recommendation, or favoring by the United States government or any agency thereof. The views and opinions of authors expressed herein do not necessarily state or reflect those of the United States government or any agency thereof.

Available electronically at <http://www.osti.gov/bridge>

Available for a processing fee to U.S. Department of Energy and its contractors, in paper, from:

U.S. Department of Energy
Office of Scientific and Technical Information
P.O. Box 62
Oak Ridge, TN 37831-0062
phone: 865.576.8401
fax: 865.576.5728
email: <mailto:reports@adonis.osti.gov>

Available for sale to the public, in paper, from:

U.S. Department of Commerce
National Technical Information Service
5285 Port Royal Road
Springfield, VA 22161
phone: 800.553.6847
fax: 703.605.6900
email: orders@ntis.fedworld.gov
online ordering: <http://www.ntis.gov/ordering.htm>



**Errata Sheet for
WindPACT Turbine Rotor Design Study
NREL/SR-500-32495**

CORRECTIONS

Page 13

Table 3-1. Summary of Cost Models Used for Major Components in Baseline Designs

6th row, first column should read –
Pitch bearings
Not used for final costing

7th row, first column should read –
Pitch bearings
(Tasks #2, #3, #5)

7th row, fourth column should read –
See text

12th row, second column should read –
Bearing mass = $(D \times 8/600 - 0.033) \times 0.00920 \times D^{2.5}$
Where D = rotor diam (m)

12th row, third column, delete “U of Sunderland [6] and”

Page 14

Table 3-1 Continued

13th row, second column should read
 $\$/kW = 3.38E-7 * Rating^2 + 9.84E-4 * Rating + 31.57$

Page 18

Section 3.2.2.1 Pitch Bearings

Starting with the second paragraph, the text in the section should be replaced with the following with the exception of the formula. The formula remains unchanged.

An initial model for the total cost was: $\$/bearing = 0.0454 * D^{2.98}$. This was found to correspond well with data obtained later from Avon Bearings (see Appendix C). These data included cost estimates for the range of ratings of interest and were based on initial estimates of peak moments. The mass and cost of the auxiliary pitch drive components were estimated to be equal to that of the pitch bearing itself and a factor of 2.0 was,

therefore, added to the cost. However, as noted below, this model was not used for the final estimates in the costing and scaling efforts.

Different bearing types were recommended by Avon at the different sizes because of the relatively small diameter of these bearings compared to the high loads they must carry. At 750 kW, a single-row ball bearing was selected, whereas at the 1.5 MW and higher ratings, triple-row bearings were recommended and quoted. The cost quoted for bearings for the 5-MW size did not fall on the same curve as for the others and it was therefore neglected in defining the cost model.

A new cost model was defined for Tasks #2, #3, and #5 that reflected cost changes due to changes in the peak loads applied. Therefore, the Avon cost data was reformatted into the following form:

NOTE – FORMULAS AS WRITTEN IN ORIGINAL SHOULD REMAIN UNCHANGED

For Tasks #2, #3, and #5, it was again assumed that the cost of the remainder of the pitch system (motor, speed reducer, controller, etc.) is equal to the cost of the bearing.

Page 19

Section 3.2.3.2 Main Bearings – the text should be replaced with the following:

The main bearing was assumed to be of a standard type and a formula for the mass was developed based on data, collected by Powertrain Engineers Inc., from wind turbines between 750 kW and 2000 kW. The second bearing was included in the gearbox assembly. The resulting expression for the bearing mass, in terms of the rotor diameter, D, was:

$$\text{Mass (kg)} = (D \times 8/600 - 0.033) \times 0.00920 \times D^{2.5}$$

The mass of the bearing housing was assumed to be the same as that of the bearing itself and a rate of \$17.60 per kg was used for both components.

To download a corrected version of this report go to:

<http://www.nrel.gov/docs/fy06osti/32495.pdf>

TABLE OF CONTENTS

EXECUTIVE SUMMARY	v
Introduction.....	v
Approach.....	v
Results.....	vi
Conclusions.....	vii
Recommendations.....	viii
1. INTRODUCTION	1
1.1 Background.....	1
1.2 Objectives	1
1.3 Scope.....	1
1.4 Results on Web Site.....	2
2. METHODOLOGY	3
2.1 Organization.....	3
2.1.1 Work Plan	3
2.1.2 Procedure	4
2.1.2.1 Blade Design File.....	6
2.1.2.2 Input Data File	6
2.1.2.3 Output Data File.....	7
2.1.2.4 Design and Cost Evaluation Process.....	7
2.1.3 Load Cases	8
2.1.4 Design Methodology.....	9
2.2 Specifications for Baseline Configurations.....	9
2.3 Simulation Software.....	9
2.4 Signals Recorded	10
3. TASK #1. DESIGN AND COST MODELS	12
3.1 General Approach	12
3.2 Rotor Components	15
3.2.1 Blade Design.....	15
3.2.1.1 Aerodynamic Specifications	15
3.2.1.2 Baseline Blade Design	15
3.2.1.3 Airfoil Schedule	16
3.2.2 Hub.....	17
3.2.2.1 Pitch Bearings	18
3.2.2.2 Teetered Hub.....	18
3.2.3 Drive Train Components.....	19
3.2.3.1 Main Shaft.....	19
3.2.3.2 Main Bearings.....	19
3.2.3.3 Gearbox.....	19
3.2.3.4 Generator.....	20
3.2.3.5 Power Electronics	20
3.2.3.6 Bedplate	20
3.2.3.7 Nacelle Cover.....	20
3.2.3.8 Yaw System	21
3.2.3.9 High-Speed Shaft, Coupler, Brakes	21
3.2.3.10 Hydraulics and Lubrication.....	21
3.2.3.11 Switchgear and Other Electrical.....	21

3.2.4	Tower	21
3.2.5	Balance of Station	22
3.2.5.1	Foundations	22
3.2.5.2	Operating Costs	22
3.3	Control Systems	23
3.4	Cost of Energy Model	23
4.	TASK #2. BASELINE DESIGNS	24
4.1	Basic Specifications	24
4.2	FAST_AD vs. ADAMS Results	24
4.3	Annual Energy Production	24
4.4	Material Properties	25
4.5	Pitch Control System	25
4.6	Results from Design Process	25
4.7	Campbell Diagram	29
4.8	Conclusions from Baseline Study	29
5.	TASK #3. CONFIGURATION VARIATIONS	30
5.1	Initial Matrix	30
5.2	Selection Approach	30
5.3	FAST_AD vs. ADAMS	33
5.4	Results from Task #3	33
5.5	Observations from Task #3 results	36
6.	TASK #5. DETAILED MODELING	37
6.1	Approach	37
6.2	Cost Models	37
6.3	Preliminary Results	37
6.4	Results from 3-Bladed Upwind Rotors	38
6.4.1	Campbell Diagram	39
6.4.2	Loads	40
6.4.3	Costs	40
6.5	Results for 2-Bladed Rotors	42
6.5.1	Loads	42
6.5.2	Costs	43
6.6	Lessons from Task #5	44
7.	TASK #6. DESIGN BARRIERS	45
7.1	Transportation	45
7.2	Installation	45
7.3	Blade Manufacturing	46
7.4	Acoustics	46
7.5	Design Load Cases	46
7.6	Non-Turbine Costs	47
8.	CONCLUSIONS	48
8.1	Assumptions within the Study	48
8.2	Summary	48
8.3	Recommendations	49
9.	REFERENCES	50
10.	BIBLIOGRAPHY	52

APPENDICES

- A Details from Task #3 Configuration Variations
- B Details from Task #5 Final Designs
- C Avon Bearing Costs
- D Calculation of Fatigue Damage Equivalent Loads
- E Description of the Blade Pitch Control System

LIST OF FIGURES

Figure S-1. Cost of energy of baseline and final 3-bladed upwind designs.....	vii
Figure S-2. Cost of energy for baseline and final 3- and 2-bladed designs at 1.5MW	vii
Figure 2-1. Organization of project personnel	3
Figure 2-2. Tasks and approximate schedule.....	4
Figure 2-3. Flow of work between GEC and Windward Engineering.....	5
Figure 2-4. Configuration control scheme for models	5
Figure 2-5. Flow of information in the design process	7
Figure 2-6. Coordinates systems used and corresponding rotations	11
Figure 3-1. Specific rating vs. rotor diameter for current commercial wind turbines.....	15
Figure 3-2. Airfoils used for baseline 1.5-MW blade model	17
Figure 4-1. Summary of cost-of-energy breakdown for baseline configurations	26
Figure 4-2. Variation of root flapwise and edgewise moments with diameter	28
Figure 4-3. Natural frequencies vs. rotor speed (Campbell diagram) of baseline 1.5-MW model	29
Figure 5-1. Rotor configurations selected.....	30
Figure 5-2. Summary of cost of energy from all Task #3 configurations	33
Figure 5-3. Cost-of-energy changes for 3-bladed configurations	34
Figure 5-4. Cost-of-energy changes for 2-bladed configurations	34
Figure 5-5. Summary of component costs for 3-bladed configurations.....	35
Figure 5-6. Summary of component costs for 2-bladed configurations.....	35
Figure 6-1. Natural frequencies vs. rpm (Campbell diagram) for Task #5 1.5-MW 3-bladed upwind turbine.....	39
Figure 6-2. Comparison of baseline loads with final Task #5 loads for 1.5-MW 3-bladed upwind turbine.....	40
Figure 6-3. Cost of energy of baseline and final 3-bladed 750-kW, 1.5-MW, and 3-MW configurations	41
Figure 6-4. Comparison of baseline and final costs of 3-bladed configurations by sub-assembly	41
Figure 6-5. Comparison of baseline and final Task #5 loads for 1.5-MW 2-bladed upwind turbine	42
Figure 6-6. Comparison of baseline and final Task #5 loads for 1.5-MW 2-bladed downwind turbine ...	43
Figure 6-7. Cost of energy for 2- and 3-bladed 1.5-MW configurations	43
Figure 6-8. Comparison of baseline and final costs of 3- and 2-bladed 1.5-MW configurations by sub-assembly	44
Figure E-1. Basic WindPACT rotor speed control system	E-4
Figure E-2. WindPACT speed control with tower acceleration feedback	E-5

LIST OF TABLES

Table S-1. Summary of Baseline Design Properties and Cost of Energy	vi
Table 2-1. Types of Files Used in Design Process.....	6
Table 2-2. Load Case Analyses Carried Out.....	8
Table 2-3. Loads and Variables Recorded During Simulations.....	10
Table 3-1. Summary of Cost Models Used for Major Components in Baseline Designs.....	13
Table 3-2. Summary of Aerodynamic and Geometrical Design of Blades.....	17
Table 3-3. Items Included in Operations & Maintenance	22
Table 4-1. Initial and Final Overall Specifications	24
Table 4-2. Material Properties Used in Design of Major Components (Task #2)	25
Table 4-3. Characteristics of Final Baseline Configurations	26
Table 4-4. Costs of All Wind Farm Items for Baseline Designs	27
Table 4-5. Trends from Baseline Designs: Dependence on Diameter	28
Table 4-6. Critical Load Cases for Baseline Turbines	28
Table 5-1. Initial Table of Configurations for Examination in Task #3	31
Table 5-2. Configuration Modifications Chosen for Study in Task #3.....	32
Table 6-1. Changes Made to Cost Models for Task #5.....	37
Table 6-2. Summary of Properties of the Baseline and Task #5 Final Configurations.....	39
Table 7-1. Transportation Costs vs. Rating.....	45
Table 7-2. Installation Costs vs. Rating	45
Table A-1. Relative Load Results from Task #3 Configurations.....	A-1
Table A-2. Governing Load Cases and Margins for Task #3 Configurations	A-2
Table A-3. Costs and Cost of Energy Summary for All Task #3 Configurations.....	A-3
Table B-1. Comparison of Baseline and Final Loads for 3-Bladed Upwind Machines.....	B-1
Table B-2. Summary of Costs of Baseline and Final 3-Bladed Machines at 750 kW, 1.5 MW, and 3.0 MW	B-2
Table B-3. Comparison of 1.5-MW Final Loads with Baseline Configurations	B-3
Table B-4. Comparison of Final Costs with 1.5-MW Baseline Configurations	B-4
Table B-5. Governing Load Cases and Margins for Baseline and Task #5 Final Configurations.....	B-5

EXECUTIVE SUMMARY

Introduction

This report presents the results of a study completed by Global Energy Concepts (GEC) as part of the U.S. Department of Energy's (DOE's) WindPACT (Wind Partnership for Advanced Component Technologies) project. The purpose of the WindPACT project is to identify technology improvements that will enable the cost of energy (COE) from wind turbines to fall to a target of 3.0¢/kWh in low-wind-speed sites. Other parts of the project have examined blade scaling, logistics, balance-of-station costs, and drivetrain design, while this project was concerned with the effect of different rotor configurations and the effect of scale on those rotors.

Approach

The original project statement of work discussed a very broad set of rotor systems to be examined. To focus the research on those areas most useful to the industry, a survey of industry participants was used to narrow the number of rotor systems evaluated. The rotor systems were grouped into four basic configurations (upwind 3-bladed, upwind 2-bladed, downwind 2-bladed, downwind 3-bladed). The rotor systems were defined by making modifications to parameters such as the root-hub attachment, the tip speed, the control system, the blade stiffness, etc. For each rotor system an aeroelastic model of the wind turbine with the appropriate properties was developed, and a series of simulations corresponding to the IEC 61400-1 design conditions were carried out. From these results, key loads were used to design all the major components using previously developed design methods in combination with cost models that were checked against current commercial data. The results of the analysis for each concept were compared to a baseline representative of current industry practice.

This work was shared between Windward Engineering, LLC, who carried out most of the aeroelastic simulations, and GEC, who were the prime subcontractors and responsible for all design and costing work. In addition, consultants were used for aspects of blade design, controls, and gearbox and bearing design. The project was divided into four major tasks:

1. Development of cost models (Task #1).
2. Establishment of 3-bladed upwind, full-span pitch-to-feather, variable-speed baseline designs of 750-kW, 1.5-MW, 3-MW, and 5-MW ratings (Task #2).
3. Examination of a series of rotor configurations and modifications and their effects on the cost of energy (Task #3).
4. Combination of the most promising features from Task #3 into final designs of 3-bladed and 2-bladed upwind and 2-bladed downwind configurations (Task #5).

Results

The Task #2 work resulted in the cost of energy for the four baseline designs shown in Table S-1. These results illustrate the increase in COE to be expected beyond 1.5 MW.

Table S-1. Summary of Baseline Design Properties and Cost of Energy

		750 kW	1.5 MW	3.0 MW	5.0 MW
Rotor Diameter	m	50	70	99	128
Hub Height	m	60	84	119	154
Max Rotor Speed	rpm	28.6	20.5	14.5	11.2
Hub Overhang	m	2.330	3.300	4.650	6.000
Tower Base Diameter	m	4.013	5.663	8.081	10.373
Cost of Energy Contributions					
Rotor	¢/kWh	0.477	0.543	0.741	0.864
Drive Train	¢/kWh	1.197	1.234	1.305	1.441
Controls	¢/kWh	0.047	0.022	0.011	0.006
Tower	¢/kWh	0.326	0.403	0.561	0.685
Balance of Station	¢/kWh	1.021	0.852	0.889	1.432
Replacement Costs	¢/kWh	0.499	0.467	0.434	0.414
O&M	¢/kWh	0.800	0.800	0.800	0.800
Total COE	¢/kWh	4.367	4.321	4.741	5.642

The modifications of Task #3 were all applied to a 1.5-MW rating while maintaining the baseline's variable speed with full-span pitch control features. A total of 23 rotor systems were examined. The following three modifications that reduced loads throughout the system and offered widespread benefits were identified:

- Tower feedback in the control system
- Passive flap-twist-to-feather coupling in the blades
- Reduced blade chord in combination with increased tip speed.

These features appeared to benefit each of the four basic rotor configurations.

In Task #5, these three features were combined in an effort to arrive at the lowest COE. This was done to the 3-bladed and 2-bladed upwind and the 2-bladed downwind 1.5-MW configurations. It was also applied to the 750-kW and the 3-MW 3-bladed upwind configurations. The results of these analyses showed that substantial load reductions were obtained. Cost of energy estimates were made for each of these configurations and compared with their corresponding baseline versions (from Tasks #2 or #3), which are illustrated in Figures S-1 and S-2.

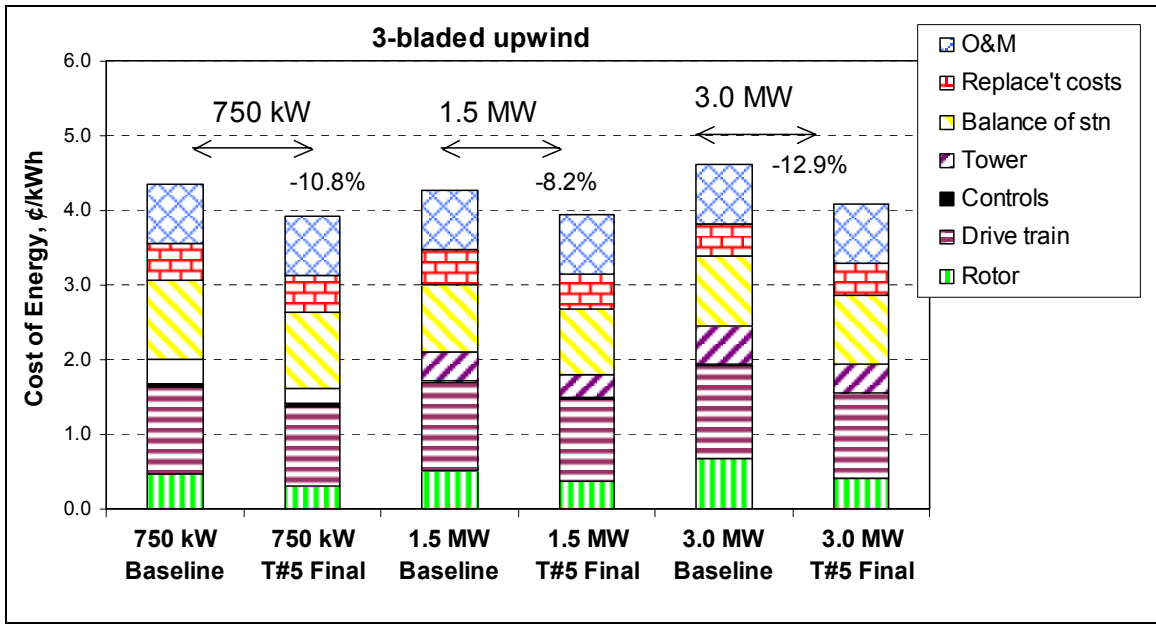


Figure S-1. Cost of energy of baseline and final 3-bladed upwind designs.

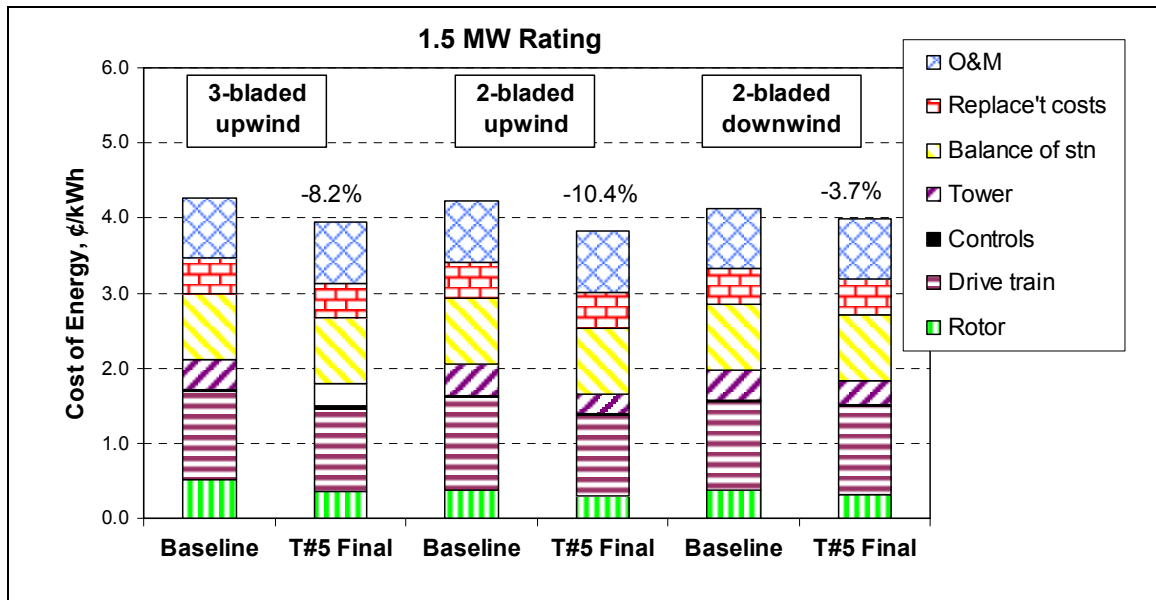


Figure S-2. Cost of energy for baseline and final 3- and 2-bladed designs at 1.5 MW.

Conclusions

- The cost of energy of the baseline designs has been reduced by up to 13%.
- The cost of energy reduction is small relative to the magnitude of the loads reductions that occurred throughout the system.
- More than 50% of the cost of energy is unaffected by rotor design and system loads. Further COE reductions may be achieved by addressing the balance-of-station costs.

- Combinations of rotor improvements with parallel improvements in the drive train design and in the tower design must be pursued. Such combinations will bring the total COE reductions closer to the 30% target.
- The cost of the rotor as a fraction of the total capital cost rises with increasing rotor size. Therefore, larger machines can benefit more from rotor improvements.
- The cost of a 3-bladed rotor is greater than the equivalent 2-bladed rotor and, for the same reason, benefits more from rotor improvements.
- No single rotor modification offered a solution to reduced rotor costs and lower system loads. Instead, there were a number of modifications that offered some general benefits, especially:
 - Inclusion of tower feedback to the blade pitch control system.
 - Incorporation of flap-twist coupling in the blade design.
 - Reduction of the blade chord combined with an increase in the tip speed.
- The Task #5 improvements were of most benefit to the 3-MW, 3-bladed upwind machine. This narrowed the difference in COE within the 750-kW to 3-MW range.
- The extensive use of carbon fibers was essential to the final blade design. Their greater stiffness (compared to glass fiber) was needed to achieve the required flap-twist coupling and to avoid contact with the tower.
- Added costs of transportation and assembly adversely affect the COE for machines rated above 1.5 MW. Alternatives to the use of conventional cranes and alternative tower designs will potentially benefit larger machines.
- The inclusion of feedback from tower motion into the control system has reduced tower loads considerably. This feature has not been optimized, and further improvements may be possible. Other control system enhancements may also have beneficial effects.

Recommendations

- Combine the findings of this study with those of the parallel WindPACT drive train configuration study and the continuing study of the effect of specific rating. This combination may offer COE improvements that approach the target COE reduction identified by the WindPACT project.
- Conduct more testing of material coupons and blade assemblies to support the use of bias-ply carbon fibers required for flap-twist coupling.
- Study the acoustic penalties associated with higher tip speeds and ways of ameliorating them.
- Develop further refinements of turbine control systems to reduce loads.
- Study various approaches for reducing COE by changes in the balance-of-station costs and in the fixed charge rate.

1. INTRODUCTION

1.1 Background

Over the past 20 years, the cost of wind energy has decreased significantly and is now close to being competitive with conventional forms of energy. To achieve the further decrease in cost of energy (COE) necessary to make wind energy truly competitive with electricity generated from fossil fuels such as coal and natural gas, further reductions in COE of up to 30% are required. To achieve this reduction, a greater level of innovation will be required in the design of wind turbines.

Over the past decades, many concepts have been proposed to reduce loads and to lower COE. However, most current commercial machines have converged toward a design consisting of an upwind 3-bladed rotor with full-span pitch control. It is difficult for a manufacturer to develop radically new designs in an aggressive market-driven environment in which availability of a product is more important than long-term innovation. In addition, there is doubt about how far the current trend toward large machines should go and where barriers to this trend will be encountered.

To deal with these issues, the U.S. Department of Energy, through the National Renewable Energy Laboratory (NREL), has implemented the Wind Partnership for Advanced Component Technologies (WindPACT) project. The purpose of this project is to provide a vehicle for exploring advanced technologies for improving machine reliability and decreasing the overall cost of energy. One element of the WindPACT project has been a series of design studies aimed at each of the major subsystems of the wind turbine to study the effect of scale and of alternative design approaches.

In June of 2000, Global Energy Concepts, LLC (GEC), was awarded contract number YAT-0-30213-01 under the WindPACT project to examine the role of the rotor design on the overall cost of energy.

1.2 Objectives

There are three principal objectives of this study.

1. Determine the impact on COE of changes to the rotor size and rating in the 750-kW to 5-MW range.
2. Determine the effect of different rotor configurations and modifications on system loads and COE.
3. Identify rotor design issues that may be barriers to the development of larger machines.

1.3 Scope

This report describes the approach and rationale used to reach the objectives of the study and the organization of the work between GEC and its subcontractors. It presents the work plan that was followed and describes the results of each task.

Detailed results of all aspects of the calculations of the cost of energy are presented together with explanations of the appraisal system used to select the most promising configurations. A set of optimized configurations is identified and compared with the initial baseline designs.

1.4 Results on Web Site

NREL plans to establish a Web site that will allow access to some of the detailed data related to this study. In addition to copies of this report, a number of input data files, ADAMS and FAST input files, and design evaluation files will be available. The Web site address is: www.nrel.gov/wind/windpact.

2. METHODOLOGY

2.1 Organization

The organization of the project and of the personnel is shown in Figure 2-1.

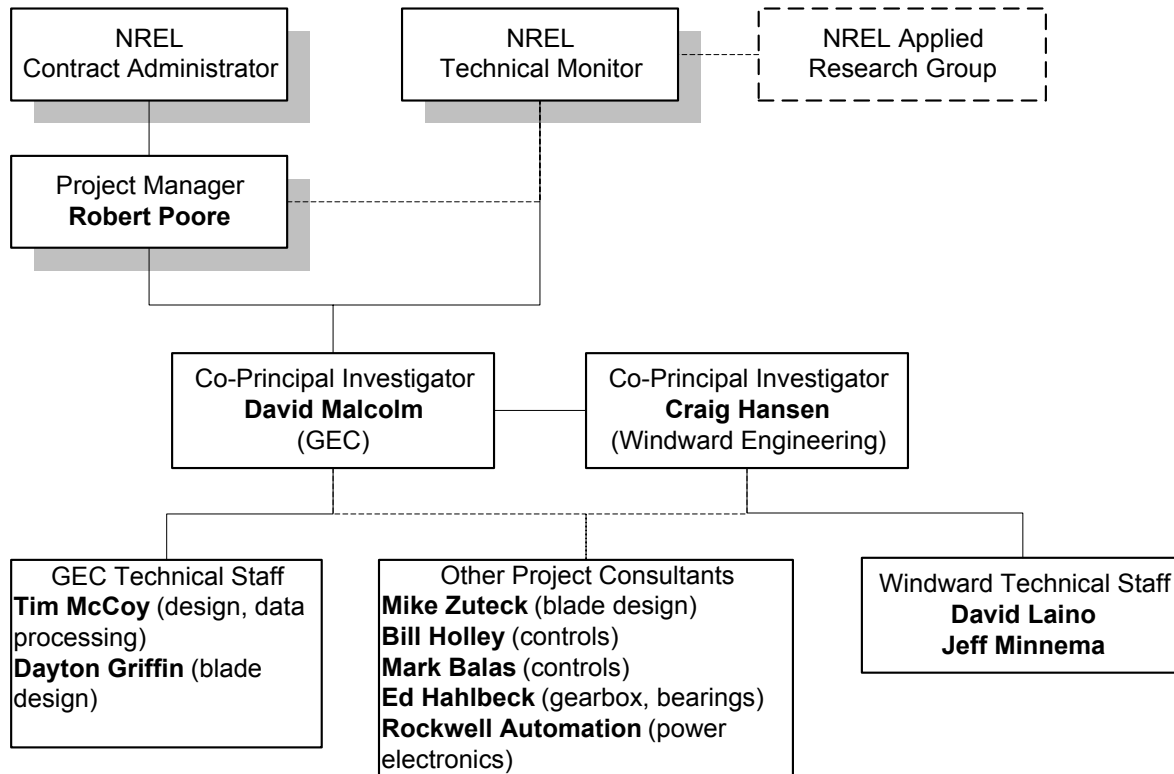


Figure 2-1. Organization of project personnel.

2.1.1 Work Plan

The project was divided into nine tasks that reflect the objectives and the organization. Figure 2-2 shows these tasks and their scheduling and gives a brief description of each.

Task #1 was a review of existing cost and optimization studies and the selection of cost models suitable for this project. The task led to a kick-off meeting at which GEC and Windward Engineering presented their intended approach to NREL.

In Task #2, a number of baseline configurations were developed in the range between 750 kW and 5.0 MW. Aeroelastic models were built and analyzed under a number of load conditions, and the major components were designed and their costs estimated.

In Task #3, a number of modifications to the rotor were selected and applied to 3-bladed upwind, 3-bladed downwind, 2-bladed upwind, and 2-bladed downwind configurations. The COE associated with each was calculated, and the most promising modifications were identified.

Task #5 examined combinations of the results of Task #3 to arrive at optimized 3-bladed designs for 750-kW, 1.5-MW, and 3-MW ratings. The 2-bladed configurations at 1.5 MW were also optimized.

The remaining tasks identified particular barriers to development and to size and presented the results of the study.

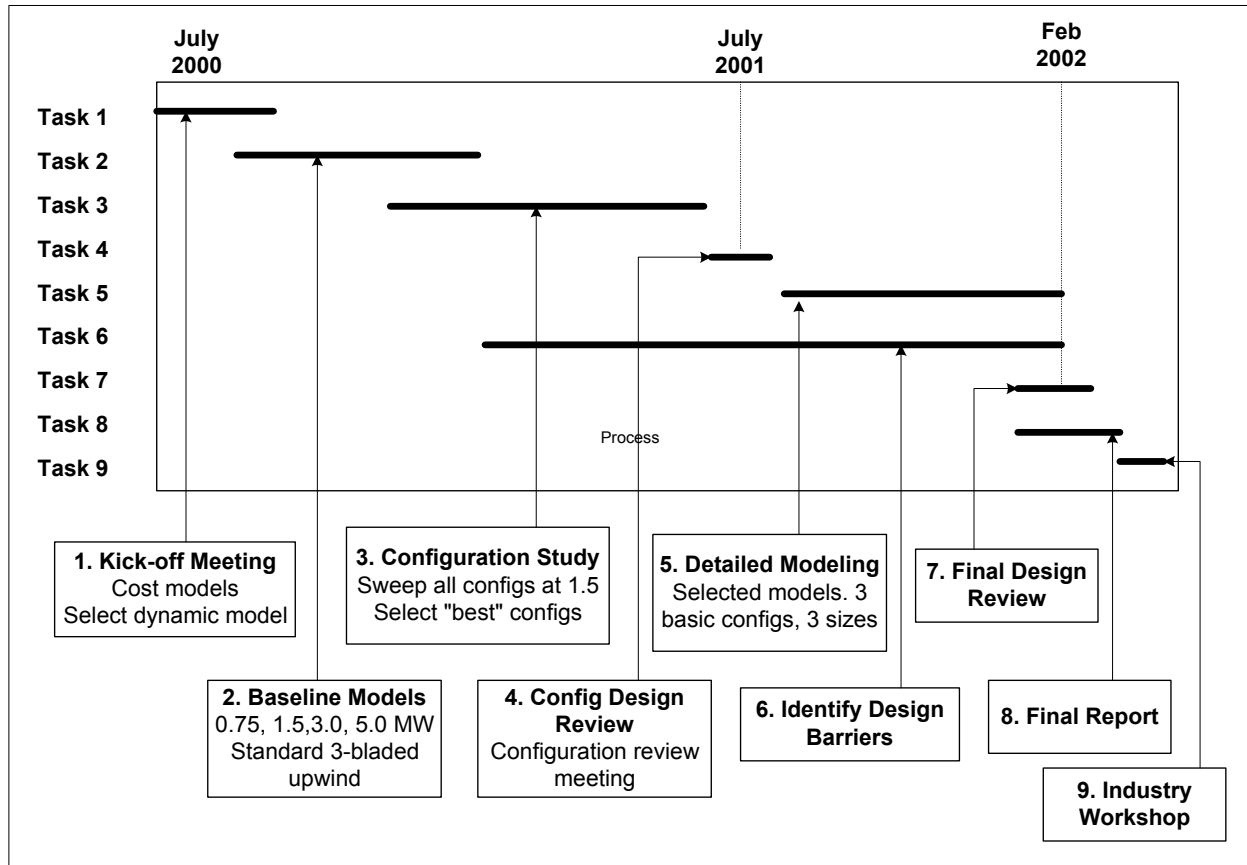


Figure 2-2. Tasks and approximate schedule.

2.1.2 Procedure

The work was divided between GEC and Windward Engineering. GEC initiated the designs and performed the evaluation and costing, while Windward carried out the majority of aeroelastic simulations. This relationship is illustrated in Figure 2-3. Excel spreadsheets were used to standardize much of the data storage and transfer.

The project involved examining a large number of different turbine configurations, and it was important to have a system to efficiently process and track these. A system of configuration control was established based on the naming scheme shown in Figure 2-4.

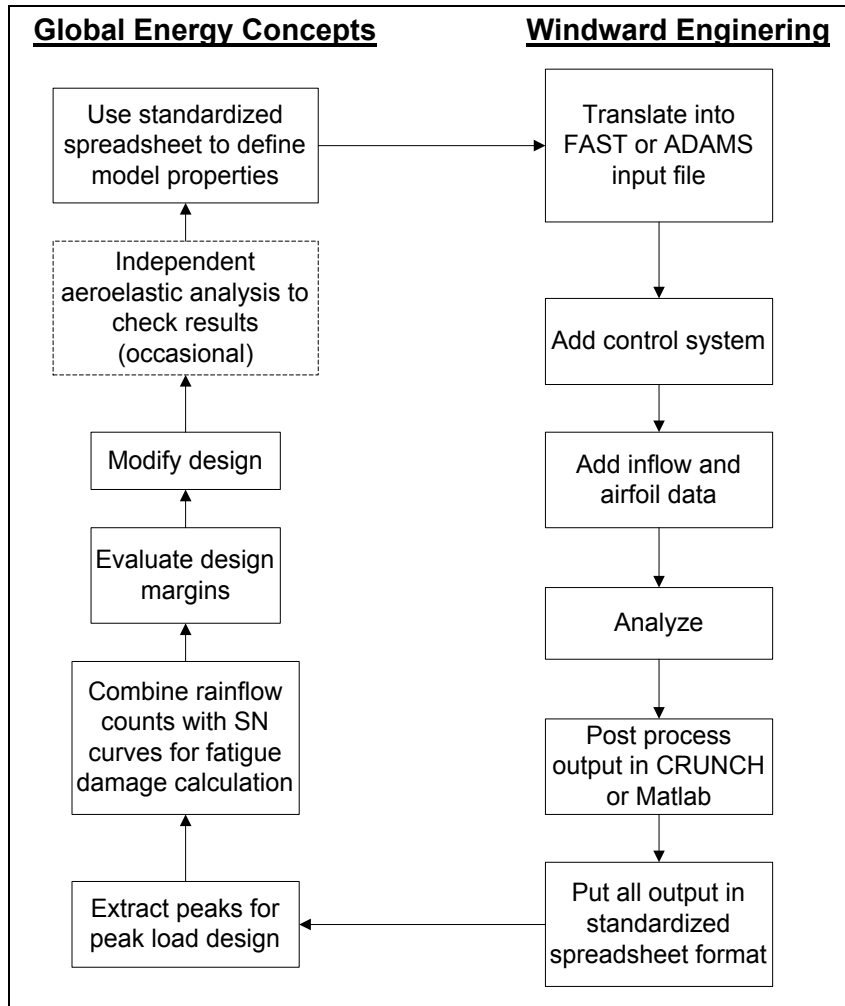


Figure 2-3. Flow of work between GEC and Windward Engineering.

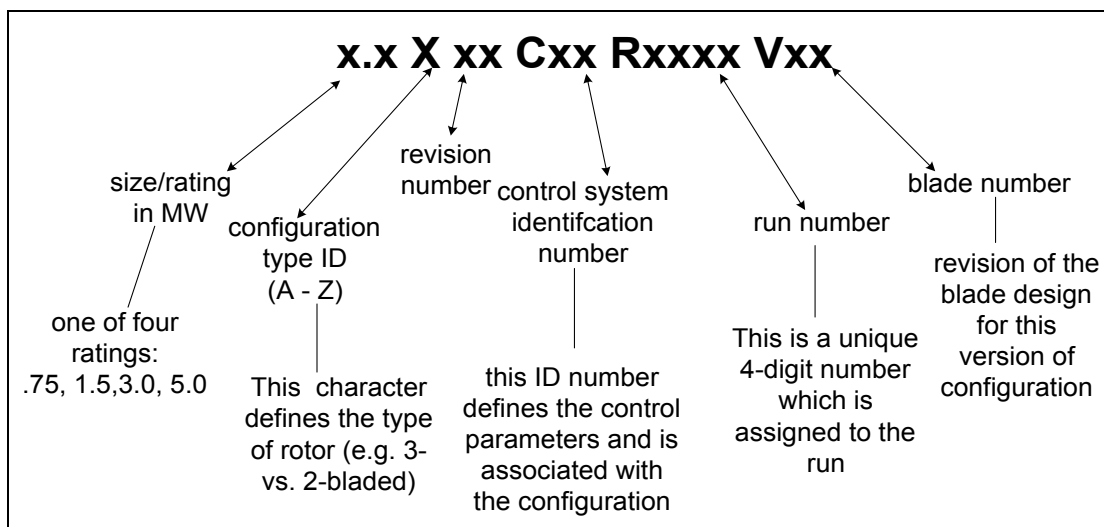


Figure 2-4. Configuration control scheme for models.

It was necessary to maintain a number of file types throughout the design process and to standardize the file formats for communications between GEC and Windward. These files are listed and described in Table 2-1.

Table 2-1. Types of Files Used in Design Process

File Type	Purpose	Format
Blade design files	Used to define the profile and structural properties of the blade	Excel
Input data files	Used to define all details of the turbine configuration, from which the simulation model was constructed	Excel
Output data file	Formulated by Windward to store all output from a certain configuration analysis	Excel
Design evaluation and cost	Using input and output data files, carried out design and cost estimate of all components	Excel
File log	Used to list and track all configurations and files listed above	Excel
ADAMS input file	Constructed by Windward from the input file to submit to the ADAMS code	*.adm
FAST_AD input file	Constructed by Windward from the input file to submit to the FAST_AD code	text

The relationship among the sets of files and how they were used in the design process and in the flow of information between GEC and Windward is shown in Figure 2-5. Information on each file was maintained in a central logging system, and samples of each file type are available through the NREL WindPACT Web site. Some details of the spreadsheet structure and format are given below.

2.1.2.1 Blade Design File

An Excel spreadsheet was prepared to supply the basic properties of the blade. The spreadsheet was based on the approach developed for the WindPACT Blade Scaling Project [3] and is described more fully in Section 3.2.1.

The inputs to the spreadsheet were the design moments at key spanwise locations: the root, 25% span, 50% span, and 75% span. The output from the spreadsheet comprised the required thickness of the box spar at those sections and the corresponding section properties and weights.

2.1.2.2 Input Data File

The input data file (see Figure 2-5) was used to transmit all information necessary to allow construction of a computer model of the entire turbine. The spreadsheet consisted of a Main Page on which all basic information was supplied and a number of pages on which further calculations were made and the data presented in a format suitable as input to the aeroelastic codes. There was one page each for definition of the blade and the tower.

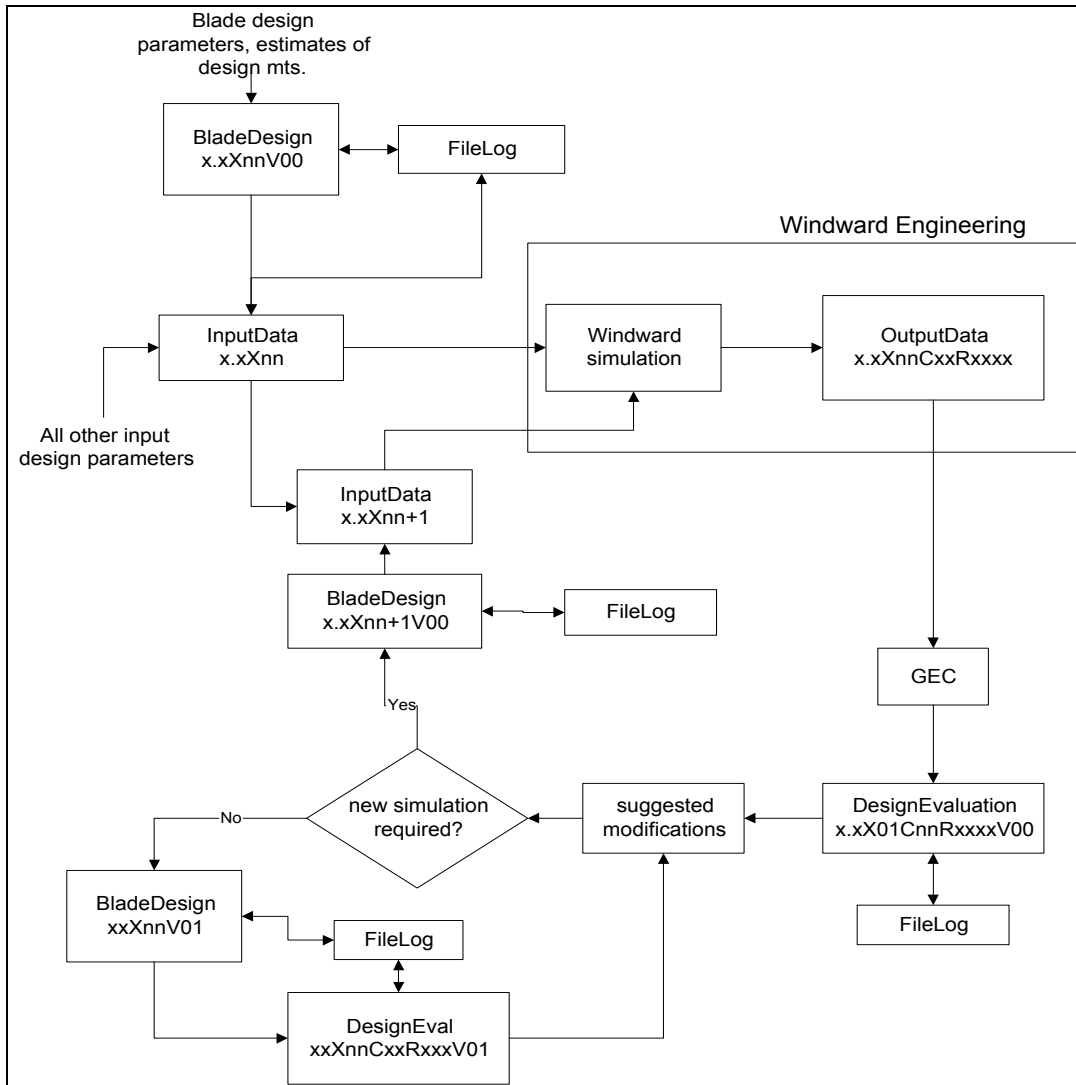


Figure 2-5. Flow of information in the design process.

2.1.2.3 Output Data File

The output data file was received from Windward Engineering and contained all output results from the various simulations. This file consisted of:

- One page with all statistics from all the required signals/loads for all the load cases.
- One page containing rainflow distributions from all the signals at each of the mean wind speeds for normal operation in turbulent conditions.
- One page with the durations spent at each range of drive train torques for each of the mean wind speeds for the normal operation.

2.1.2.4 Design and Cost Evaluation Process

This spreadsheet combined the configuration definition and the simulation outputs and determined whether the major components were adequately designed. Therefore the Main Page from the input data file was copied into the design spreadsheet along with all pages from the output data file. The design spreadsheet contained one page for design calculations for each of the following: blades, hub, low-speed shaft, gearbox, mainframe, and tower.

A sheet titled *Materials* contained all the design properties for all the materials used in the design. Another sheet titled *Evaluation* calculated the margin of safety in the various modes for all components. The calculation of the margin of safety for peak loads and for fatigue loading is shown below.

$$\text{margin of safety (peak loads)} = \frac{\text{characteristic_strength} * \text{material_safety_factor}}{\text{characteristic_load} * \text{loading_safety_factor}} - 1$$

$$\text{margin of safety (fatigue loading)} = 1 - (\text{fraction of fatigue damage done by factored loads})$$

A positive margin indicated that there was spare safety and that the component could be made lighter, whereas a margin of zero indicated that the design was critical. The intent was to adjust all components so that all margins of safety were at or very close to zero. Margins for peak loads indicated the amount by which the load and/or the static strength could be adjusted. Margins for fatigue load cases indicated the amount by which the fatigue life was over or below the 20-year target.

The *Evaluation* sheet contained factors by which the major component dimensions could be adjusted. This allowed the user to make corrections until all the margins became zero. This process was valid if the adjustments were small (less than about 10%) and the required changes would not lead to any significant change in loads. However, if the required changes were more substantial, then a new simulation was carried out to ensure that the properties used in the aeroelastic analysis were consistent with the final configuration.

2.1.3 Load Cases

The load cases set out in IEC 61400-1 [1] were used as a basis for the loads simulated in the analysis. All the extreme events were simulated and are listed in Table 2-2. None of the fault conditions, such as overspeed and emergency stops, were included. The operation in turbulence was carried out with the standard IEC Kaimal spectrum [1] for IEC class 2, intensity option A, at mean wind speeds of 8, 12, 16, 20, and 24 m/s. At each mean wind speed, three 10-minute periods were simulated using different random seeds. Emergency stops were added in Task #5.

Table 2-2. Load Case Analyses Carried Out

Type of Load	Acronym	Mean or Initial Wind Speeds (m/s)	Directions	Return Periods (Years)
Normal turbulence model, IEC class 2a, Kaimal spectrum	NTM	8, 12, 16, 20, 24 (@ 3 seeds each)	N/A	N/A
Extreme coherent gust with direction change	ECD	12, 16, 20, 24	Positive, negative	N/A
Extreme coherent gust	ECG	12, 16, 20, 24	N/A	N/A
Extreme direction change	EDC	12, 16, 20, 24	Positive, negative	1, 50 years
Extreme operating gust	EOG	12, 16, 20, 24	N/A	1, 50 years
Extreme vertical wind shear	EWSV	12, 16, 20, 24	N/A	N/A
Extreme horizontal wind shear	EWSH	12, 16, 20, 24	Positive, negative	N/A
Extreme wind model	EWM	42.5 (@ 5 seeds)	Turbulent	50
Emergency stops (Task 5 only)	Estop	12, 16, 20, 24	N/A	N/A

2.1.4 Design Methodology

The following rules were observed in the design process:

- The limit states approach was used wherever applicable.
- The partial safety factors for loads (load factors) were in accordance with IEC 61400-1 [1].
- The partial safety factors for material strength were in accordance with IEC 61400-1 [1] and with the applicable industry design codes.
- For fiberglass blade design, the material factors from the Germanischer Lloyd regulations [2] were used.

2.2 Specifications for Baseline Configurations

The NREL Statement of Work included the following specifications for the baseline configurations:

- Three blades
- Upwind
- Full-span variable-pitch control
- Rigid hub
- Blade flapwise natural frequency between 1.5 and 2.5 per revolution
- Blade edgewise natural frequency greater than 1.5 times flapwise natural frequency
- Rotor solidity between 2% and 5%
- Variable-speed operation with maximum power coefficient = 0.50
- Maximum tip speed ≤ 85 m/s
- Air density = 1.225 kg/m³
- Turbine hub height = 1.3 times rotor diameter
- Annual mean wind speed at 10-m height = 5.8 m/s
- Rayleigh distribution of wind speed
- Vertical wind shear power exponent = 0.143
- Rated wind speed = 1.5 times annual average at hub height
- Cut-out wind speed = 3.5 times annual average at hub height
- Dynamically soft-soft tower (natural frequency between 0.5 and 0.75 per revolution)
- Yaw rate less than 1 degree per second.

These initial specifications were modified and reinterpreted as the project progressed. The basic specifications were revised partway through Task #2; as a result, reference in this document will be made to the first and second sets of specifications. No comparisons were made between results using the two sets of specifications. All results in this report are based on the second set of specifications.

2.3 Simulation Software

There are several codes that are intended for or can be adapted to the aeroelastic analysis of a horizontal-axis wind turbine. The two that were considered for this project were the proprietary code ADAMS™, available from MSC Software of Santa Ana, California (formerly Mechanical Dynamics of Ann Arbor, Michigan) [4], and FAST_AD [5], which has been developed by Oregon State University and NREL. The former has been used in conjunction with aerodynamic routines to provide a versatile tool able to represent any configuration and to include all nonlinear effects. FAST_AD works with the same aerodynamic routines but is limited in the types of rotor that can be modeled, and the deformation is limited to a number of preselected mode shapes. These limitations are balanced by shorter computer run times.

It was recognized that although FAST_AD would speed the analysis process, only ADAMS could model some of the intended configurations. In addition, FAST_AD had not been used in conjunction with any control systems, while there was some experience incorporating control systems into ADAMS models. For this reason, Task #1 included an item to modify the FAST_AD code for controlling the blade pitch and the electrical torque to simulate the modern variable-pitch, variable-speed wind turbine.

2.4 Signals Recorded

Table 2-3 lists the loads/measurements that were collected in the aeroelastic simulations, and Figure 2-6 shows the various coordinate systems that are referenced. Note that the sign convention refers to the load applied to the part farther down the load path. For example, the blade root flapwise bending moment refers to the moment applied by the blade to the hub.

Table 2-3. Loads and Variables Recorded During Simulations

Variable	Notation	Units
Time		Seconds
hub height wind speed	WShh	m/s
hub height wind direction	WDhh	degrees (positive, yaw ccw about Z axis)
low speed shaft speed	RpmLss	rpm (positive, cw about X axis)
high speed shaft speed	Rpmgen	rpm
aerodynamic power	RotorPower	kW
generator electrical power	GenPower	kW
yaw angle	YawAng	degrees (positive ccw about Z axis)
pitch angle of blade #1	PitchAngB1	degrees (positive moves leading edge upwind)
Azimuth angle	AzimHub	degrees (positive cw about X axis)
out-of-plane displacement of blade tip #1	DxTipOutB1	m (positive downwind)
in-plane displacement of blade tip #1	DyTipInB1	m (measured in hub coordinates)
out-of-plane displacement of blade tip #2	DxTipOutB2	m (positive downwind)
in-plane displacement of blade tip #2	DyTipInB2	m (measured in hub coordinates)
out-of-plane displacement of blade tip #3	DxTipOutB3	m (positive downwind)
in-plane displacement of blade tip #3	DyTipInB3	m (measured in hub coordinates)
longitudinal displacement of tower top	DxLongT	m (positive downwind)
lateral displacement of tower top	DyLatT	m
edgewise bending moment at 75% span, blade #1	Mx75EdgeB1	kN m (positive, trailing edge in tension)
Flapwise bending moment at 75% span, blade #1	My75FlapB1	kN m (positive, upwind face in tension)
edgewise bending moment at 50% span, blade #1	Mx50EdgeB1	kN m (positive, trailing edge in tension)
Flapwise bending moment at 50% span, blade #1	My50FlapB1	kN m (positive, upwind face in tension)
edgewise bending moment at 25% span, blade #1	Mx25EdgeB1	kN m (positive, trailing edge in tension)
Flapwise bending moment at 25% span, blade #1	My25FlapB1	kN m (positive, upwind face in tension)
Flapwise shear force at root of blade #1	FxRtFlapB1	kN (positive in blade x direction)
edgewise shear force at root of blade #1	FyRtFlapB1	kN (positive in blade y direction)
axial force at root of blade #1	FzRtExtB1	kN (positive in tension)
edgewise bending moment at root of blade #1	MxRtEdgeB1	kN m (positive, trailing edge in tension)
Flapwise bending moment at root of blade #1	MyRtFlapB1	kN m (positive, upwind face in tension)
Flapwise shear force at root of blade #2	FxRtFlapB2	kN (positive in blade x direction)
edgewise shear force at root of blade #2	FyRtFlapB2	kN (positive in blade y direction)
axial force at root of blade #2	FzRtExtB2	kN (positive in tension)
edgewise bending moment at root of blade #2	MxRtEdgeB2	kN m (positive, trailing edge in tension)
Flapwise bending moment at root of blade #2	MyRtFlapB2	kN m (positive, upwind face in tension)
Flapwise shear force at root of blade #3	FxRtFlapB3	kN (positive in blade x direction)
edgewise shear force at root of blade #3	FyRtFlapB3	kN (positive in blade y direction)
axial force at root of blade #3	FzRtExtB3	kN (positive in tension)
edgewise bending moment at root of blade #3	MxRtEdgeB3	kN m (positive, trailing edge in tension)

Table 2-3 (Continued). Loads and Variables Recorded During Simulations

Variable	Notation	Units
Flapwise bending moment at root of blade #3	MyRtFlapB3	kN m (positive, upwind face in tension)
axial thrust in low speed shaft	FxThrustS	kN
shear force in shaft edgewise to blade #1	FyS	kN
shear force in shaft parallel to blade #1	FzS	kN
torque in low speed shaft	MxTorqS	kN m
bending in low speed shaft at hub center about axis parallel to blade #1 chord	MyS	kN m
bending in low speed shaft at hub center about axis parallel to blade #1 span	MzS	kN m
bending in low speed shaft at main bearing about axis parallel to blade #1 chord	MyBrgS	kN m
bending in low speed shaft at main bearing about axis parallel to blade #1 span	MzBrgS	kN m
electrical torque applied to drive train	GenTorq	kN m
downwind thrust at yaw bearing	FxAxialN	kN
lateral thrust at yaw bearing	FyLat	kN
Vertical load at yaw bearing	FzVertN	kN
Pitching moment at yaw bearing	MypitchN	kN m
yawing moment at yaw bearing	MzYawN	kN m
lateral bending moment at base of tower	MxLatT	kN m
longitudinal bending moment at base of tower	MyLongT	kN m
torsional moment at base of tower	MzYawT	kN m

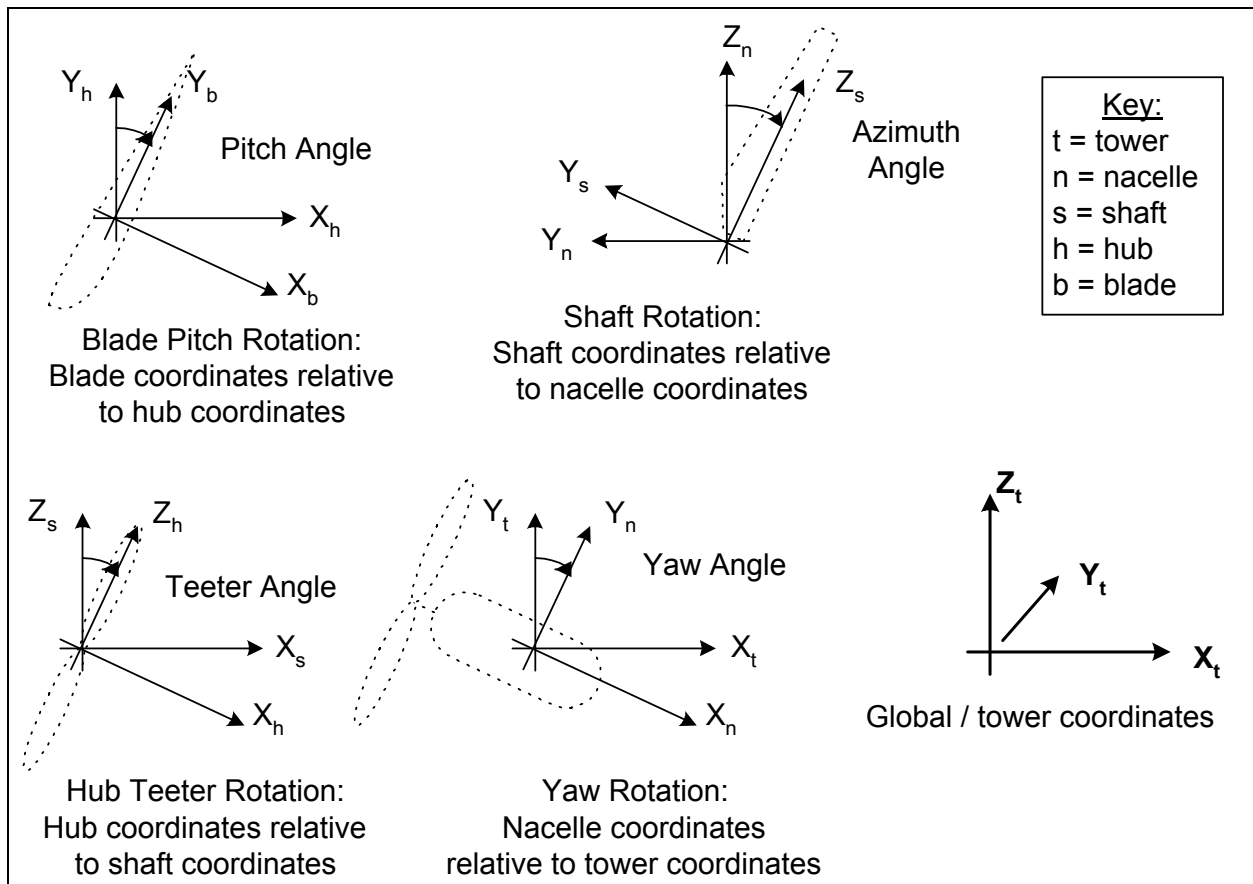


Figure 2-6. Coordinates systems used and corresponding rotations.

3. TASK #1. DESIGN AND COST MODELS

3.1 General Approach

In order to calculate the effect of rotor changes on the final cost of energy, it was necessary to be able to estimate the cost of all major wind turbine components and to know how those costs change with perturbations in the rotor design. Task #1 of the project consisted largely of developing these cost relations.

The following general approaches and guidelines were used:

- Apart from the rotor, all components or subassemblies were assumed to be of a “standard” design.
- The wind farm was assumed to be of 50 MW rated power for all the turbine sizes considered.
- The costs of all components corresponded to “mature production,” implying that further economies of scale of manufacture are not available.
- It was important to obtain cost estimates that were realistic, but the exact cost of components was not as important as the changes due to rotor configuration changes.
- In general, all components were checked for their adequacy under both peak and fatigue loads.
- The cost of each major component was checked against at least one known commercial example.
- For most components, the cost was considered to be a function of the weight.
- The size and weight of many components were expressed as functions of the rotor diameter.
- Expressions from other cost models were checked for their applicability to current designs.
- Smooth functions were developed for all items, although the data from which they were derived may have contained discrete steps.

Table 3-1 summarizes the approaches and formulas used for costing all items.

As the project progressed, some of the initial cost models became inadequate. For example, during the Task #2 baseline study when different rotor sizes were being compared, it was important for the cost of items such as pitch bearings to reflect the changes in rotor diameter. However, in Task #3 when the effect of different configurations and associated load changes were being studied, a cost model that could reflect the effects of small changes in peak loads was required. For reasons such as this, some cost models were revised during the project. In these cases, Table 3-1 includes multiple entries for those items.

Table 3-1. Summary of Cost Models Used for Major Components in Baseline Designs

Component	Cost Model/Formula	Verification/Comparison	Comment
Blades (Task #2)	WindPACT blade scaling design [3], \$10.95 /kg	750 kW Class 1 wind: 2130 kg Class 2 wind: 1660 kg av. commercial: 2200 kg	E-glass with structural spar
Blades (Tasks #3, #5)	\$16.42/kg for hybrid carbon-glass spar \$16.42/kg for bias-ply carbon-glass skins	Costs from a range of commercial data [7]	
Hub (Tasks #2, #3)	Static analysis using peak root mt with scale factor of 2.5 \$4.25 /kg	Scale factor selected to give 750kW weight = 3100 kg compared with a commercial 750/50 machine	Cast ductile iron sphere with openings, grade 65-45-18
Hub (Task #5)	Static analysis using peak root mt. with scale factor of 1.92 \$4.25 /kg	Scale factor selected to give better agreement with hub of 47-m machine	
Teeter hub	Static analysis of cylindrical tube using peak root mt with scale factor = 3.50. Mass x 2 for teeter and dampers. Overall \$7.70/kg.	Overall costs from AWT-27	Total mass less than 3-bladed hub, but cost is greater
Pitch bearings Not used for final costing.	\$/bearing = $0.0454 * D^{2.98}$ Cost doubled for remaining system and drives	Data from Avon bearings (Appendix C). 750-kW costs and weights compared with commercial data	See text
Pitch bearings (Tasks #2, #3, #5)	Mass [kg] = $0.0110 (mt/diam)^{1.489}$ cost[\$] = $6.689 * kg + 953$	Curve fit through Avon data	See text
Gear box	Life_factor [1/Nm] = $0.1628 * mass^{-1.340}$ \$/kg = $0.000647 * rating[kW] + 13.26$	Ed Hahlbeck/Powertrain Engineers Inc. [8]. Unit_stress vs. mass curve fitted to 4 point designs	Final relationship: $mass \approx const * D^{2.2}$
Generator (Tasks #2, #3)	\$65.00/kW rating mass[kg] = $3.3 * rating[kW] + 471$	Mass model from U of Sunderland [6]. Cost checked with commercial data	1800-rpm wound rotor induction motor with power electronics
Generator (Task #5)	\$52.00/kW rating mass[kg] = $3.3 * rating[kW] + 471$	Cost model made consistent with WindPACT Drive Train study [9]	
Main shaft	\$7.00/kg, length = $0.03 * D$, scale factor = 4.0, ID = 0.5OD. Diameter kept constant in Task #3 changes and thereafter	U of Sunderland [6] and current commercial designs	Shaft often governed by stiffness rather than by strength
Main bearings	Bearing mass = $(D \times 8/600 - 0.033) \times 0.00920 \times D^{2.5}$ Where D = rotor diam (m) cost = \$17.60/kg	Powertrain Engineers Inc.	
Bedplate	Ductile iron casting, grade 60-45-18 \$4.25/kg	Scale factor included to obtain agreement with industry (5800 kg for 750-kW turbine)	Stress analysis of channel section using moments at yaw bearing
Nacelle cover (Tasks #2, #3)	Area = length ² length[m] = 2*yaw brg to outer main brg mass = 84.1 kg/m ² cost = \$10.00/kg	U of Sunderland formula for kg/m ² . Cost from Morrison Fiberglass	
Nacelle cover (Task #5)	Area = length*(width+height) length[m] = 2*yaw brg to outer main brg mass = 84.1 kg/m ²	Area formula modified to be less sensitive to length	

Note: Unless specified otherwise, quantities use the units of m, kg, kW, and kN m.

Table 3-1 (Continued). Summary of Cost Models Used for Major Components in Baseline Designs

Component	Cost Model/Formula	Verification/Comparison	Comment
Hydraulics	\$4.50/kW	GEC estimate	
Brakes, couplings	Mass [kg] = 0.025*ratedHStorque[Nm] \$10.00/kg	Mass from U of Sunderland [6]	
Yaw system (Task #2)	\$/bearing = 0.0339*D ^{2.96} cost doubled for remaining system and drives	Data from Avon bearings. Initial estimates from [6]	See text
Yaw system (Tasks #3, #5)	Mass [kg] = 0.0152(max_mt/bearing_diam – 36) ^{1.489} \$ = 6.689*mass + 953	Mass and cost made dependent on peak load	
Switchgear	\$40.00/kW	Industry data	
Power electronics (Tasks #2, #3)	\$67.00/kW (total electrical)	U.S. manufacturing industry	Variable-speed system using wound rotor induction motor
Power electronics (Task #5)	\$54.00/kW (total electrical)	Comparison with data from WindPACT Drive Train study [9]	
Controls	\$9500 + 10*D	[6]	
Tower	\$1.50/kg	Initial design tuned to agree with commercial 750/50 data	Costs per U.S. steel fabricating industry
Foundations (Task #2)	\$/kW = 584*Rating ^{0.377}	Adjusted to agree with quotes from Patrick & Henderson for 750- and 1500-kW machines	The steel caisson design of P&H is cheaper than traditional concrete slab designs
Foundations (Tasks #3, #5)	\$ = 510 * (Max_base_mt[kN m]) ^{0.465}	Adjusted to agree with updated quotes from Patrick & Henderson for a range of machine sizes	Includes influence of changes in base loads
Transportation	\$/kW = 1.581E-5*Rating ² – 0.0375*Rating + 54.7	Obtained from WindPACT logistics study [12]	Reflects large increases associated with 3- and 5-MW turbines
Assembly, installation	\$/kW = 3.38E-7*Rating ² + 9.84E-4*Rating + 31.57	Obtained from WindPACT logistics study [12]	
Roads, civil works	\$/kW = 2.17E-6*Rating ² – 0.0145*Rating + 69.54	Obtained from WindPACT report [13]	Modifications to width of roads and cost of crane pads
Electrical interface	\$/kW = 3.49E-6*Rating ² – 0.0221*Rating + 109.7	Obtained from WindPACT report [13]	Includes turbine transformers and cables to substation
Permits, engineering	\$/kW = 9.94E-4*Rating + 20.31	Obtained from WindPACT report [13]	
Long-term replacement	\$15/kW/year	Based on Danish survey of experience in that country [18]	Replacement of blades, gearbox, generator, etc.
Operations and maintenance	\$0.008/kWh	Flat rate adopted so that other trends can be investigated later	Excludes taxes, lease costs, and insurance

Note: Unless specified otherwise, quantities use the units of m, kg, kW, and kN m.

3.2 Rotor Components

3.2.1 Blade Design

3.2.1.1 Aerodynamic Specifications

The blades are at the focus of this project, and it was therefore necessary to model them in some detail. As part of the study, the blades in current use in the industry were reviewed, and the following guidelines were adopted as being typical of current commercial practice.

- Maximum tip speed = 65 m/s
- Ratio of maximum chord to rotor radius = 0.09
- Tip speed ratio for maximum power coefficient = 7.0
- Ratio of maximum (electrical) power to swept area = 0.44 kW/m^2 (“specific rating”)

The data used to select the specific rating are illustrated in Figure 3-1, in which a value of 0.44 kW/m^2 is close to an average value. The NREL specification relating the rated wind speed to the hub-height mean wind speed, combined with the presence of vertical wind shear, leads to a variation of specific rating with hub height and hence to rotor diameter. This relationship is also shown in Figure 3-1 and is close to the line representing commercial data.

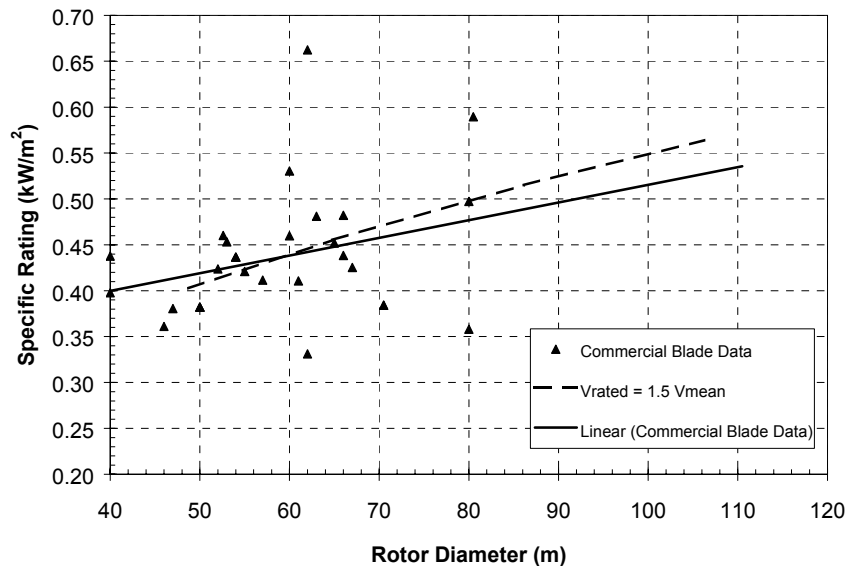


Figure 3-1. Specific rating vs. rotor diameter for current commercial wind turbines.

3.2.1.2 Baseline Blade Design

The final design and cost of the blades were determined through an iterative process using the results of the loads from the aeroelastic simulations. However, an initial design model was needed. The design of the rotor blades for the baseline configurations followed the results from the WindPACT blade-scaling project [3] that was completed at GEC near the same time that this project began. The blade-scaling project examined the feasibility and cost of increasing the scale of “current technology” in blade design and was based on the following approach:

- The blades were assumed to consist of a fiberglass skin of largely triaxial material sandwiching a balsa core for stability. Each skin thickness was 1.78 mm.
- Each blade included a longitudinal box spar that spanned from 0.15 of the chord position to 0.50 of the chord. This spar was composed mainly of uniaxial glass fibers. This spar began at the 25% span location (corresponding to maximum chord) and tapered off to zero at the tip.
- The blade section was circular between the root at 5% span and 7% span, and then it transformed to the S818 30% airfoil shape at 25% span location.
- The section was reinforced at the root to accommodate the attachment studs for which a weight estimate was made.
- The loading used to obtain the first design estimate was the 50-year extreme wind on the stationary blade using the maximum lift coefficient along the entire blade.
- Designs were generated for four sections: 7%, 25%, 50%, and 75%.
- Designs for the required spar were based on interpolation between results for total spar thickness values of 0%, 5%, and 10% of the airfoil thickness.
- Input to the blade design spreadsheet consisted of the material properties and a set of flapwise design moments. The output consisted of the spar thickness required to resist the design moments together with the corresponding section properties and the surface strains due to a unit bending moment.

A number of weight and cost models are included in the University of Sunderland report [6], but we did not make use of these for the initial design since the model from the WindPACT Blade Scaling project [3] was available and could be tailored to this project. The WindPACT model is based on the extreme 50-year gust, assuming that the maximum lift occurs simultaneously along the entire blade. It also includes a check for edgewise fatigue due to gravity loads plus the torque at rated power.

The WindPACT blade-scaling study also considered the cost of tooling and the implications of the size of the production run. The current project assumes that all costs correspond to “mature production,” which means that at least 100 blades are produced per year. This value will be reached earlier when 750-kW machines are used than when 5-MW machines are involved.

3.2.1.3 Airfoil Schedule

The NREL S-series airfoils were used for the blade designs of this study. In the work of References [19] and [20], the S818/S825/S826 family was identified as having desirable aerodynamic properties. However, the airfoils were deemed to be too thin for efficient application to large blades (assuming current commercial materials were used). A more structurally suitable set of airfoil shapes was derived by scaling the S818/S825/S826 foils and by the addition of a finite-thickness trailing edge. The shape modifications and locations of airfoils along the blade are summarized in Table 3-2; the resulting airfoil shapes are shown in Figure 3-2.

In Task #3 some of the configurations were composed of a hybrid carbon-glass spar. The cost of this construction was taken from [3]. In Task #5, the blade construction was further altered to include carbon-glass skins with a bias angle to incorporate flap-twist coupling. The cost of this was based on estimates in [7].

Table 3-2. Summary of Aerodynamic and Geometrical Design of Blades

		750 kW	1.5 MW	3.0 MW	5.0 MW
Airfoils type / aspect ratios / twist (degrees) used	@ 5% span	cylinder // 10.5	cylinder // 10.5	cylinder // 10.5	cylinder // 10.5
	@ 7% span	cylinder // 10.5	cylinder // 10.5	cylinder // 10.5	cylinder // 10.5
	@ 25% span	S818 / 0.27 / 10.5	S818 / 0.30 / 10.5	S818 / 0.33 / 10.5	S818 / 0.33 / 10.5
	@ 50% span	S825 / 0.24 / 2.5			
	@ 75% span	S825 / 0.21 / 0.0			
	@ 100% span	S826 / 0.16 / -0.6			
Rotor diameter	first specification	46.6	66.0	93.0	120.0
	second specification	50.0	70.0	99.0	128.0
Chord at 25%/radius	first specification	0.09	0.09	0.09	0.09
	Second specification	0.08	0.08	0.08	0.08
Tip speed ratio for max Cp		7.0	7.0	7.0	7.0
Root section diameter		0.054*D	0.054*D	0.054*D	0.054*D
Spanwise radius at root		0.025*D	0.025*D	0.025*D	0.025*D

Note: D is the diameter of the rotor.

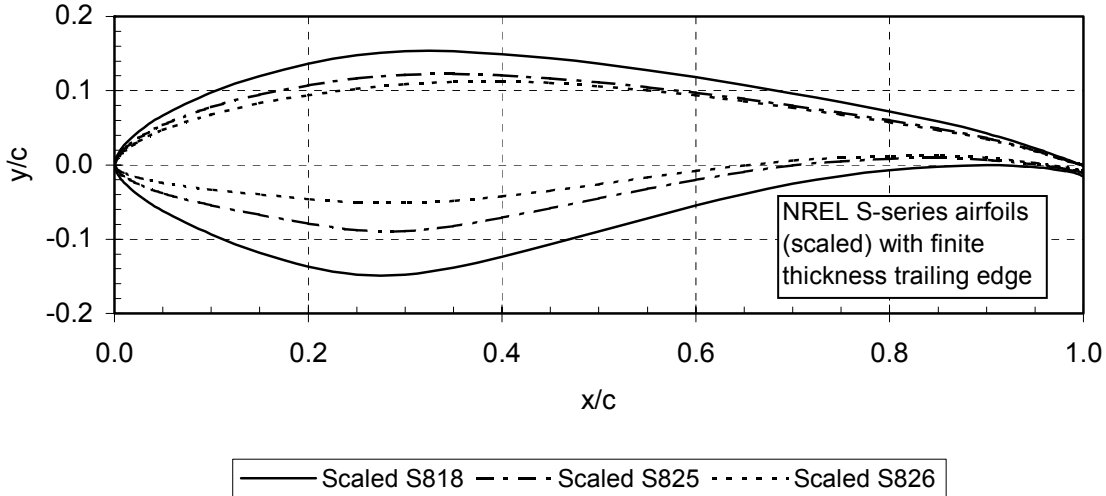


Figure 3-2. Airfoils used for baseline 1.5-MW blade model.

3.2.2 Hub

Most current 3-bladed rotors use a hub made from a ductile iron casting in the shape of a sphere with openings for the blades and for the shaft connections. The stress analysis and design of these components are done by finite element analysis of multiple load cases, which this project could not attempt to duplicate. Instead, a simplified approach based on static analysis and a suitable “scale factor” was used. The approach consisted of calculating the membrane stress due to the maximum applied moment at the

opening as a function of sphere diameter, opening diameter, and shell thickness. This membrane stress was increased by a scale factor, which accounted for the stress concentrations around the opening, and combined with appropriate material properties to arrive at a design.

The final mass was calculated as a complete sphere with the prescribed diameter and wall thickness. This implied that the reinforcements around the four openings were equivalent to a uniform sphere. The total mass of the hub obtained in this manner was compared with some commercial hubs and the scale factor was tuned so that the model and commercial values were in good agreement. Initial comparisons indicated that a scale factor of 2.5 was appropriate. Further comparisons carried out later in the project, during Task #3, suggested that this value was too high, and a value of 1.92 was adopted from then onwards. The lower value was used for all results presented in this report.

3.2.2.1 Pitch Bearings

It was assumed that each of the blades is pitched independently. The pitch system for each blade consists of a bearing, a speed reducer, an electric drive motor, a controller, and a power supply. Each blade is mounted to the hub via turntable bearings with an internal slewing ring for engagement with a drive pinion. The pinion is driven through a speed reducer by a high-rpm electric motor.

An initial model for the total cost was: $\$/bearing = 0.0454 * D^{2.98}$. This was found to correspond well with data obtained later from Avon Bearings (see Appendix C). These data included cost estimates for the range of ratings of interest and were based on initial estimates of peak moments. The mass and cost of the auxiliary pitch drive components were estimated to be equal to that of the pitch bearing itself and a factor of 2.0 was, therefore, added to the cost. However, as noted below, this model was not used for the final estimates in the costing and scaling efforts.

Different bearing types were recommended by Avon at the different sizes because of the relatively small diameter of these bearings compared to the high loads they must carry. At 750 kW, a single-row ball bearing was selected, whereas at the 1.5 MW and higher ratings, triple-row bearings were recommended and quoted. The cost quoted for bearings for the 5-MW size did not fall on the same curve as for the others and it was therefore neglected in defining the cost model.

A new cost model was defined for Tasks #2, #3, and #5 that reflected cost changes due to changes in the peak loads applied. Therefore, the Avon cost data was reformatted into the following form:

$$mass[kg] = 0.0110 \left(\frac{\max_applied_moment[kN\ m]}{diameter[m]} \right)^{1.489}$$

$$cost[\$] = mass * 6.689 + 953$$

For Tasks #2, #3, and #5, it was again assumed that the cost of the remainder of the pitch system (motor, speed reducer, controller, etc.) is equal to the cost of the bearing.

3.2.2.2 Teetered Hub

The concept adopted for the design of the teetered hub was of a cylindrical tube that mated with the blade pitch bearings at either end and was attached to the shaft through a central teeter pin. The wall thickness of the tube was designed by the peak moment from the blade roots and was adjusted by a scale factor to give agreement with known data (the AWT-27) and to be comparable to the mass of the equivalent 3-bladed hubs. The mass of the remaining items (modifications to the single tube, the teeter pin, the dampers, etc.) was assumed to be equal in weight to the cylindrical tube. The cost of the total assembly was calculated using a value of \$7.70/kg, which was calculated from the known cost and mass of the AWT-27 turbine components.

A scale factor of 3.50 was used. This value resulted in total hub weights that were slightly less than the total weights of corresponding 3-bladed hubs. The cost of the teetered hub was higher than that of the 3-bladed hub due to the costs involved in the teeter pin and damper units.

3.2.3 Drive Train Components

The drive train includes all components from the main shaft to the connection to the pad mount transformer including any power electronics and electrical switches. In addition to the mechanical and electrical power delivery and conversion equipment, all the structural components and auxiliary mechanical and electrical components between the hub and the tower top are included in the drive train group. The following sections address the sizing, weight, and cost modeling of these components.

3.2.3.1 Main Shaft

The main shaft was assumed to be a hollow cylinder with a flanged end for a bolted connection to the hub. The length was initially fixed at 0.03*(rotor diameter) and the inner-to-outer-diameter ratio was fixed at 0.5. Determination of the outer diameter was based on an analysis of the stress at the bearing closest to the rotor (the location of peak bending) with an added scale factor of 4.0 to allow for stress concentrations and to obtain initial agreement with current designs and with the University of Sunderland report [6]. Both peak stresses and fatigue were considered. The shaft was assumed to be made from high-strength steel with a characteristic yield of 828 MPa. The mass of the shaft, calculated from the length and diameter, was used to assess the cost at \$7.00/kg.

The cost of the main shaft was initially allowed to change with the changes in loads created in Task #3. However, it was determined that the shaft diameter was usually dictated by stiffness rather than strength considerations, so that the mass and cost of the main shaft should remain constant with these perturbations. This approach was adopted throughout Task #3 and for the remainder of the project.

3.2.3.2 Main Bearings

The main bearing was assumed to be of a standard type and a formula for the mass was developed based on data, collected by Powertrain Engineers Inc., from wind turbines between 750 kW and 2000 kW. The second bearing was included in the gearbox assembly. The resulting expression for the bearing mass, in terms of the rotor diameter, D, was:

$$\text{Mass (kg)} = (D \times 8/600 - 0.033) \times 0.00920 \times D^{2.5}$$

The mass of the bearing housing was assumed to be the same as that of the bearing itself and a rate of \$17.60 per kg was used for both components.

3.2.3.3 Gearbox

For the design of the gearbox, Ed Hahlbeck of Powertrain Engineers was contracted to provide point designs for the 750-kW, 1.5-MW, 3-MW and 5-MW baseline turbines. These design results included detailed fatigue analyses, mass estimates, and costs. Powertrain Engineers was given the baseline turbine parameters and a requirement to operate at rated torque for a lifetime of 200,000 hours. The analysis was based on the standard AGMA methodology combined with experience in wind turbine gearbox design. The analyses and results can be found in Reference [8].

GEC used a combination of the resulting gearbox masses and the intermediate stress results to develop a model of gearbox mass based on the torque histograms from the simulations at each turbine rating. The unit stresses from the gears with the lowest safety margins were curve fit to the total mass of the

corresponding four gearbox point designs. The critical unit stress in the gearbox could then be calculated from a gearbox mass estimate. This unit stress, when combined with the torque histogram from the simulations, was used in a fatigue analysis using standard AGMA SN curves. If the predicted life was above or below that required, the mass was adjusted and the stress and life recalculated until a converged mass estimate was reached.

The life factor (stress divided by maximum allowable stress) is used in fatigue life calculations and was related to the gearbox mass by the following formula:

$$\text{Life factor per unit torque [1/(N m)]} = 0.1628 * (\text{gearbox mass [kg]})^{-1.3405}$$

The gearing for large turbine ratings becomes very large and the costs per unit mass tend to rise and the cost function used was: $(0.000647 * \text{rating [kW]} + 13.26) \text{ \$/kg}$.

3.2.3.4 Generator

The baseline turbine assumes a wound rotor induction generator with slip rings, which allows variable-speed operation. The generator mass model was taken from the University of Sunderland report [6] for an 1800-rpm wound rotor with slip rings. The cost models were verified with data from commercial data. The initial models used were:

$$\begin{aligned} \text{mass [kg]} &= 3.3 * \text{rating [kW]} + 471 \\ \text{cost} &= \$65.00 / \text{kW} \end{aligned}$$

In Task #5, this cost model was compared with information used in the parallel WindPACT Drive Train study [9]. In order to be compatible with the more detailed study of electrical components in that project, the generator cost was reduced to \$52.00/kW.

3.2.3.5 Power Electronics

No mass estimates were made for the power electronic system because it is assumed that they are inside the tower at the base and do not affect the turbine dynamic simulation.

The initial cost model used was \$67.00/kW, where the kW is from the total system rating rather than the rating of the power electronics. This value was based on data related to a major manufacturer. Later in the project, this cost was also compared with information available from the WindPACT Drive Train study [9] and, as a result, the cost was reduced to \$54.00/kW.

3.2.3.6 Bedplate

The bedplate was assumed to be a 60-45-18 grade ductile iron casting with a tapered channel shape. A stress function was developed based on bottom and side wall thickness, and cross section width and depth. The overhanging moment and yaw moment at the yaw bearing were used to calculate the required dimensions to meet both peak and fatigue analysis requirements. An additional scale factor of 9.0 was applied to the stress analysis to obtain agreement with current industry data.

The cost of the bedplate was assessed by calculating the mass that satisfied the stress analysis and adding 50% to cover additional material not directly required to support the rotor, such as the section for the generator, etc.. The cost function used was \$4.25/kg, which includes casting and machining costs.

3.2.3.7 Nacelle Cover

The nacelle cover was assumed to be fiberglass and to cover the entire length of the nacelle. A mass per unit area equal to 84.1 kg/m^2 [6] and a cost of \$10.00/kg was applied (as quoted by Morrison Molded Fiberglass). The estimated surface area was initially calculated as the square of the length where the length is twice the distance from the yaw axis to the outer main bearing [6].

This formula for the cladding area is very sensitive to the length of the nacelle because the formula assumes that the width and the height also increase with the length. In Task #5, the mass model was changed to be dependent on the width and the height of the drive train, as well as the length.

3.2.3.8 Yaw System

The yaw system consists of a turntable bearing and slew ring driven by multiple electric drives that are connected to the slew ring through a speed reducer and pinion. The mass, calculated for use in the simulations, was estimated from the equation in the University of Sunderland report [6]. This equation is a function of the rotor diameter and the initial estimates for rotor thrust, tower head mass, and tower top diameter.

The yaw bearing costs were based on quotes from Avon Bearings (see Appendix C) for the four baseline turbines. These quotes were curve fit to the rotor diameter, resulting in the following relation:

$$\text{yaw bearing cost [\$]} = 0.0339 * (\text{Rotor diameter[m]})^{2.96}$$

This formula is dependent only on the rotor diameter and was not suitable for reflecting cost changes due to changes in the loads for configurations having the same rotor diameter. The masses and costs from Avon Bearings were reexamined and reformatted to be dependent on the maximum moment applied.

$$\text{mass[kg]} = 0.0152 \left(\frac{\text{max_applied_moment[kN m]} - 36}{\text{diameter[m]}} \right)^{1.489}$$

$$\text{cost[\$]} = \text{mass} * 6.689 + 953$$

The diameter of the yaw bearing was calculated as 0.03 times the rotor diameter. The total cost of the yaw system was estimated to be equal to twice the cost of the bearing.

3.2.3.9 High-Speed Shaft, Coupler, Brakes

The mass of the high-speed shaft and coupler were estimated based on the equation in Reference [6] as follows:

$$\text{Mass [kg]} = 0.025 * \text{rated HSS torque [N m]}$$

The mass of the brake calipers and additional disk mass on the coupler were estimated as an additional 50% of the shaft and coupler mass. The cost for all of these items was assumed to average out to \$10.00/kg.

3.2.3.10 Hydraulics and Lubrication

It was assumed that the hydraulic system is used only for the brakes and that the lubrication includes equipment for cooling the gearbox and bearings.

$$\text{Cost} = \$4.50/\text{kW}$$

3.2.3.11 Switchgear and Other Electrical

The cost of the electrical systems (switchgear, transformer, cables, cabinets) exclusive of controls and power electronics was assumed to increase directly with rating. The cost model used was \$40.00/kW.

3.2.4 Tower

The tower was assumed to be a tapered steel tube and was designed for peak and fatigue bending moments at the base and at the top. The total mass was calculated using a linear taper of both diameter and wall thickness between the top and bottom, and a rate of \$1.50/kg was used to arrive at a total cost.

This rate was obtained by consultation with members of the steel fabricating industry and by comparison with known costs of towers in the Turbine Verification Project [10].

The design check of the tower sections used a material yield stress of 350 MPa and a fatigue strength defined by BS7608 class D. A check was also carried out for local stability using formula 14.16 from [11]. In order to maintain the diameter/wall thickness ratio to values that are acceptable to manufacturers, a maximum ratio of 320 was adopted. In addition, the diameter of the top of the tower was specified to be no less than 0.5 of the base diameter. This was done for reasons of access, accommodation of the yaw bearing, and for aesthetics.

3.2.5 Balance of Station

The costs of most items in the balance-of-station category were obtained from the earlier WindPACT studies on logistics [12] and balance of station [13]. The scenarios used in these reports referred to a selected site in South Dakota and are appropriate for the current study. Trend lines were developed from the WindPACT results and were used in this project. The trend line formulas are listed in Table 3-1.

The WindPACT values for Roads & Civil Works from [13] were considered unrealistic and were modified. The costs of the gravel pads for the cranes were reduced by a factor of 2, and the roads for the 2.5-MW and 5-MW machines were adjusted to have a 40-ft (12-m) width.

3.2.5.1 Foundations

The costs of the foundations were based on information received from Patrick & Henderson, Inc. of Bakersfield, California. That company has developed a cost-effective system of wind turbine foundations utilizing a post-tensioned, concrete-filled steel caisson. Their costs were adjusted for the hub heights of the current project and were fit to a power curve resulting in the formula below. These costs assume soil conditions typical of the Great Plains.

$$$/kW = 584 * \text{Rating}[kW]^{-0.377}$$

This formula was found inadequate for Task #3 when the effects of small changes in loads were required. Therefore the costs were reevaluated and also updated with additional data from Patrick & Henderson to arrive at the following expression, which was used for Tasks #3 and #5:

$$\text{Cost } [\$] = 510 * (\text{max_base_moment}[kN\ m])^{0.465}$$

3.2.5.2 Operating Costs

There are several types of costs that are sometimes included in the category of “operations and maintenance.” They may be divided into those associated with operations and those associated with maintenance.

Table 3-3. Items Included in Operations & Maintenance

Class of O&M Cost	
Operations	Maintenance
Local property taxes	Regular scheduled maintenance
Insurance	Unscheduled maintenance
Land lease	Long-term replacement
Project administration	
Local utilities	

A number of sources were used to survey current costs, and the results varied widely, in part because they did not all include the same items and because the circumstances of each information source are always different [16, 17]. In addition, operators are naturally reluctant to disclose information that may be proprietary.

It was especially difficult to obtain data that could help to predict the effect of scale on O&M costs for which it is necessary to separate the effects of age from the effects of size. One source used was a report by Lemming & Morthorst [15].

In order to simplify this situation, the following decisions were made:

- All the operations costs were included in the 10.6% financing charge rate (this was approved by the staff of the NWTC).
- The long-term replacement costs were fixed at \$15.00/kW/year (based on reports from Europe [18]).
- The remaining operations costs were fixed at \$0.008/kWh in accordance with NREL guidelines.

No attempt was made to vary the costs with machine size. It is recognized that different models may affect the trends observed in this study.

3.3 Control Systems

The cost of the control and protection system must include the cost of the necessary sensors, the microprocessor, and the housing and interface equipment. The cost of the development and testing is not included here.

These costs are affected very little by the size of the machine, which is reflected in the formula quoted in Table 3-2.

3.4 Cost of Energy Model

The formula used to calculate the cost of energy was specified by NREL and is given below.

$$\text{COE} = \frac{(\text{FCR} \times \text{ICC}) + \text{LRC}}{\text{AEP}_{\text{net}}} + \text{O\&M}$$

- where
- COE = Levelized cost of energy (\$/kWh)
 - FCR = Fixed charge rate (0.106 /yr was used)
 - ICC = Initial capital cost (\$)
 - LRC = Levelized replacement cost (\$/yr)
 - AEP_{net} = Net annual energy production (kW/yr)
= AEP_{gross} adjusted for availability, array losses, soiling, etc.
 - O&M = Operating and maintenance cost (\$/kWh)

4. TASK #2. BASELINE DESIGNS

The objective of Task #2 was to generate designs for four wind turbines with ratings from 750 kW to 5.0 MW and to use these designs as standards to which later designs could be compared. Because the baseline designs did not involve unusual features, the FAST_AD code was initially used to generate results. However, ADAMS models were developed for some of the turbines, and results from the two sets of models were compared. It became apparent that some loads did not agree, and finally all turbines were analyzed using ADAMS. More details concerning this comparison are given in Section 4-2.

4.1 Basic Specifications

An initial set of configurations and the rationale for them were presented to NREL staff at the kick-off meeting in August 2000. These configurations were used in Task #2 until, in December 2000, the NREL project monitor questioned whether those specifications represented the class of rotor that was of most interest. The discussion that ensued resulted in the adoption of a second set of specifications and a second series of simulations and design evaluations. The two sets of specifications are listed in Table 4-1.

Table 4-1. Initial and Final Overall Specifications

Parameter	Initial Specification	Revised Specification
Design wind regime	IEC class 1	IEC class 2
Rated tip speed	65 m/s	75 m/s
Hub height	1.3 x rotor diameter	1.2 x rotor diameter
Rotor diameters (m)	46.6, 66.0, 93.0, 120.0	50.0, 70.0, 99.0, 128.0
Hub heights (m)	61.0, 86.0, 121.0, 156.0	60.0, 84.0, 119.0, 154.0
Ratings (kW)	750, 1500, 3000, 5000	750, 1500, 3000, 5000

4.2 FAST_AD vs. ADAMS Results

The initial intention was to use the FAST_AD code for all of Task #2 and for as much as possible of Task #3. Therefore, Task #1 included the addition of a suitable PID controller routine into FAST_AD, and a number of additional output signals were added to FAST_AD in Task #2.

Comparisons were made between equivalent FAST_AD and ADAMS models, and it was noticed that the results for axial and shear forces from FAST_AD were erratic and did not compare well. It was agreed that the axial and shear force results from FAST_AD should not be used in design. Later it was found that the tower base bending moments from FAST_AD were also substantially different from the ADAMS model results. The cause and resolution of the discrepancies were developed by Windward Engineering, but it was decided that all subsequent analyses in Task #2 would be made using ADAMS. The improved version of FAST_AD was used in a number of analyses in Task #3.

4.3 Annual Energy Production

For each blade design and schedule, the PROP code [14] was used to generate a table of power-coefficient against tip-speed ratios. This table was incorporated into a spreadsheet to calculate total annual energy production (AEP) under specified wind regimes, which were functions of the wind at the reference height of 10 m and the tower height. Sea-level density and the specified drive train efficiencies were used in the calculation of AEP, and the following additional losses were included:

- Availability 95%
- Blade soiling losses 2%
- Array losses 5%

The AEP calculation assumed sharp transitions in the power curve with no smoothing.

4.4 Material Properties

The static strength, the fatigue strength details, and the partial safety factors used in the principal components are listed in Table 4-2.

Table 4-2. Material Properties Used in Design of Major Components (Task #2)

Component	Material	Stress Ratio	Static Design Strength/ Strain	Fatigue Design SN Slope	Partial Safety Factor, Material (including consequences of failure factor)	
					Static	Fatigue
Blade	Fiberglass	R=0	7586 $\mu\epsilon$	m = 8.0	2.9	1.93
		R=-1	3620 $\mu\epsilon$	m = 13.0	2.9	1.93
		R=10	3620 $\mu\epsilon$	m = 16.0	2.9	1.93
Hub	Ductile iron		Yield stress = 310 Mpa	m = 16.8	1.1	1.25
Shaft	HS steel		Yield stress = 828 Mpa	m = 6.5	1.1	1.25
Mainframe	Ductile iron		Yield stress = 310 Mpa	m = 16.8	1.1	1.25
Tower	Structural steel		Yield stress = 350 Mpa	BS 7608 class D m = 3	1.1	1.25

4.5 Pitch Control System

All rotors used full-span collective pitch control to maintain constant rotor speed above rated wind speed. Details of the pitch controller are provided in Appendix E.

A torque-speed look-up table was provided to the simulation, which maintained the rotor operating at maximum power coefficient in the variable-speed range. Above the rated torque value, the look-up table provided a near-constant torque with increasing rotor speed. Once the specified maximum speed or maximum power was reached, the rotor no longer operated at peak efficiency, and the blades were pitched to maintain the specified maximum speed.

The pitch control system was provided with maximum and minimum values of the pitch angle. The minimum was chosen for peak aerodynamic efficiency, and the maximum value was set at approximately 90 degrees (corresponding to fully feathered). The pitch rate was limited to 10 degrees/second.

4.6 Results from Design Process

Table 4-3 contains results of the configurations adopted for the four baseline machines. The corresponding costs, energy production, and the cost of energy are presented in Table 4-4 and are summarized in Figure 4-1.

Table 4-3. Characteristics of Final Baseline Configurations

	Units	750 kW	1.5 MW	3.0 MW	5.0 MW
File Name		.75A08C01V00c	1.5A08C01V03c Adm	3.0A08C01V02c	5.0A04C01V00c
Rotor diameter	m	50	70	99	128
Max rotor speed	rpm	28.6	20.5	14.5	11.2
Max tip speed	m/s	75	75	75	75
Rotor tilt	degrees	5	5	5	5
Blade coning	degrees	0	0	0	0
Max blade chord	m	8% of radius	8% of radius	8% of radius	8% of radius
Radius to blade root	m	5% of radius	5% of radius	5% of radius	5% of radius
Blade mass	kg	1818	4230	12,936	27,239
Rotor solidity		0.05	0.0500	0.05	0.05
Hub mass	kg	5086	15,104	50,124	101,014
Total rotor mass	kg	12,381	32,016	101,319	209,407
Hub overhang	m	2.330	3.300	4.650	6.000
Shaft length x diam	m	1.398 x 0.424	1.980 x 0.560	2.790 x 0.792	3.600 x 1.024
Gearbox mass	kg	4723	10,603	23,500	42,259
Generator mass	kg	2946	5421	10,371	16,971
Mainframe mass	kg	5048	15,057	45,203	102,030
Total nacelle mass	kg	20,905	52,839	132,598	270,669
Hub height	m	60	84	119	154
Tower base diam x thickness	mm	4013 x 12.9	5663 x 17.4	8081 x 25.5	10,373 x 33.2
Tower top diam x thickness	mm	2000 x 6.7	2823 x 8.7	4070 x 13.0	4851 x 17.6
Tower mass	kg	46,440	122,522	367,610	784,101

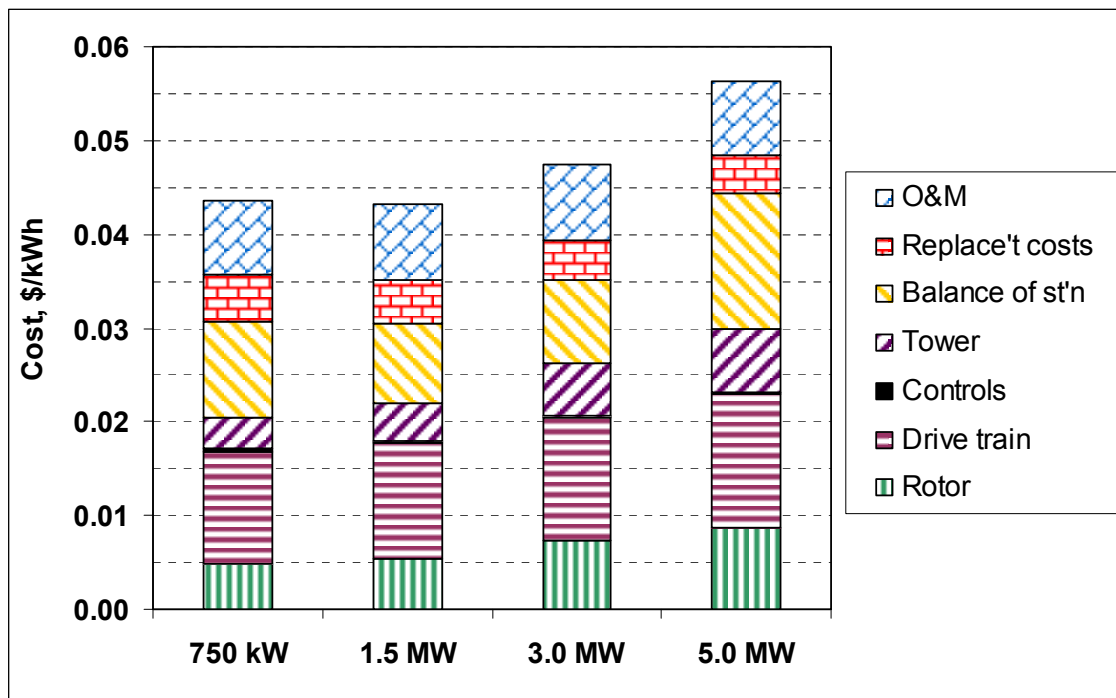


Figure 4-1. Summary of cost-of-energy breakdown for baseline configurations.

Table 4-4. Costs of All Wind Farm Items for Baseline Designs

Rating	kW	750 kW	1.5 MW	3.0 MW	5.0 MW
Rotor	\$	101,897	247,530	727,931	1,484,426
Blades	\$	64,074	147,791	437,464	905,903
Hub	\$	21,617	64,191	213,027	429,307
Pitch mechanism and bearings	\$	16,205	35,548	77,440	149,216
Drive train, nacelle	\$	255,631	562,773	1,282,002	2,474,260
Low-speed shaft	\$	8,433	19,857	56,263	120,903
Bearings	\$	3,794	12,317	41,436	101,834
Gearbox	\$	64,919	150,881	357,224	697,062
Mechanical brake, HS coupling, etc.	\$	1,492	2,984	5,968	9,947
Generator	\$	48,750	97,500	195,000	325,000
Variable-speed electronics	\$	50,250	100,500	201,000	335,000
Yaw drive and bearing	\$	5,268	12,092	28,213	109,705
Main frame	\$	21,452	63,992	192,115	433,627
Electrical connections	\$	30,000	60,000	120,000	200,000
Hydraulic system	\$	3,375	6,750	13,500	22,500
Nacelle cover	\$	17,898	35,901	71,283	118,682
Control, safety system	\$	10,000	10,200	10,490	10,780
Tower	\$	69,660	183,828	551,415	1,176,152
Balance of station	\$	217,869	388,411	873,312	2,458,244
Foundations	\$	34,919	48,513	76,765	108,094
Transportation	\$	26,586	51,004	253,410	1,312,150
Roads, civil works	\$	44,896	78,931	136,359	255,325
Assembly and installation	\$	24,374	50,713	112,714	224,790
Electrical interface/connections	\$	71,304	126,552	224,196	431,500
Permits, engineering	\$	15,790	32,698	69,868	126,385
Initial capital cost (ICC)	\$	655,057	1,392,741	3,445,150	7,603,862
Initial capital cost (ICC)	\$/kW	873	928	1,148	1,520
Net annual energy production	kWh	2,254,463	4,816,715	10,371,945	18,132,994
Rotor	¢/kWh	0.477	0.543	0.741	0.864
Drive train	¢/kWh	1.197	1.234	1.305	1.441
Controls	¢/kWh	0.047	0.022	0.011	0.006
Tower	¢/kWh	0.326	0.403	0.561	0.685
Balance of station	¢/kWh	1.021	0.852	0.889	1.432
Replacement costs	¢/kWh	0.499	0.467	0.434	0.414
O&M	¢/kWh	0.800	0.800	0.800	0.800
Total COE	¢/kWh	4.367	4.321	4.741	5.642

Table 4-5 shows how some of the key loads vary with rotor diameter. Most loads that are due mainly to aerodynamic forces vary approximately with the diameter to the power of 3.0; this agrees with simple estimates. Loads that involve gravity forces vary with the diameter to a greater power, which also is in keeping with expectations. For comparison, the energy yield of these systems varies with the diameter to the power 2.2, which is greater than 2.0 due to the increase in tower height and mean wind speed.

There is a considerable difference in the dependence on rotor diameter for the flapwise and edgewise fatigue loads at the blade root. This leads to the trend of larger blades being governed by edgewise gravity forces in place of aerodynamic flapwise forces. Figure 4-2 illustrates how, for this series of baseline designs, the edgewise fatigue loading becomes critical between the 3- and the 5-MW sizes.

Table 4-6 shows critical load cases for each component. It also shows the next critical load case and the available margin for that loading.

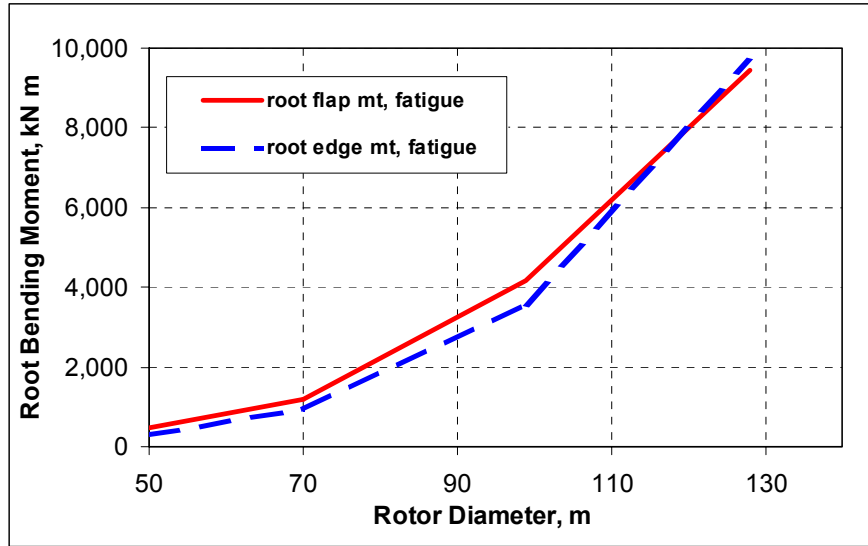


Figure 4-2. Variation of root flapwise and edgewise moments with diameter.

Table 4-5. Trends from Baseline Designs: Dependence on Diameter

Load	Exponent of Diameter in Trend Line	
	Peak Loads	Equivalent Fatigue Loads
Root flapwise bending moment	2.911	3.192
Root edgewise bending moment	3.362	3.645
50% span flapwise bending moment	2.946	3.053
50% span edgewise bending moment	3.460	3.464
Pitching moment at yaw bearing	3.317	2.924
Fore-aft bending at tower base	3.266	2.959

Table 4-6. Critical Load Cases for Baseline Turbines

Component		Machine rating			
		750 kW	1.5 MW	3.0 MW	5.0 MW
		.75A08C01V01c	1.5A08C01V04c	3.0A08C01V03c	5.0A01C01V01c
Blade root	governing load	EWM	EWM	Fatigue (TE)	Fatigue (TE)
	Next critical load margin to that load	Fatigue 2%	Fatigue 11%	EWM 1%	EWM 25%
Blade @ 50% (flapwise mt)	governing load	Fatigue	Fatigue	Fatigue	Fatigue (TE)
	Next critical load margin to that load	EWM 19%	EWM 45%	EWM 30%	EWM 31%
Hub (blade root mt)	governing load	Fatigue	Fatigue	Fatigue	Fatigue
	Next critical load margin to that load	EWM 41%	EWM 67%	EWM 68%	EWM 76%
Mainframe (pitch bending)	governing load	Fatigue	Fatigue	Fatigue	Fatigue
	Next critical load margin to that load	ECD 50%	ECD 27%	NTM 60%	ECD 10%
Tower base (fore-aft mt)	governing load	Fatigue	Fatigue	Fatigue	Fatigue
	Next critical load margin to that load	EWM 12%	EWM 35%	EWM 84%	EOG 21%

Note: For the meaning of the loading acronyms, see Table 2-2.

TE indicates Trailing Edge (associated with edgewise bending in contrast to flapwise bending).

4.7 Campbell Diagram

Figure 4-3 shows the predicted natural frequencies vs. rotor speed for the baseline model of the 1.5-MW configuration. The figure also shows the harmonic frequencies at 1P, 3P, and 6P and also shows the maximum operating speed of the rotor (20.5 rpm). The diagram shows the fundamental fore-aft mode to be close to the 1P excitation and also that the first blade mode is close to the 3P excitation at the maximum operating speed.

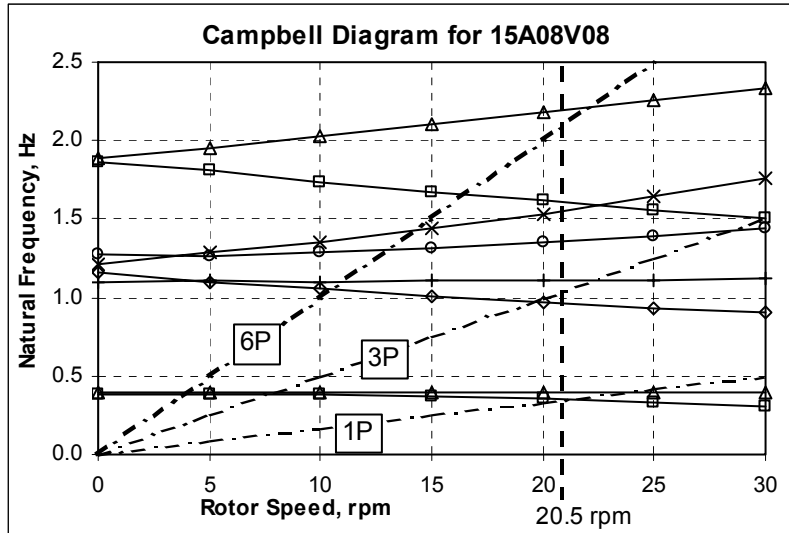


Figure 4-3. Natural frequencies vs. rotor speed (Campbell diagram) of baseline 1.5-MW model.

4.8 Conclusions from Baseline Study

The study of the baseline configuration at the range of sizes has led to the following observations:

- The rotor cost comprises between 10% and 15% of the total cost of energy. A change of 10% in the rotor cost will therefore translate into only 1% to 1.5% change in the COE.
- There are considerable costs that are affected only slightly or not at all by load variation. These include some electrical drive train costs and balance-of-station costs. Approximately 50% of the total costs are unaffected by changes in rotor loads.
- Considerable reductions in COE may still be achieved by rotor changes if the load reductions affect the entire load path.
- The rotors of the larger machines represent higher fractions of the total costs. This is because the mass and cost of the rotors increase with diameter faster than other costs, such as balance-of-station costs. Improvements in rotor design will, therefore, benefit larger turbines more than smaller turbines.

5. TASK #3. CONFIGURATION VARIATIONS

The purpose of Task #3 was to determine the effect on COE of changes to the rotor configuration. These changes were to the type of rotor (3 blades/2 blades, etc.) and to details of the rotor, such as the tip speed or the stiffness of the blade. The objective was to identify those configurations that had the most beneficial effect on COE and to determine how these effects were influenced by scale or rating. The changes were made one at a time so that, within a certain range, their effects could be superimposed.

5.1 Initial Matrix

Table 5-1 shows the list of configurations initially considered, requiring a total of 58 designs to be evaluated. It became apparent that resource limitations would prevent a thorough analysis of this number of configurations, and a process was therefore begun to reduce that number to a more manageable one.

5.2 Selection Approach

A questionnaire was sent to staff at the NWTC, at GEC, at Woodward Engineering, and to participants at the WindPACT Workshop (in October 2000), to solicit opinions about what configurations were expected to be the most cost effective and what configurations might be deleted from consideration. The results of that survey indicated that the following were not favored: pitch-to-stall rotors; those with constant speed, teetered hubs with delta-3; or stiff towers. The decision was made to eliminate those options and also to remove the simulations at all four ratings for the three non-baseline configurations. It was agreed that the simulations of the reduced number of configurations of 1.5-MW rating should be followed by a study of the effect of certain selected configurations, or combination of configurations, on the range of ratings.

The list of final configurations included upwind and downwind machines, although the preferred configurations tended to be the 3-bladed upwind and the 2-bladed downwind. This is reflected in the diagram of final selections illustrated in Figure 5-1 and in the accompanying list shown in Table 5-2.

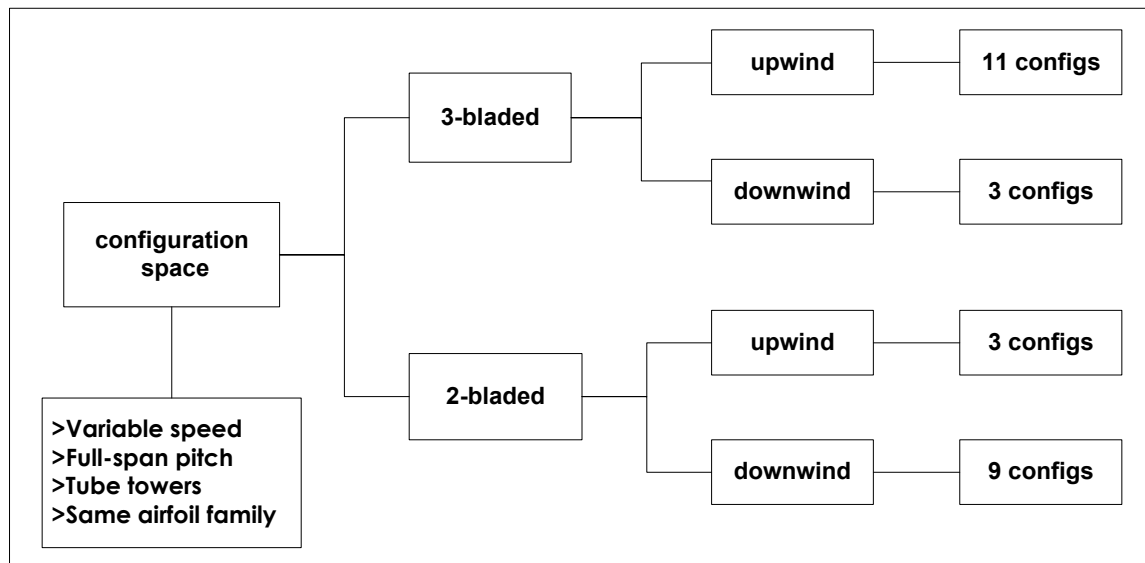


Figure 5-1. Rotor configurations selected.

Table 5-1. Initial Table of Configurations for Examination in Task #3

Rotor size (1.5 MW or all)	Number of blades	Orientation: upwind (Up) or downwind (Down)	Hub type: rigid (R), teeter (T), flapping hinge (F), teeter with d3 (Td)	Blade type: regular (R) or soft (S)	Fixed pitch (F), pitch to feather (PF), pitch to stall (PS)	Tip speed: standard (S) or modified (M)	Diameter: standard (S) or modified (M)	Variable (VS) or constant speed (CS)	Tower stiffness: soft-soft (SS) or soft (S)	Tower feedback to pitch control	Yaw drive: active (A) or free (F)	Model: FAST_AD (F) or ADAMS (A)	Number of new models (not incl. struct. iterations)
All	3	Up	R	R	PF	S	S	VS	S	No	A	F	4
1.5						S	M						1
						M	S						1
1.5							S	VS, CS					2
								VS	SS	Yes			1
									SS, S,	No			2
				S	F, PF				S				2
All	3	Down	R	R	PF	S	S	VS	S	No	A	F	4
1.5			R	R, S	F, PF, PS				SS	Yes			6
			F	R	PF, PS				S	No		A	2
			R		PF						F	F	1
All	2	Up	T	R	PF	S	S				A	F	4
1.5						M							1
						S	M						1
				R, S	PF, PS		S	VS	S				4
				R	F			VS					1
					PF				SS	Yes			1
				S					S	No			1
All	2	Down	T	R	PF	S	S	VS	S	No	F	F	4
1.5				R, S	F, PF, PS				S	No			6
				R	PF	M							1
						S	M						1
							S		SS	Yes			3
			Td		F				S	No	F		1
			F		F, PF, PS							A	3
1.5	5	Down	R		F, PF						A	F/A	2
Total												58	

Note: A blank cell indicates that it is unchanged from the cell above.

Table 5-2. Configuration Modifications Chosen for Study in Task #3

ID Letter	No. of Blades	Rotor Orientation	Feature Modified	Comments	Results Summary
A	3	Upwind	Baseline		
B	3	Upwind	12% increase in rotor diameter	Blade dimensions were increased by same ratio	Loads in and cost of rotor increased as expected. Other loads also increased
C	3	Upwind	13% increase in tip speed	Blade was unchanged from baseline	Gearbox cost reduced, but all other loads and costs up
D	3	Upwind	feedback from tower motion in control system	See Appendix E	Tower loads and cost down significantly. Other loads largely unchanged
E	3	Upwind	soft-soft tower, feedback from tower, and increased tip speed	Achieving a soft-soft tower led to a very thick tube. In E02, the soft-soft tower (with no other changes) was achieved by reducing the elastic modulus of the tower material	Tower for config. E very expensive. In config. E02, most loads were higher than in baseline
F	3	Upwind	stiff blades	Added stiffness was achieved through the use of carbon fiber in the spar	Loads generally unchanged. Lighter rotor led to greater rpm fluctuations
G	3	Upwind	blades with flap-twist coupling	The stiffness matrices in the ADAMS models were adjusted (see Ref. [25]) to incorporate an "alpha" value of approximately 0.17	Most loads were reduced significantly
H	3	Upwind	flap-pitch feedback in control system	An attempt to incorporate the algorithm from Ref. [26]. Root flap mt from each blade compared to mean from all three blades	Costs of all components were increased slightly
X	3	Upwind	increased tip speed, reduced chord, high-strain blade material	Material as in config. Y. Tip speed increased to 85 m/s. Max chord reduced from 8% to 6% of radius	Significant decrease in the loads in all components
Y	3	Upwind	high-strain blade material	Prepreg fiberglass has greater quality control; permissible strains are higher; fatigue SN curve is flatter	Lower flapwise fatigue loads in blade. Reduced rotor cost but other costs unchanged
J	3	Downwind	intermediate baseline	Similar to A but downwind with tower shadow	All loads and costs up slightly
K	3	Downwind	soft blades	Material as in configuration Y	Blade softness reduced most blade loads and tower loads
L	3	Downwind	hinged blades	Flapwise hinges installed at blade roots, together with necessary restraints to ensure tower clearance	Most blade loads reduced, but hub cost difficult to estimate. Tower clearance a potential problem.
M	2	Upwind	intermediate baseline	Max chord = 10% of radius	Rotor cost much reduced from 3-bladed baseline
N	2	Upwind	12% increase in diameter	Similar to configuration B	All loads up, especially those due to teeter restraint
P	2	Upwind	13% increase in tip speed	Similar to configuration C	Slight increase in rotor loads and cost
Q	2	Downwind	intermediate baseline	All downwind configurations incorporated free yaw	All rotor loads increased from upwind case
R	2	Downwind	soft blades	High strain blade material, as in Y	Hub and nacelle loads increased due to higher teeter restraint forces
S	2	Downwind	12% increase in diameter	Similar to configuration B	Higher rotor loads and cost balance increase in AEP
T	2	Downwind	13% increase in tip speed	Similar to configuration C	Higher loads and higher final COE
U	2	Downwind	feedback from tower included in control system	Similar to configuration D	Tower loads reduced and other loads unchanged
V	2	Downwind	positive delta-3	For details of delta-3 feature, see Ref. [27]	Some loads reduced but final COE unchanged
W	2	Downwind	hinged blades	Flapwise hinges in each blade at root, together with necessary restraints for tower clearance	High blade root loads required to avoid tower strike. More sophisticated analysis and design needed

5.3 FAST_AD vs. ADAMS

As described earlier (Sections 2-3, 4-2), two simulation codes were used: FAST_AD, and ADAMS. Care was taken to compare results only from the same code.

5.4 Results from Task #3

Details of the loads from selected locations from all the configurations studied are presented in Table A-1 (Appendix A). In that table, the loads have been normalized with respect to appropriate baseline models to allow quick and meaningful evaluation. Some analyses were carried out using ADAMS and some using FAST_AD. This is noted, and the relevant normalization basis was selected.

Table A-2 refers to the same load locations but gives the governing load case and the margin to the next critical load case. Table A-3 presents cost information from all subassemblies for all configurations. It includes the net annual energy production and the COE from each major assembly, as well as the final COE.

Some of the important results of the configuration changes are included in Table 5-2. The final cost of energy from all the configurations is summarized in Figure 5-2. Figures 5-3 and 5-4 graphically present some of the same COE information but separate the 3- and 2-bladed results and show the COE changes relative to the baseline models. Figures 5-5 and 5-6 present similar COE information according to subassembly.

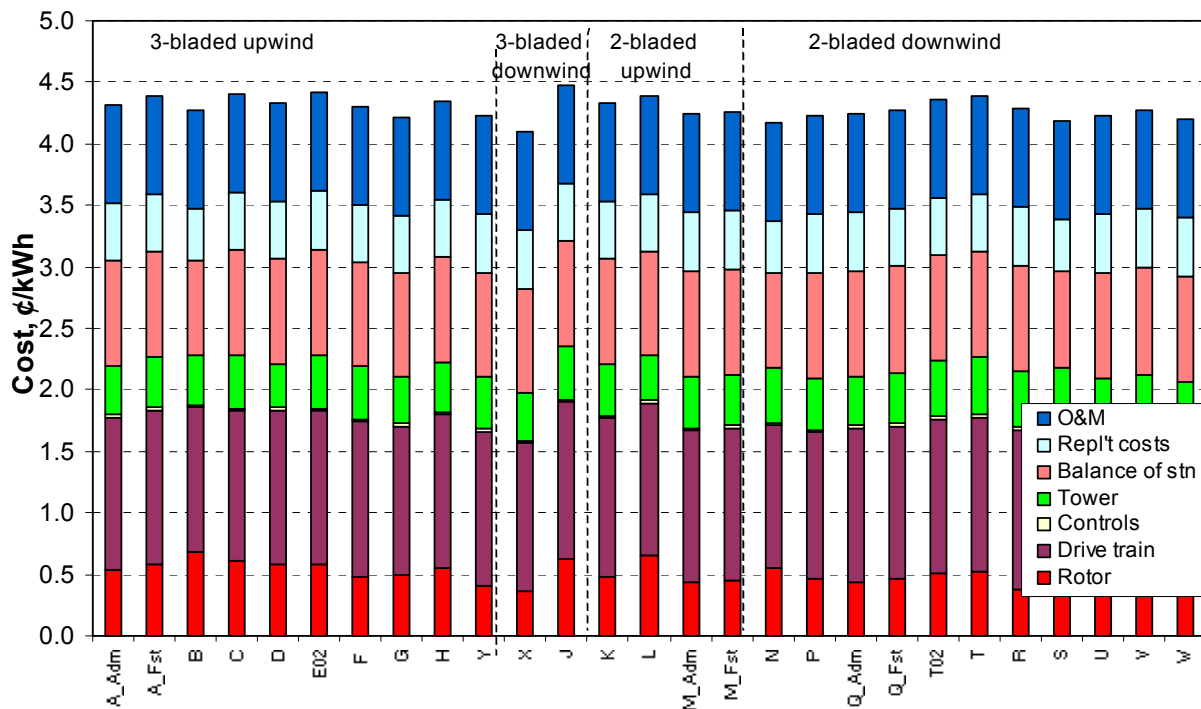


Figure 5-2. Summary of cost of energy from all Task #3 configurations.

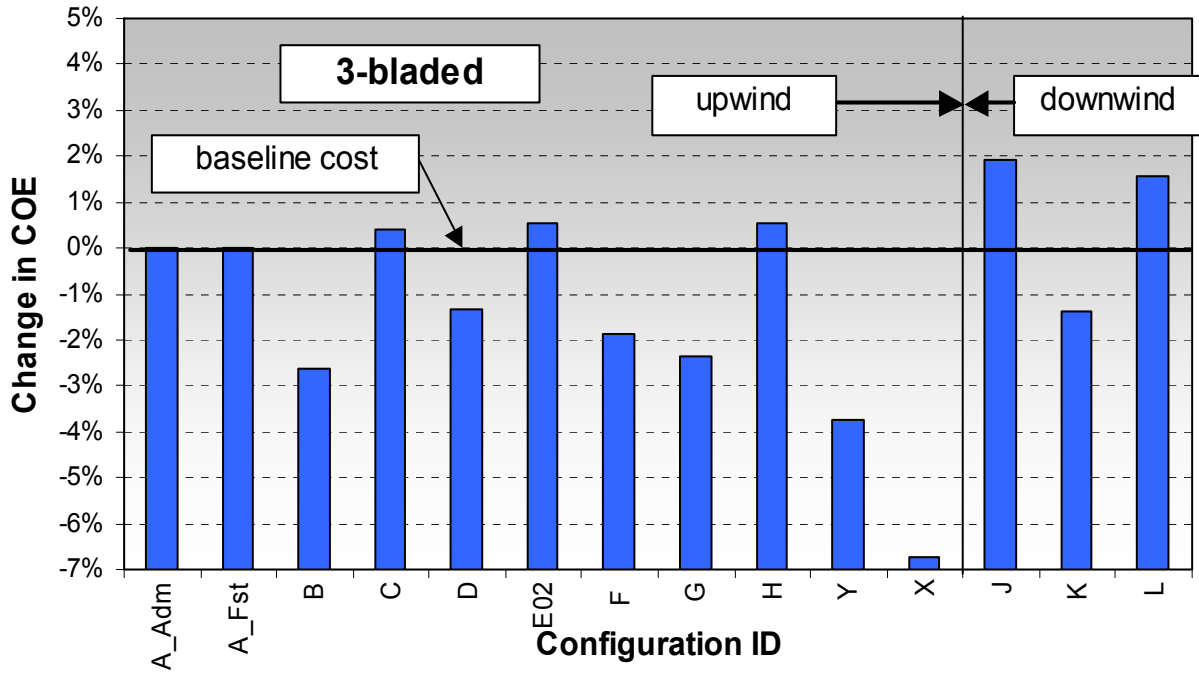


Figure 5-3. Cost-of-energy changes for 3-bladed configurations.

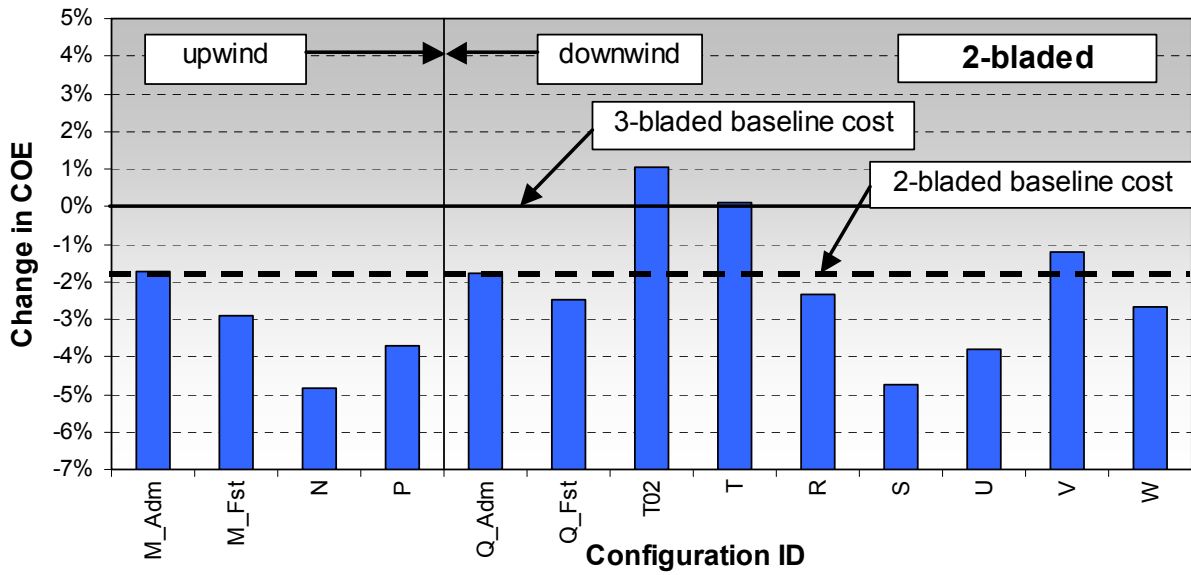


Figure 5-4. Cost-of-energy changes for 2-bladed configurations.

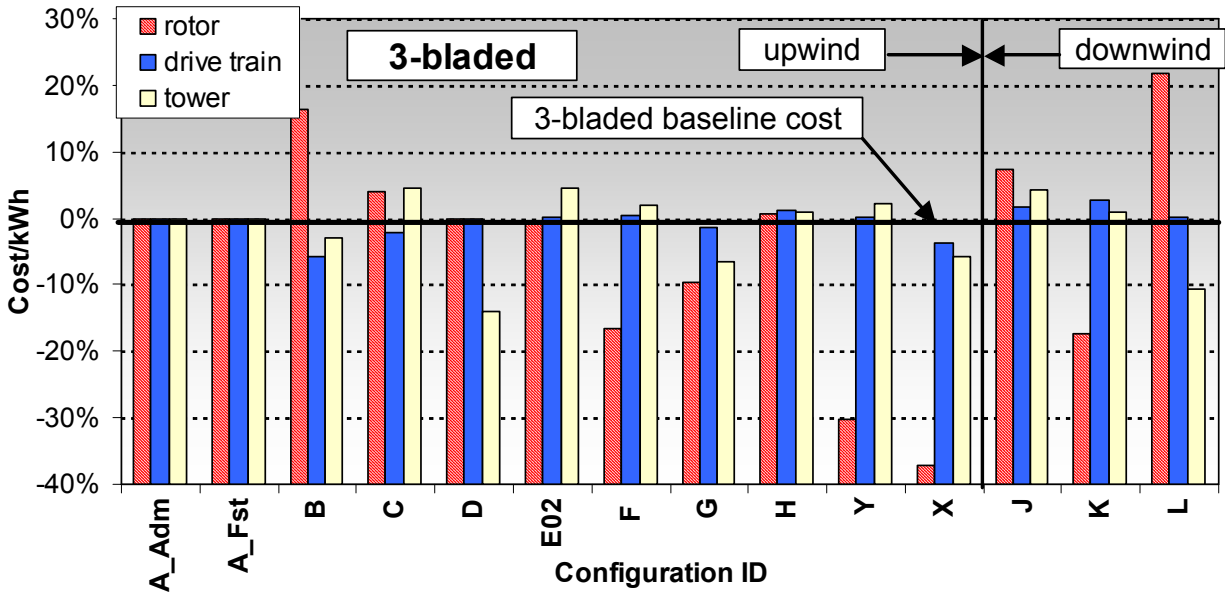


Figure 5-5. Summary of component costs for 3-bladed configurations.

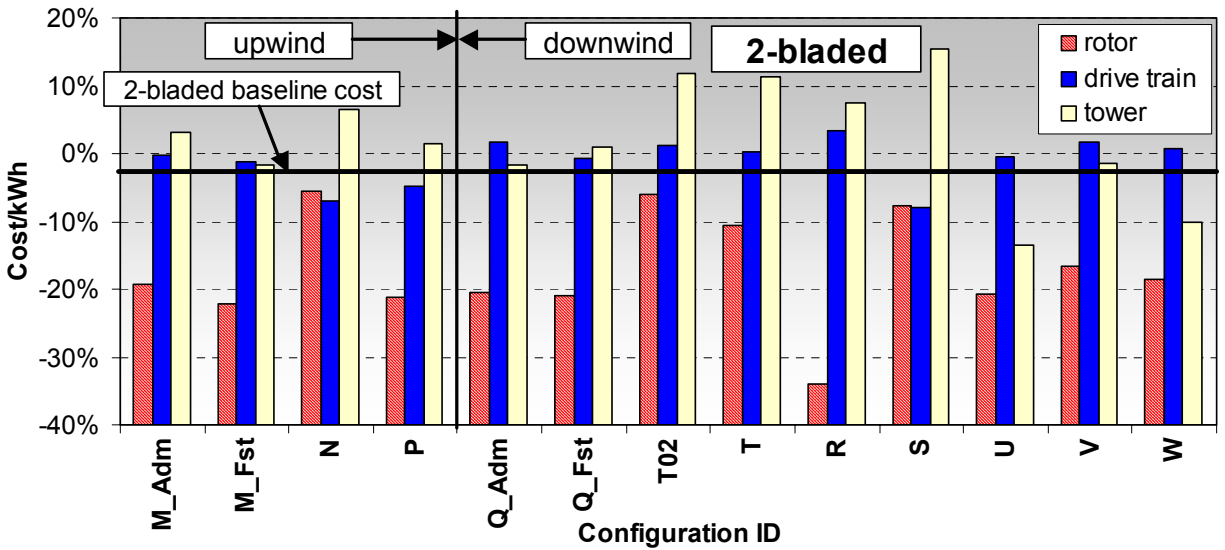


Figure 5-6. Summary of component costs for 2-bladed configurations.

5.5 Observations from Task #3 results

A number of principles should be kept in mind when evaluating the Task #3 results presented above.

- The results should be regarded as indicating trends rather than absolute values.
- Some of the trends can be applied in either direction. For example, the effects of decreasing the tip speed can be considered to be the opposite of the effects of increasing the tip speed.
- Some results may not be realizable. For example, configurations X and Y show considerable cost reductions but also have blade-tower interference problems. In addition, the manner in which the flap-twist coupling would be implemented in configuration G and the cost involved have not been fully determined. Furthermore, the higher tip speeds adopted in configurations C and X may lead to unacceptable acoustic emissions.
- Comparisons must be done using the same aeroelastic code. The differences between the two codes are of the same order as the differences between the configurations.
- Several of the modifications need to be optimized for best performance. For example, the tower feedback in the controls could be refined for improved results.

The following conclusions were drawn from the Task #3 results:

- The final cost of energy is much more sensitive to the energy capture than it is to changes in the loads. The approximately 2% energy loss associated with changing from three to two blades (due to tip losses) is significant.
- All of the basic configurations (upwind/downwind, 3-/2-bladed) are affected in a similar manner by some modifications. These include changes to the tip speed, the diameter, and tower feedback.
- The analysis of the rotors with hinged blades (configurations L and W) requires much care because the results are very sensitive to the restraints offered to the flapping motion. A more complete analysis should give more attention to the transient conditions, such as emergency stops. Nevertheless, the load reductions obtained from these configurations did not exceed those that were offered by other modifications, and these configurations were not selected for further study in Task #5. This omission was not intended to detract from current attempts at commercializing such rotors; it was a reaction to the rigorous demands of this configuration.
- Two-bladed teetered rotors are also sensitive to transients and peak load conditions because the restraining force from the teeter restraints may occur at these times. Downwind rotors would probably benefit from an increased hub overhang and a tuning of the teeter restraints.
- The incorporation of soft blades (configuration K) did lead to some attenuation of loads. The relationship among tip flexibility, blade materials, and blade weight is not completely clear.
- Although increasing the tip speed alone had deleterious effects (configuration C and P), the combination of increased tip speed with decreased blade chord (configuration X) had considerable benefits. The interpretation of these results is that it is more efficient for a blade of lower solidity to move faster and to do the same mechanical work with lower loads.
- The following features were recommended for further study in Task #5 in all three basic configurations (3-bladed upwind, 2-bladed upwind, and 2-bladed downwind):
 - Tower feedback
 - Reduced chord with increased tip speed
 - Flap-twist coupling.

6. TASK #5. DETAILED MODELING

6.1 Approach

The purpose and approach of Task #5 was discussed and finalized at the Preliminary Design Review (PDR) meeting. The decision was made to consider separately the three basic configurations (3-bladed upwind, 2-bladed upwind, and 2-bladed downwind) because the results of Task #3 showed that the COE from all three could be improved by similar modifications. The most promising features identified in Task #3 were to be combined and applied to the three basic configurations at the 1.5-MW size. The effect of size would also be examined.

In addition, it was agreed at the PDR that the cost models would be reviewed and that the power curve implied by the simulations would be compared with the results from aerodynamic models using the PROP code.

6.2 Cost Models

A review of the cost models resulted in the changes listed in Table 6-1.

Table 6-1. Changes Made to Cost Models for Task #5

Component	Change in Cost or Design Model
Hub	Scale factor reduced to give hub weights and costs more consistent with a range of commercial data. This was applied to the spherical hub of the 3-bladed configurations and a corresponding change was made to the teetered hubs of the 2-bladed rotors.
Nacelle cover	Made dependent on width of nacelle, as well as length. This led to more realistic cost changes due to changes in the hub overhang.
Generator	The cost per kW was reduced from \$65/kW to \$52/kW to reflect costs used in the WindPACT drive train design study.
Power electronics	The cost per kW was reduced from \$67/kW to \$54/kW to reflect costs used in the WindPACT drive train design study.
Foundations	Algorithm adjusted upward to reflect the costs of foundations quoted more recently by Patrick and Henderson.
Blades	A price of \$16.42/kg was adopted for material containing bias-ply carbon fibers. Adjustment was made in the spreadsheets to separate the inboard material (glass fiber) from the carbon-dominated spar and outboard skin.

The same cost model changes were made to the corresponding baseline (Task #2) configurations so that comparisons of the two sets would be valid.

6.3 Preliminary Results

The results from Task #3 indicated that the following features had beneficial effects on loads and costs throughout the turbine system:

- Tower feedback in the control system
- Incorporation of flap-twist coupling in the blade
- Reduced blade solidity in conjunction with higher tip speeds.

There was little problem in implementing the first of these three features because no change was required from its implementation in Task #3. However, the application of flap-twist coupling in the blade used in

Task #3 lacked rigorous modeling of the necessary composites, and there was inadequate information for the accompanying cost models. It was, therefore, decided to delay incorporation of this feature until these deficiencies could be corrected.

The results from studying the third feature, lower solidity and higher tip speed, in Task #3 showed lower loads but at the expense of a negative tower clearance margin. Therefore, in Task #5 some coning was added to the rotor and the extent of the lower solidity was reduced. Models of this 3-bladed upwind configuration, using hand lay-up fiberglass in the blades, indicated continued tower clearance problems and little or no reduction in loads.

To address the problem of blade-tower clearance, the decision was made to change from using fiberglass to the same carbon-glass hybrid that was examined in Task #3 configuration F. It was found that this change permitted the incorporation of the full solidity reduction without any tower clearance problem so long as some coning was added to the blades and a modest addition was made to the hub overhang.

The reduction in loads from combining the tower feedback with the reduced solidity led to a substantial reduction in the tower section and in the tower flexural stiffness. This, in turn, led to a lowering of the fundamental natural frequency of the turbine and to a resonance with the 1P excitation frequency. To address this, while not artificially strengthening some components, the decision was made to reduce the hub height from 84 m to 80 m, thereby restoring the natural frequency to approximately 1.2P.

In parallel with these preliminary results, GEC staff made progress in the modeling of flap-twist blades and their fabrication costs. Work on adaptive blades on behalf of Sandia National Laboratories (Reference [7]) showed that the necessary coupling could best be achieved by incorporation of carbon fibers at 20° to the longitudinal axis. Furthermore, it appeared that the resulting blade could have the required overall flexural stiffness if the off-axis carbon fibers were placed in the skin while the spar was composed of uniaxial carbon-glass hybrid.

Another parallel study for Sandia National Laboratories (Reference [22]) resulted in a procedure to extract the equivalent set of beam properties from a 3-dimensional finite element model of the blade. This meant that the exact lay-up of off-axis and uniaxial fibers could be modeled in ANSYS using the NuMAD interface (Reference [23]), and the equivalent beam properties could be extracted and included in the input file that was, in turn, converted into the ADAMS model.

With these new design tools available, it was possible to combine all three of the chosen features and to ascribe accurate cost models to the blades. It was found that the combination of the three features further reduced the loads in the tower, allowing a smaller section, a softer tower, and allowing the hub height to be restored to 84 m in conjunction with a natural frequency comfortably below the 1P resonance. The models, therefore, also incorporated a soft-soft tower feature.

The elastic twist that occurred due to the blade flap-twist coupling reduced the loads throughout the structure but also slightly reduced the energy captured. The maximum performance coefficient was reduced by up to 4%, which resulted in an annual energy production loss of up to 2%. To balance this effect, the initial twist schedule and the minimum pitch angle were modified so that the addition of the elastic twist during operation resulted in the desired optimum shape and pitch angle. In this manner the AEP was completely restored.

6.4 Results from 3-Bladed Upwind Rotors

Table 6-2 presents a summary of some of the properties of the final 3-bladed configurations developed in Task #5.

Table 6-2. Summary of Properties of the Baseline and Task #5 Final Configurations

		750 kW		1.5 MW		3.0 MW	
		Baseline	Task #5 Final	Baseline	Task #5 Final	Baseline	Task #5 Final
		.75A08C01V 00c	.75AA04C01V 00	1.5A08C01V03 cAdm	1.5AA12C05V 00	3.0A08C01V0 2c	3.0AA02C01V 00
Rotor diameter	m	50	50	70	70	99	99
Max rotor speed	rpm	28.6	32.4	20.5	23.2	14.5	16.4
Max tip speed	m/s	75	85	75	85	75	85
Rotor tilt	Deg	5	5	5	5	5	5
Blade coning	Deg	0	3	0	3	0	3
Max blade chord	M	8% R	6% R	8% R	6% R	8% R	6% R
Blade mass	kg	1818	868	4230	2281	12,936	5463
Rotor solidity		0.05	0.038	0.0500	0.038	0.05	0.038
Hub mass	kg	5086	2464	15,104	8063	50,124	21,270
Total rotor mass	kg	12,381	6063	32,016	17,882	101,319	49,498
Hub overhang	mm	2300	2330	3300	3500	4650	4950
Shaft length x diam	mm	1398 x 424	1398 x 400	1980 x 560	2185 x 560	2790 x 792	3100 x 800
Gearbox mass	kg	4723	4816	10,603	10,083	23,500	22,111
Generator mass	kg	2946	2949	5421	5421	10,371	10,371
Mainframe mass	kg	5048	3689	15,057	12,319	45,203	33,795
Total nacelle mass	kg	20,905	19,143	52,839	45,917	132,598	111,868
Hub height	m	60	60	84	84	119	119
Tower base diam x thickness	mm	4013 x 12.9	3296 x 10.4	5663 x 17.4	4969 x 15.4	8081 x 25.5	6691 x 21.3
Tower top diam x thickness	mm	2000 x 6.7	1525 x 4.8	2823 x 8.7	2461 x 7.6	4070 x 13.0	3280 x 10.2
Tower mass	kg	46,440	29,054	122,522	94,869	367,610	246,992

6.4.1 Campbell Diagram

Figure 6-1 shows the predicted natural frequencies vs. rotor speed for the final Task #5 model of the 3-bladed upwind 1.5-MW configuration. The figure also shows the harmonic frequencies at 1P, 3P, and 6P and shows the maximum operating speed of the rotor (23.2 rpm).

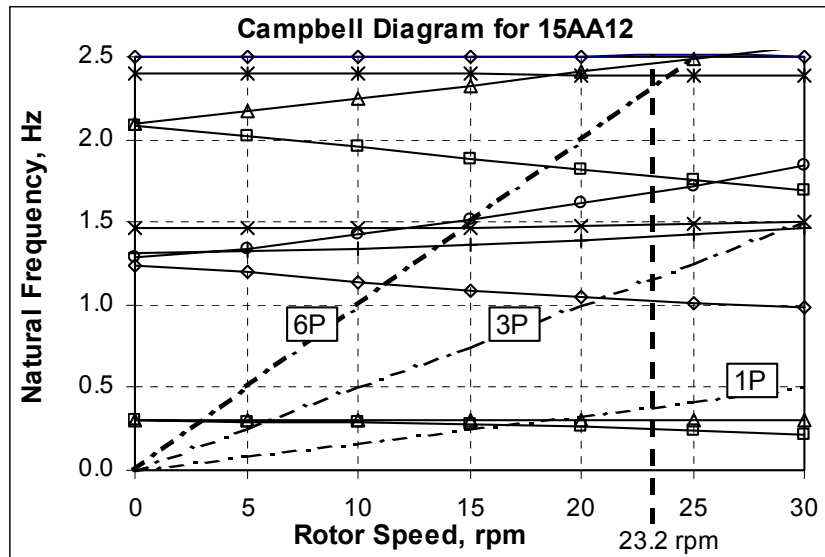


Figure 6-1. Natural frequencies vs. rpm (Campbell diagram) for Task #5 1.5-MW 3-bladed upwind turbine.

6.4.2 Loads

A detailed compilation of system loads for the baseline and final Task #5 3-bladed upwind 750-kW, 1.5-MW, and 3-MW configurations is presented in Appendix B as Table B-1. A sample of these results is shown in Figure 6-2, in which some loads from the 1.5-MW final configuration are compared with the corresponding baseline loads. As well as showing the final peak and equivalent fatigue loads normalized with respect to the baseline loads, Figure 6-1 indicates which load condition governs the baseline and Task #5 final designs.

Figure 6-2 shows considerable reductions in all loads except for the peak loads at the tower base. That load is due to the extreme wind condition on the stationary rotor (EWM), which is unaffected by tower feedback and by flap-twist coupling.

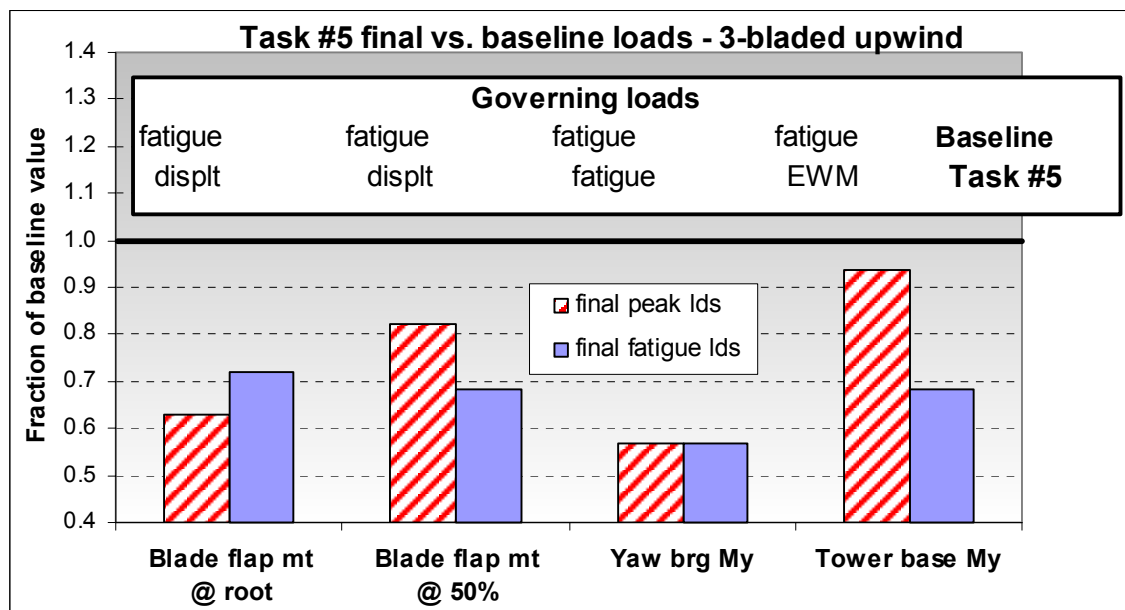


Figure 6-2. Comparison of baseline loads with final Task #5 loads for 1.5-MW 3-bladed upwind turbine.

Table B-5 in Appendix B gives full information on which loads govern the baseline and final designs and how much margin there is to the next most critical load.

6.4.3 Costs

Details of the costs of all components for the baseline and final 3-bladed upwind machines for the 750-kW, 1.5-MW, and 3-MW ratings are included in Table B-2 in Appendix B. The COE data are shown schematically in Figures 6-3 and 6-4.

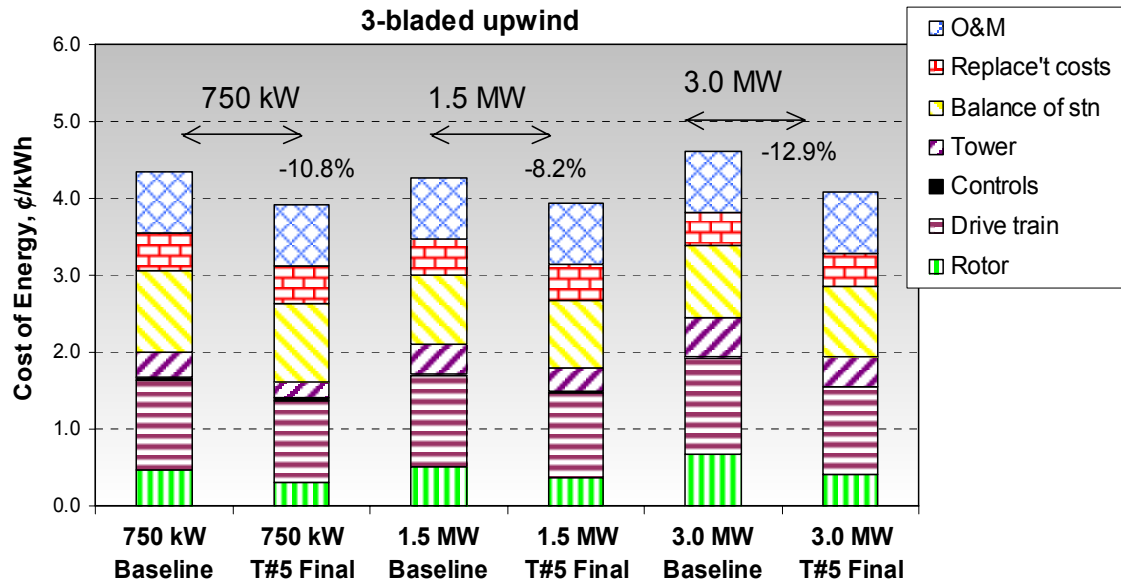


Figure 6-3. Cost of energy of baseline and final 3-bladed 750-kW, 1.5-MW, and 3-MW configurations.

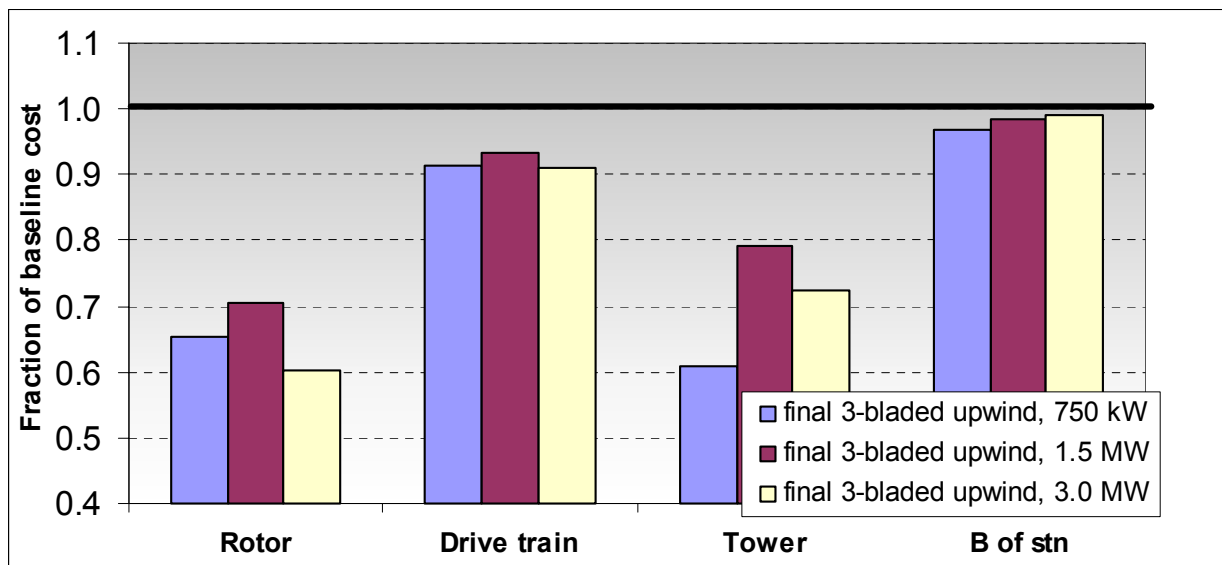


Figure 6-4. Comparison of baseline and final costs of 3-bladed configurations by sub-assembly.

6.5 Results for 2-Bladed Rotors

6.5.1 Loads

A detailed compilation of system loads for the baseline and final Task #5 2-bladed upwind and downwind 1.5-MW configurations is presented in Appendix B as Table B-3. Samples of these results are shown in Figures 6-5 and 6-6, in which selected loads from the final configurations are shown normalized by the corresponding baseline loads. As well as showing the final peak and equivalent fatigue loads, Figures 6-5 and 6-6 indicate what load condition governs the baseline and Task #5 final designs. Figures 6-5 and 6-6 show considerable reductions in peak and fatigue loads, especially to the fatigue load at the tower base.

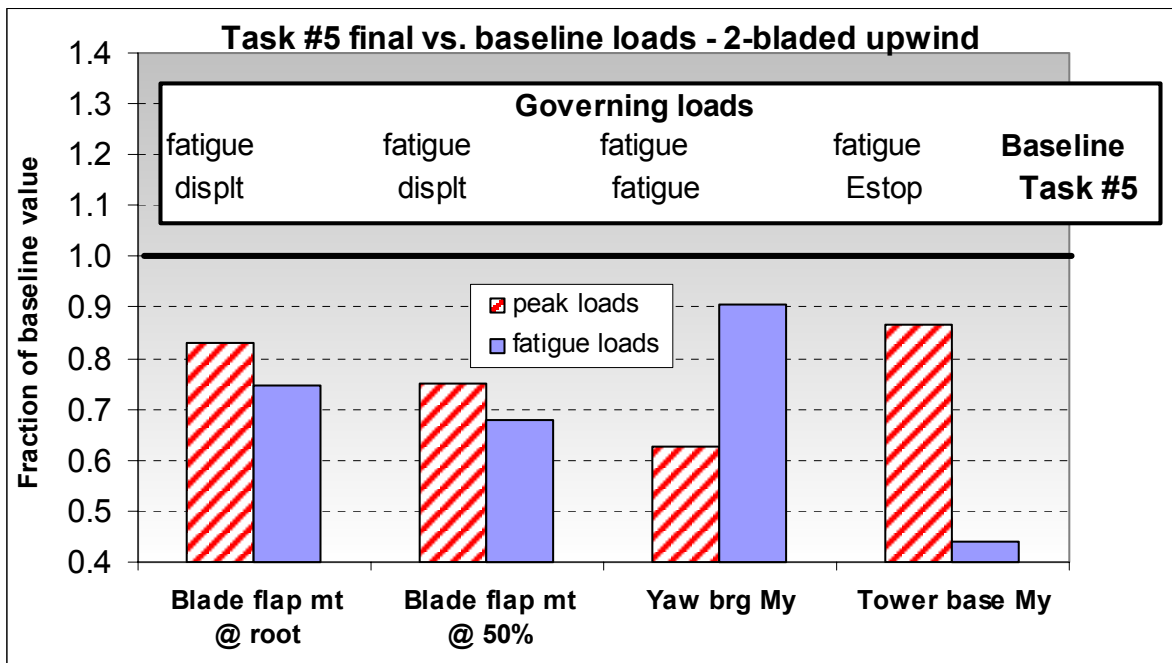


Figure 6-5. Comparison of baseline and final Task #5 loads for 1.5-MW 2-bladed upwind turbine.

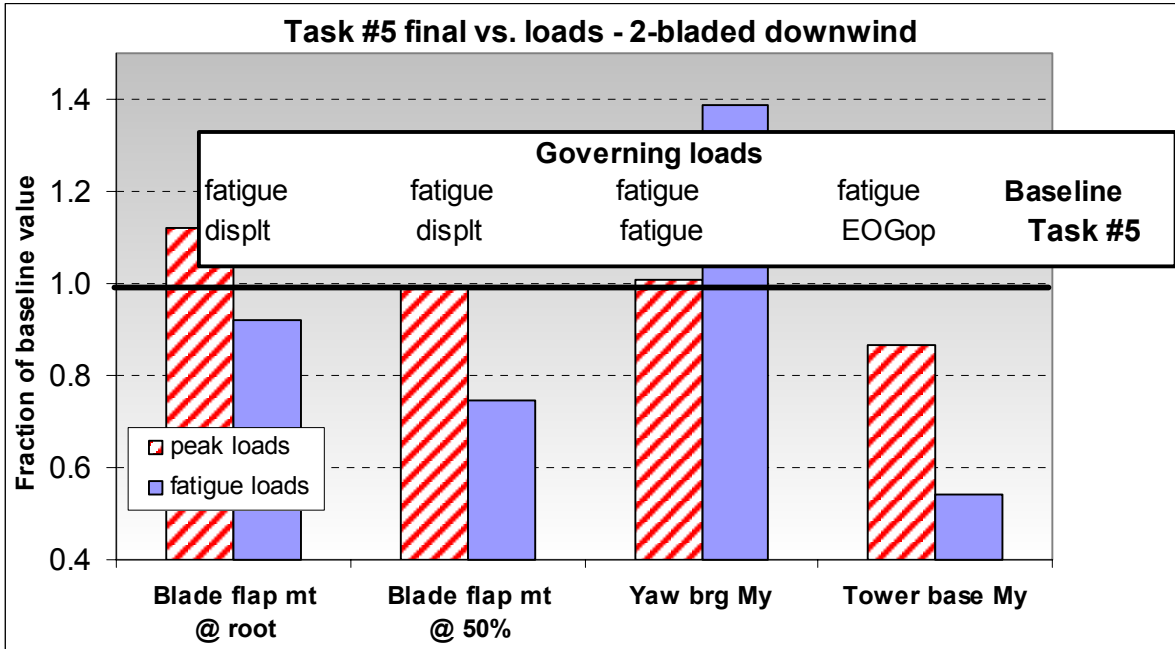


Figure 6-6. Comparison of baseline and final Task #5 loads for 1.5-MW 2-bladed downwind turbine.

6.5.2 Costs

Full details of the costs and cost of energy for the baseline and final 2-bladed 1.5 MW configurations are given in Table B-3 in Appendix B. Summaries of this information are shown in Figures 6-7 and 6-8.

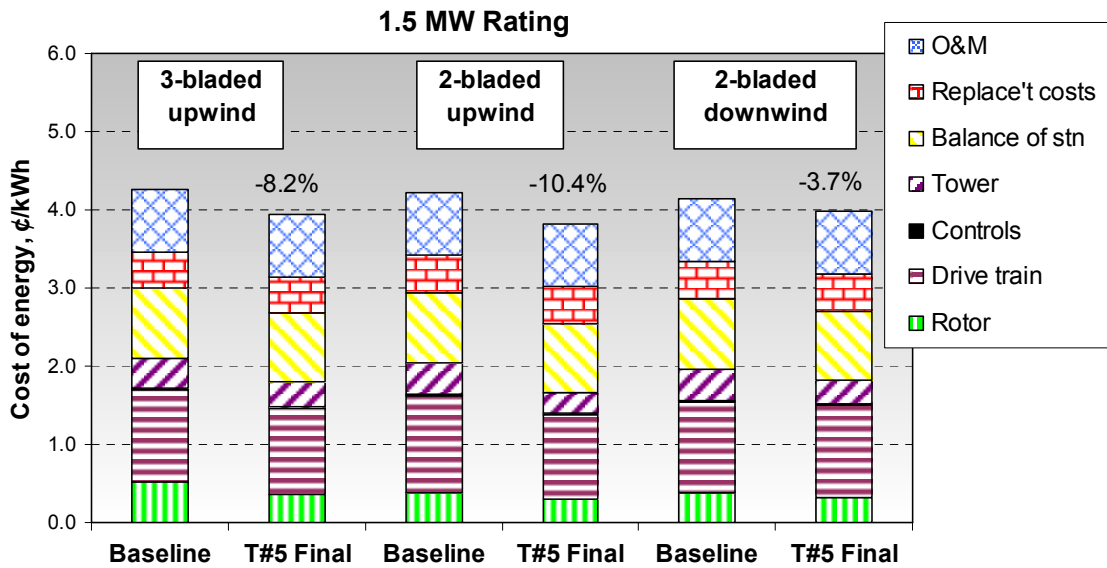


Figure 6-7. Cost of energy for 2- and 3-bladed 1.5-MW configurations.

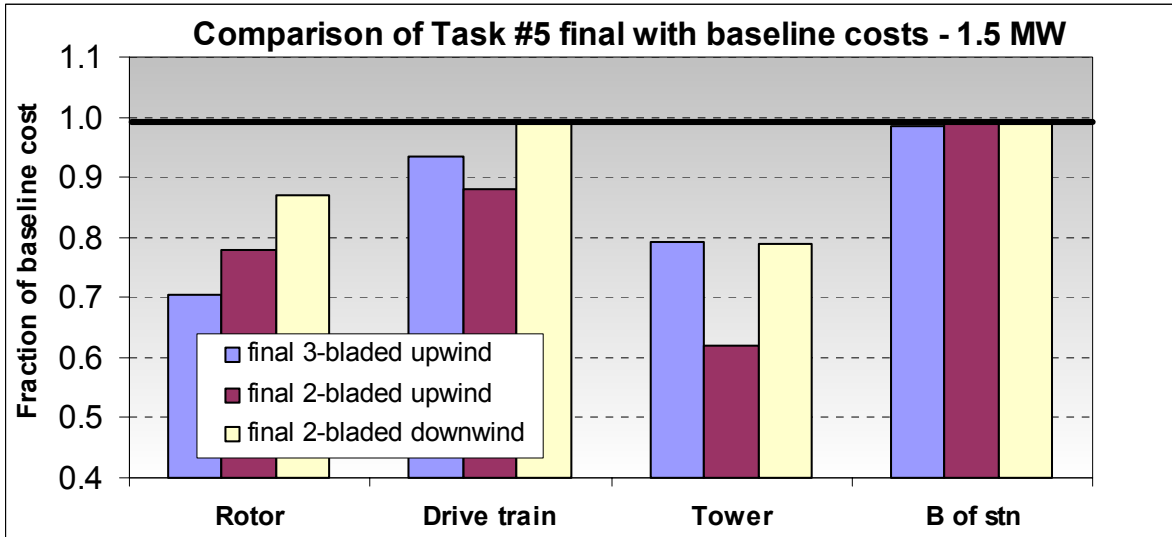


Figure 6-8. Comparison of baseline and final costs of 3- and 2-bladed 1.5-MW configurations by sub-assembly.

6.6 Lessons from Task #5

The following observations can be made from the results presented above:

- The combination of features adopted in Task #5 (tower feedback, flap-twist coupling, and reduced chord with higher tip speed) appears to be effective.
- It has been necessary to incorporate a large amount of carbon fiber in the blade to successfully incorporate flap-twist coupling without incurring blade-tower clearance problems.
- The blades have become governed by stiffness to avoid tower clearance problems. There is an uncertain balance between the cost of blades on one hand and the cost of additional hub overhang and the penalties of added tilt and/or coning.
- There can be an energy loss associated with flap-twist coupling unless the initial twist and the minimum pitch of the blade are corrected.
- Lower COE can be achieved by reducing the chord and increasing the tip speed with attention to the spanwise tapering of the blade. The optimum level for this approach must depend on further investigation of system design, especially the blade design, and must be balanced by consideration of the acoustic penalties.
- It is possible that the inclusion of flap-twist coupling into a 2-bladed, teetered, free-yaw rotor is not as productive as when applied to a rotor with a rigid hub. The reason for this is that a teetered hub uses the 1 per rev loads due to yaw error to teeter into a new direction, which then allows the thrust to realign the nacelle in yaw.
- The downwind 2-bladed rotors also experience strong harmonic loading from the tower shadow, which may excite natural frequencies. The identification of natural frequencies for 2-bladed rotors is more complex than for 3-bladed machines, and there were insufficient resources in this project to develop the Campbell diagram for these configurations.

7. TASK #6. DESIGN BARRIERS

During execution of this project, it became apparent that some costs rose especially steeply with size. In addition, it was difficult to prescribe costs to some designs because they were novel and there was not a reliable base of information. These factors are possible barriers to the increased size of machines or to the reduction of costs of a given rating. They are discussed further in the subsequent sections.

7.1 Transportation

Reference [12] examines in detail the costs and logistics of transporting the various components for large wind turbines. These costs depend on the relative location of the manufacturer of these components and the site of the wind farm; for the current project, a site in the Midwest United States, such as South Dakota, has been assumed.

The items that pose the most transportation problems are the tower sections, the nacelle, and the blades. Movement of these items is limited by weight, length, height, or width. Table 7-1 shows how the cost of transportation varies with machine rating:

Table 7-1. Transportation Costs vs. Rating

Rating	Transportation Cost per Turbine	Cost per kW
750 kW	\$26,586	\$35.4
1.5 MW	\$51,004	\$34.0
3.0 MW	\$253,410	\$84.4
5.0 MW	\$1,312,150	\$262.4

It is clear from Table 7-1 that machines of 3.0 MW and greater are significantly penalized by transportation costs. To reduce these costs, the following changes would have to take place:

- Tower sections can be transported in partial cylinders and fastened together on the site, or an alternative tower construction approach can be adopted.
- Blades can be designed to be manufactured in parts that are assembled in the field or manufactured at a project site.
- Nacelle parts can be transported separately and assembled on site.

7.2 Installation

The installation costs quoted in Table 4-6 were also obtained from Reference [12] and are summarized in Table 7-2.

Table 7-2. Installation Costs vs. Rating

Rating	Installation cost per Turbine	Cost per kW
750 kW	\$24,374	\$32.5
1.5 MW	\$50,713	\$33.8
3.0 MW	\$112,714	\$37.5
5.0 MW	\$224,790	\$44.9

The costs per kW of installed power increase only slightly up to ratings of 3.0 MW, but there is a more substantial increase at 5.0 MW. The reason for this is largely due to the cost of the crane required to lift parts into place. This cost could be reduced by incorporating a self-erecting tower scheme that would also allow installation of the nacelle and rotor parts.

7.3 Blade Manufacturing

Reference [3] concluded that the weights and costs of scaling up conventional blades increase approximately with the diameter to the power of 3.0, implying that the cost of the blades per kW will increase linearly with diameter. Hence the blade costs for larger machines will comprise a greater fraction of the total cost. However, the cost of the rotor is not greater than about 15% of the total cost so that a certain increase in rotor costs has only 0.15 of that effect on the final COE.

Nevertheless, the design of the blade is important because the blades generate loads that are seen by all parts of the turbine. This has been illustrated in the current project by the introduction of lower solidity blades accompanied by flap-twist coupling in the blade material. The latter property raises questions of fabrication methods and final costs. Although this project was able to estimate the costs of fabrication of one type of construction, the subject of adaptive blades is one that is undergoing considerable study at present, and more information will be available in due course. In the meantime, uncertainty about costs and reliability of adaptive blades must be considered a barrier to implementing this technology.

7.4 Acoustics

Acoustic emission from wind turbines is a matter that is critical to the acceptance of the industry and is one that is subject to considerable research (Reference [21]). In general, much of the emission is from the blade tips and increases with the tip speed. Therefore, the proposal in Task #5 to increase the tip speed from 75 to 85 m/s is one that may be criticized for potentially increasing acoustic emission to an unacceptable level.

The high tip speeds proposed may be more acceptable in regions such as the Midwest than in more populated areas. However, some Midwest residents may object to undue noise level, and it is recommended that research continue into the design of blade details that will attenuate the emissions.

7.5 Design Load Cases

All the simulations and the loads in this project have been based on use of the standard Kaimal spectrum of turbulence from Reference [1]. It is known that this spectrum (and the alternative von Karman spectrum) does not satisfactorily include all extreme events that may occur during operation, and this is why the separate inclusion of deterministic extreme events is also required. (This may change in the future when extrapolation techniques are improved.) Recent field studies (Reference [24]) have demonstrated that taller machines, especially in locations such as the Midwest, can be subject to a phenomenon known as the low-level jet stream. This phenomenon may subject a turbine to violent coherent turbulence and high loads. It is possible, therefore, that the loads used for design in this project may underestimate those that may occur in some locations, especially when combined with greater tower heights.

However, this possibility does not invalidate the conclusions drawn from the project. The designs and modifications use the same loads, and the relative appraisal of the configurations will be unaffected.

7.6 Non-Turbine Costs

Approximately 50% of the cost of energy is from items that are unaffected by rotor design. These are the balance of station, land, maintenance, replacement, etc. costs which may not be barriers to lowering the cost but do make it more difficult to bring about a reduced COE purely by improved rotor design.

Another relevant fact is that changes to the various components of the wind turbine affect only part of the total COE equation, whereas a change to the aerodynamic performance and the annual energy production will have a direct effect on the COE. Hence, any rotor change that may reduce the energy production by even a small amount must be offset by a considerable reduction in material cost.

8. CONCLUSIONS

8.1 Assumptions within the Study

The basic assumptions used in this study must always be borne in mind. These include:

- All the costs presented in this study are intended to be used to compare one set against another. They should not be regarded as absolute although much effort has been made to ensure that they are consistent with typical commercial costs.
- All non-recurring manufacturing costs have been neglected. This includes all development, tooling, and marketing costs.
- All costs assume that a mature production rate or number has been achieved. This will be harder to achieve for components for larger turbines than it will be for smaller turbines.
- The emphasis in this study has been on the different configurations of the rotor. The configurations of the drive train and tower have been assumed to be of a standard type, and no effort has been made to optimize them.
- This also applies to the operating and maintenance costs, which have been assumed to be a constant per kWh for all configurations and for all ratings.
- A number of types of rotors and control strategies were eliminated at the start of Task #3. The remaining configurations have all featured full-span pitchable blades, continuously variable speed, and a pitch-to-feather control strategy.
- The specific rating (rated power/swept area) of all configurations has been maintained at 0.39 kW/m^2 . This value was agreed on after reviewing common commercial practice and the apparent trends.

8.2 Summary

The cost of energy of the baseline designs has been reduced by no more than 13%, although considerable reductions have occurred to the loads throughout the system. In the course of achieving this, several trends and conclusions have become apparent.

- More than 50% of the COE is unaffected by rotor design and system loads. Further COE reductions may be achieved by addressing the balance-of-station costs.
- Combinations of rotor improvements with parallel improvements in the drive train design and in the tower design must be pursued. Such combinations will bring the total COE reductions closer to the 30% target.
- The cost of the rotor as a fraction of the total capital cost rises with increasing rotor size. Therefore, larger machines can benefit more from rotor improvements.
- The cost of a 3-bladed rotor is greater than the equivalent 2-bladed rotor and, for the same reason, benefits more from rotor improvements.
- No single rotor modification offered a solution to reduced rotor costs and lower system loads. Instead there were a number of modifications that offered some general benefits.
- The three modifications that resulted in the most general reductions in system loads and in a subsequent reduction in the cost of energy were:
 - Inclusion of tower feedback to the blade pitch control system.
 - Incorporation of flap-twist coupling in the blade design.
 - Reduction of the blade chord combined with an increase in the tip speed.

- Combination of these three modifications (in Task #5) resulted in further COE improvements in the 3-bladed upwind configuration.
- The Task #5 improvements were of most benefit to the 3-MW 3-bladed upwind machine. This narrowed the difference in COE within the 750-kW to 3-MW range.
- The selected rotor modifications benefited all three basic configurations. However, the benefit to the 2-bladed configurations, especially the downwind machine, was less than the benefit to the 3-bladed configuration.
- Several loads in the final 2-bladed downwind machine were higher than the corresponding loads in the baseline design. This is attributed to dynamic issues caused by the strong harmonic loading due to the tower shadow. It is likely that correct tuning will reduce the loads to be equal to or less than the baseline values.
- The COE is very sensitive to changes in the annual energy production. Therefore, the added tip losses associated with larger chords penalize the 2-bladed rotors.
- Likewise, the COE is sensitive to any performance loss due to the flap-twist coupling, and care must be taken to adjust the initial twist schedule to compensate for elastic deformations.
- The extensive use of carbon fibers was essential to the final blade design. Their greater stiffness (compared to glass fiber) was needed to achieve the required flap-twist coupling and to avoid contact with the tower.
- The use of carbon fiber was accompanied by a change from a fatigue-governed blade to one governed by peak loads or by deflection.
- Added costs of transportation and assembly adversely affect the COE for machines rated above 1.5 MW. Alternatives to the use of conventional cranes and alternative tower designs will benefit larger machines.
- The inclusion of feedback from tower motion into the control system reduced tower loads considerably. This feature has not been optimized, and further improvements may be possible. Other control system enhancements may also have beneficial effects.

8.3 Recommendations

The following recommendations are made:

- Combine the findings of this study with those of the parallel WindPACT drive train configuration study and the continuing study of the effect of specific rating. This combination may offer COE improvements that approach the target COE reduction identified by the WindPACT project.
- Conduct more testing of material coupons and blade assemblies to support the use of bias-ply carbon fibers required for flap-twist coupling.
- Study the acoustic penalties associated with higher tip speeds and ways of ameliorating them.
- Develop further refinements of turbine control systems to reduce loads.
- Study various approaches for reducing COE by changes in the balance-of-station costs and in the fixed charge rate.

9. REFERENCES

1. International Electrotechnical Commission. *Safety of Wind Turbine Conversion Systems*. 61400-1. 1998.
2. Germanischer, Lloyd. *Regulations for the Certification of Wind Energy Conversion Systems*. 1999.
3. Griffin, D.A. *WindPACT Turbine Design Scaling Studies Technical Area 1 – Composite Blades for 80- to 120-Meter Rotor*. Global Energy Concepts, LLC for National Renewable Energy Laboratory. Golden, CO. NREL/SR-500-29492. March 2001.
4. Mechanical Dynamics Inc. *ADAMS/Solver Reference Manual, Version 11, 2002*.
5. Wilson, R.E.; Freeman, L.N.; Walker, S.N.; and Harman, C.R. *Users' Manual for the FAST_AD Advanced Dynamics Code*. OSU/NREL Report 95-01. September 1995.
6. Harrison, R. and Jenkins, G. *Cost Modeling of Horizontal Axis Wind Turbines*. For ETSU W/34/00170/REP. University of Sunderland. 1994.
7. Griffin, D.A. *WindPACT Blade System Design Studies – Task #2 Blade Study Report*. Sandia National Laboratories. Albuquerque, NM. SAND2001-XXXX.: (publication pending).
8. Powertrain Engineers. *Wind Turbine Gearbox Mass – A Parametric Study for Global Energy Concepts*. Document # 20189-1. August 10, 2000.
9. Global Energy Concepts, LLC. *WindPACT Drive Train Study, Preliminary Design Status Summary*. December 2001.
10. *Wind Turbine Verification Project Experience*. Global Energy Concepts LLC on behalf of EPRI. EPRI #1000961. December 2000.
11. Galambos, T.V. *Guide to Stability Design Criteria for Metal Structures, 5th Edition*. John Wiley & Sons. 1998.
12. Global Energy Concepts LLC. *WindPACT Turbine Design Scaling Studies. Technical Area 2 – Turbine, Rotor and Blade Logistics. Final Report*. NREL Subcontract YAM-0-30203-01. December 2000.
13. Commonwealth Associates Inc. *WindPACT Turbine Scaling Studies, Technical Area 4, Balance of Station Cost*. prepared for National Renewable Energy Laboratory. July 2000.
14. Selig, M.S.; Tangler, J.L. (May 10-13, 1994). “A Multipoint Inverse Design Method for Horizontal Axis Wind Turbines.” Presented at the AWEA Windpower ‘94 Conference. Minneapolis, MN.
15. Lemming, J. and Morthorst, P.E. “O&M Costs and Economical Life Time of Wind Turbines.” EWEC '99. March 1-5, 1999. Nice, France.

16. National Wind Coordinating Council. "Wind Energy Costs," *Wind Energy Series No. 11*, January 1997.
17. Harrison, R., Hau, E., and Hermann, S. "Large Wind Turbines, Design and Economics." John Wiley & Sons, Ltd. 2000.
18. "Predictions on Costs. Associations Warn Turbine Owners." *Windpower Monthly*. April 2000.
19. Tangler, J.L. and Somers, D.M. "NREL Airfoil Families for HAWTS." American Wind Energy Association. *Windpower '95*.
20. Somers, D.M. and Tangler, J.L. "Wind Tunnel Tests for Two Airfoils for Wind Turbines Operating at High Reynolds Numbers." AIAA/ASME Wind Energy Symposium. Reno, Nevada. January 2000.
21. Migliore, P.G. (Editor). "Fundamentals of Aeroacoustics with Applications to Wind Turbine Noise." Proceedings of a workshop held at NWTC. Colorado. July 24-26, 2001.
22. Global Energy Concepts. *Development of Blade Property Extraction Code to Interface with NumMAD, Phase 2*. On behalf of Sandia National Laboratories. Document 20173. March 2002.
23. Laird, D.L. "A Numerical Manufacturing Odyssey." Proceedings of ASME/AIAA Wind Energy Symposium. Reno, Nevada. January 2001.
24. Kelley, N.D.; Hand, M.; Larwood, S.; and McKenna, E. "The NREL Large Scale Turbine Inflow and Response Experiment – Preliminary Results." Proceedings of ASME/AIAA Wind Energy Symposium. Reno, Nevada. January 2002.
25. Lobitz, D.W., Veers, P.S., and Laino, D.J. "Performance of Twist-Coupled Blades on Variable Speed Rotors." Proceedings of AIAA/ASME Wind Energy Symposium. Reno, Nevada. January 2000.
26. Rock, S.M.; Eggers, A.J.; Moriarty, P.J.; and Chaney, K. "Tradeoffs in Active Control of Aerodynamic Power and Loads on a HAWT Rotor." Proceedings AIAA/ASME Wind Energy Symposium. Reno, Nevada. January 2000.

10. BIBLIOGRAPHY

- Giguere, P. and Selig, M.S. "Blade Geometry Optimization for the Design of Wind Turbine Rotors." Proceedings of AIAA/ASME Wind Energy Symposium. Reno, Nevada. January 2000.
- Fuglsang, P.L., and Madsen, H.A. "Optimization Method for Wind Turbine Rotors." *Journal of Wind Engineering and Industrial Aerodynamics*. Vol. 80, 1999. pp.191-306.
- Bulder, G.H. and Hagg, F. 'BLADOPT' – "A Numerical Optimization Tool for Rotor Blades using Cost of Energy as the Target Function." European Wind Energy Conference. Dublin, Ireland. October 1997.
- Madsen, P., Pierce, K. and Buhl, M. "Predicting Ultimate Loads for Wind Turbine Design." Proceedings of AIAA/ASME Wind Energy Symposium. Reno, Nevada. January 1999.
- Madsen, P., Pierce, K. and Buhl, M. "Predicting Ultimate Loads for Wind Turbine Design." Proceedings of AIAA/ASME Wind Energy Symposium. Reno, Nevada. January 1999.
- Snel, H., Van Holten, Th., and Follings, F. "Study on the Next Generation of Large Wind Turbines, Part 1, Technical Concept Analysis." European Community Wind Energy Conference. Madrid. September 1990.
- Harrison, R., Jenkins, G., and Macrae, A. N. "Study on the Next Generation of Large Wind Turbines, Part 2, Manufacturing Cost Analysis." European Community Wind Energy Conference. Madrid. September 1990.
- Milborrow, D. J. "Will Multi-Megawatt Wind Turbines Ever Be Economic?" European Wind Energy Conference and Exhibition. Glasgow. July 1989.
- Follings, F. "Economic Optimization of Wind Power Plants." European Wind Energy Conference and Exhibition. Glasgow. July 1989.
- Follings, F.J. "Design Recommendations for Large WECS." European Community Wind Energy Conference. Madrid. September 1990.
- EWEA, European Commission, Directorate-General for Energy. *Wind Energy – The Facts. Volume 1: Technology*. 1998.
- EWEA, European Commission, Directorate-General for Energy. *Wind Energy – The Facts. Volume 2: Costs, Prices and Values*. 1998.
- EWEA, European Commission, Directorate-General for Energy. *Wind Energy – The Facts. Volume 3: Industry and Employment*. 1998.
- EWEA, European Commission, Directorate-General for Energy. *Wind Energy – The Facts. Volume 4: Environment*. 1998.
- EWEA, European Commission, Directorate-General for Energy. *Wind Energy – The Facts. Volume 5: Market Development*. 1998.
- "Audit and Review of the IDWGP Operations." *Wind Utility Consulting*. May 2000.
- Thresher, R.W. and Dodge, D.D. "Evolution of Wind Turbine Generator Configurations." *Wind Energy*. Vol. 1, pp. 70-85. 1998.
- Schontag, C. and van Bussel, G.J.W. *Opti-OWECS Final Report Vol. 2: Methods Assisting the Design of OWECS Part B: Optimization of Operation and Maintenance*. Contract JOR3-CT95-0087 for The European Commission, Non Nuclear Energy Programme. December 1997.

Appendix A

Details from Task #3 Configuration Variations

Table A-1. Relative Load Results from Task #3 Configurations

Configuration						Load Location and Type												
Type	Letter ID	Model ID	Description	Code Used	Normalize Base	Root Flap		Blade 50% Flap		Hub-Shaft My		Shaft Torque		Yaw Bearing My		Tower Base My		Tower Clrnce
						peak	fatig	peak	fatig	peak	fatig	peak	fatig	peak	fatig	peak	fatig	margin
3-bl upwind	A (Adm)	1.5A08C01V03cAdm	baseline	Adams	A (Adm)	1.00	1.00	1.00	1.00	1.00	1.00	1.00	1.00	1.00	1.00	1.00	1.00	0.16
3-bl upwind	A (Fst)	1.5A08C01_3V02c	baseline	FAST	A(Adm)	0.92	1.11	1.36	1.15	1.19	1.12	1.06	1.07	1.07	1.08	1.02	1.03	0.16
3-bl upwind	B	1.5B01C01V01e	diam + 12%	FAST	A (Fst)	1.42	1.38	1.45	1.36	1.42	1.44	1.43	1.21	1.42	1.41	1.05	1.16	0.34
3-bl upwind	C	1.5C02C01V01c	tip spd + 13%	FAST	A (Fst)	0.99	1.07	1.01	1.06	1.05	1.14	0.99	0.92	1.03	1.12	1.04	1.08	0.25
3-bl upwind	D	1.5D01C07V00c	+ twr feedback	FAST	A (Fst)	1.00	1.00	1.00	1.00	0.96	1.00	1.00	1.01	1.00	1.00	0.92	0.75	0.32
3-bl upwind	E02	1.5E02C01V00c	soft-soft tower	FAST	A (Fst)	0.96	1.01	1.01	1.01	1.02	1.02	0.96	0.99	1.04	1.00	1.27	1.05	0.23
3-bl upwind	F	1.5F02C01V00c	stiff blades	FAST	A (Fst)	0.99	0.90	1.00	0.98	0.95	0.94	0.97	1.19	0.94	0.92	1.07	1.14	0.04
3-bl upwind	G	1.5G05C01V01	flap twist coupling	Adams	A (Adm)	0.92	0.84	0.90	0.80	0.79	0.81	0.81	1.03	0.83	0.79	0.94	0.89	0.24
3-bl upwind	H	1.5H01C01V01c	flap pitch feedback	Adams	A (Adm)	1.00	0.96	1.00	1.02	0.87	1.20	1.00	1.05	0.77	1.14	1.00	1.04	0.40
3-bl upwind	Y	1.5Y01C01V01c	high strain blades	FAST	A (Fst)	1.02	0.85	1.00	0.89	0.98	0.86	1.04	1.25	0.93	0.82	0.99	1.06	-0.31
3-bl upwind	X	1.5X01C01V01c	high strain, low chrd, tp spd +13%	FAST	A (Fst)	0.77	0.76	0.77	0.75	0.77	0.73	0.74	1.17	0.69	0.64	0.95	0.93	-0.55
3-bl dwnwind	J	1.5J01C01V01c	baseline, downwind	FAST	A (Fst)	1.07	1.14	1.02	1.10	1.16	1.17	0.96	1.34	1.25	1.17	1.14	1.08	1.27
3-bl dwnwind	K	1.5K02C01V00c	downwind, soft blades	FAST	A (Fst)	0.96	0.91	1.04	0.85	0.99	0.89	1.06	1.11	1.00	0.85	0.95	0.93	0.39
3-bl dwnwind	L	1.5L01C01V01cAdm	hinged blades	Adams	A (Adm)	1.19	0.80	0.79	0.82	0.81	1.19	1.13	1.17	0.84	0.78	0.95	0.82	0.00
2-bl upwind	M	1.5M03C01V00c	int. baseline	FAST	A (Fst)	0.93	0.98	0.88	1.03	0.80	0.58	0.70	1.19	0.55	0.48	0.89	1.02	-0.08
2-bl upwind	N	1.5N02C01V00c	diam + 12%	FAST	M (Fst)	1.47	1.40	1.43	1.39	2.26	1.53	1.40	1.26	1.66	1.76	1.13	1.36	-0.08
2-bl upwind	P	1.5N02C01V00c	tip spd + 13%	FAST	M (Fst)	1.47	1.40	1.43	1.39	2.26	1.53	1.40	1.26	1.66	1.76	1.13	1.36	0.02
2-bl dwnwind	Q	1.5Q02C03V01cAdm	int. baseline	Adams	A (Adm)	0.65	1.05	0.98	1.14	0.74	1.37	0.74	1.21	0.85	0.91	0.90	1.01	0.04
2-bl dwnwind	Q	1.5Q02C01V01cFst	int baseline	FAST	A (Adm)	0.92	1.09	1.00	1.21	0.71	1.27	0.70	1.66	0.72	0.64	0.85	1.07	
2-bl dwnwind	R	1.5R01C01V01c	soft blade	FAST	Q (Fst)	0.96	1.05	0.93	0.93	2.01	1.37	1.03	1.24	1.67	1.74	1.08	1.14	0.17
2-bl dwnwind	S	1.5S01C01V00c	diam + 12%	FAST	Q (Fst)	1.44	1.40	1.33	1.40	1.82	1.46	1.47	1.32	1.42	1.60	1.36	1.50	0.10
2-bl dwnwind	T	1.5T01C01V01cAdm	Ti spd + 13%	Adams	Q (Adm)	1.50	1.27	1.19	1.22	1.34	0.81	1.04	0.89	1.26	1.43	1.15	1.21	0.03
2-bl dwnwind	U	1.5U01C01V00c	tower feedback	FAST	Q (Fst)	1.08	0.99	1.01	1.00	1.12	1.00	1.03	1.01	1.13	1.01	0.96	0.81	0.22
2-bl dwnwind	V	1.5V01C07V02Adm	positive delta-3	Adams	Q (Adm)	1.42	1.04	1.34	1.05	1.37	1.08	1.20	0.99	1.18	0.82	1.04	0.97	0.08
2-bl dwnwind	W	1.5W02C01V01	hinged blades	Adams	Q (Adm)	1.95	0.82	1.09	0.84	1.42	1.28	1.16	0.96	0.96	0.97	0.92	0.86	-0.08

Table A-2. Governing Load Cases and Margins for Task #3 Configurations

Configuration				Governing load case and margin to next critical load															
Type	Letter ID	Model ID	Description	Code Used	Root Flap			50% Flap			Hub			Mainframe			Tower Base		
					Gov load	Next load	Mrgn to nxt Id	Gov load	Next load	Mrgn to nxt Id	Gov load	Next load	Mrgn to nxt Id	Gov load	Next load	Mrgn	Gov load	Next load	Mrgn to nxt Id
3-bld upwind	A (Adm)	1.5A08C01V03cAdm	baseline	Adams	fatigue	ECD	52%	fatigue	EWM	45%	fatigue	EWM	67%	fatigue	ECD	27%	fatigue	EWM	35%
3-bld upwind	A (Fst)	1.5A08C01_3V02c	baseline	FAST	fatigue	EWM	6.3%	fatigue	EWM	24%	fatigue	EWM	55%	fatigue	ECD	43%	fatigue	EWM	44%
3-bld upwind	B	1.5B01C01V01c	diam + 12%	FAST	fatigue	EWM	3%	fatigue	EWM	16%	fatigue	EWM	43%	fatigue	ECD	39%	fatigue	ECD	37%
3-bld upwind	C	1.5C02C01V01c	tip spd + 13%	FAST	fatigue	EWM	14%	fatigue	EWM	30%	fatigue	EWM	68%	fatigue	ECD	41%	fatigue	EWM	43%
3-bld upwind	D	1.5D01C07V00c	+ twr feedback	FAST	fatigue	EWM	6%	fatigue	EWM	24%	fatigue	EWM	55%	fatigue	ECD	43%	fatigue	EWM	3%
3-bld upwind	E02	1.5E02C01V00c	soft-soft tower	FAST	fatigue	EWM	10%	fatigue	EWM	23%	fatigue	EWM	38%	fatigue	ECD	61%	fatigue	EWM	24%
3-bld upwind	F	1.5F02C01V00c	stiff blades	FAST	fatigue	EOG	31%	fatigue	ECD	43%	fatigue	EWM	42%	fatigue	ECD	48%	fatigue	EWM	66%
3-bld upwind	G	1.5G05C01V01	flap twist coupling	Adams	fatigue	EOG	??	fatigue	EWM	27%	fatigue	EWM	56%	fatigue	ECD	20%	fatigue	EWM	49%
3-bld upwind	H	1.5H01C01V01c	flap pitch feedback	Adams	fatigue	EOG	53%	fatigue	EWM	48%	fatigue	EOG	112%	fatigue	ECD	72%	fatigue	EWM	97%
3-bld upwind	Y	1.5Y01C01V01c	high strain blades	FAST	EWM	Fatigue	52%	EWM	ECD	17%	fatigue	EWM	23%	fatigue	ECD	38%	fatigue	EWM	110%
3-bld upwind	X	1.5X01C01V01c	high strain, low chrd, tip spd + 13%	FAST	EWM	NTM	22%	EWM	fatigue	12%	fatigue	EWM	49%	fatigue	ECD	43%	fatigue	EOG	63%
3-bld downwind	J	1.5J01C01V01c	baseline, downwind	FAST	fatigue	EWM	12%	fatigue	EWM	32%	fatigue	EWM	62%	fatigue	ECD	12%	fatigue	ECD	44%
3-bld downwind	K	1.5K02C01V00c	downwind, soft blades	FAST	EWM	fatigue	23%	EWM	fatigue	18%	fatigue	EWM	54%	fatigue	ECD	7%	fatigue	EWM	36%
3-bld downwind	L	1.5L01C01V01cAdm	hinged blades	Adams	EWM	ECD	117%	fatigue	ECD	43%	fatigue	EWM	150%	fatigue	ECD	22%	fatigue	EWM	32%
2-bld upwind	M	1.5M03C01V00c	int. baseline	FAST	fatigue	EWM	10%	fatigue	EWM	45%	fatigue	EWM	55%	fatigue	ECD	22%	fatigue	NTM	95%
2-bld upwind	N	1.5N02C01V00c	diam + 12%	FAST	fatigue	EWM	10%	fatigue	EWM	39%	fatigue	EWM	49%	fatigue	ECD	28%	fatigue	EWM	130%
2-bld upwind	P	1.5N02C01V00c	tip spd + 13%	FAST	fatigue	EOG	17%	fatigue	EOG	49%	fatigue	EOG	66%	fatigue	ECD	20%	fatigue	NTM	100%
2-bld downwind	Q	1.5Q02C03V01cAdm	int. baseline	Adams	fatigue	EOG	39%	fatigue	EOG	68%	fatigue	EOG	100%	fatigue	EWM	55%	fatigue	EOG	83%
2-bld downwind	Q	1.5Q02C01V01cFst	int baseline	FAST	fatigue	EWM	3%	fatigue	NTM	76%	fatigue	EWM	48%	fatigue	NTM	47%	fatigue	EOG	26%
2-bld downwind	R	1.5R01C01V01c	soft blade	FAST	EWM	fatigue	1%	fatigue	NTM	33%	fatigue	EWM	65%	fatigue	NTM	52%	fatigue	NTM	120%
2-bld downwind	S	1.5S01C01V00c	diam + 12%	FAST	fatigue	EWM	1%	fatigue	EWM	86%	fatigue	EWM	43%	fatigue	NTM	50%	fatigue	NTM	130%
2-bld downwind	T	1.5T01C01V01cAdm	Ti spd + 13%	Adams	fatigue	EWM	16%	fatigue	NTM	73%	fatigue	EWM	74%	fatigue	NTM	80%	fatigue	EOG	74%
2-bld downwind	U	1.5U01C01V00c	tower feedback	FAST	EWM	fatigue	1%	fatigue	NTM	72%	fatigue	EWM	34%	fatigue	NTM	30%	fatigue	EOB	72%
2-bld downwind	V	1.5V01C07V02Adm	positive delta-3	Adams	fatigue	EWM	5%	fatigue	EWM	34%	fatigue	EWM	44%	ECD	fatigue	1%	fatigue	NTM	75%
2-bld downwind	W	1.5W02C01V01	hinged blades	Adams	EWM	fatigue	39%	fatigue	ECD	35%	EWM	fatigue	22%	fatigue	EDC	22%	fatigue	NTM	72%

Table A-3. Costs and Cost of Energy Summary for All Task #3 Configurations

Configuration		A bsline 3-bld upwnd	A bsline 3-bld upwnd	B bsline diam +12%	C bsline tipspd +13%	D bsline twr fdbck	E02 bsline + sft sft twr	F bsline stiff bld s	G bsline flp- twst cplng	H bsline flp- ptch fdbck	Y bslin high strain blds	X Tp spd +13% lwr chrdr	J 3-bld dwnwnd	K 3-bld dwnwnd soft bld	L 3-bld hinged dwnwnd	M 2-bld upwnd	M 2-bld upwnd	N 2-bld upwnd diam +12%	P 2-bld upwnd +13% tpspd	Q 2-bld dwnwnd	Q 2-bld dwnwnd	T02 2-bld dwnwnd tp spd +13%	R 2-bld dwnwnd soft bld	S 2-bld dwnwnd diam +12%	U 2-bld dwnwnd twr fdbck	V 2-bld dwnwnd D3=+45	W 2-bld dwnwnd hngd	
Model Used		Adams	FAST	FAST	FAST	FAST	FAST	FAST	Adams	Adams	FAST	FAST	FAST	FAST	Adams	FAST	FAST	FAST	Adams	FAST	Adams	FAST	FAST	FAST	Adams	Adams		
Rotor	\$k	248	265	346	276	265	263	222	223	249	185	167	285	219	301	195	202	277	206	192	205	229	171	271	206	202	197	
Blades	\$k	148	162	214	171	162	162	125	140	148	95	90	173	115	138	98	100	134	104	97	100	113	64	134	101	101	89	
Hub	\$k	64	71	89	73	71	71	64	51	63	58	52	77	71	118	81	85	119	86	83	86	98	90	110	85	83	80	
Ptch mch, brngs	\$k	36	32	43	32	32	31	32	32	38	33	24	35	33	44	16	17	24	16	13	19	18	17	26	20	18	28	
Drve trn, nacelle	\$k	563	571	602	559	571	571	574	555	570	572	549	581	586	563	549	551	586	535	559	554	561	576	579	554	559	554	
Low-speed shaft	\$k	20	20	20	20	20	20	20	20	20	20	20	20	20	20	21	20	20	20	20	20	20	20	20	20	20	20	20
Bearings	\$k	12	12	12	12	12	12	12	12	12	12	12	12	12	12	13	12	12	12	12	12	12	12	12	12	12	12	12
Gearbox	\$k	151	154	169	142	154	154	159	151	160	158	146	160	166	159	155	159	176	146	155	155	146	162	171	155	159	153	
Mech brk, cplng	\$k	3	3	3	3	3	3	3	3	3	3	3	3	3	3	3	3	3	3	3	3	3	3	3	3	3	3	3
Generator	\$k	98	98	98	98	98	98	98	98	98	98	98	98	98	98	98	98	98	98	98	98	98	98	98	98	98	98	98
Var spd elctmcs	\$k	101	101	101	101	101	101	101	101	101	101	101	101	101	101	101	101	101	101	101	101	101	101	101	101	101	101	101
Yw drve, bearing	\$k	12	13	18	14	13	14	12	10	9	12	8	18	18	10	7	6	10	5	6	5	8	9	8	6	7	6	
Main frame	\$k	64	68	79	68	68	68	67	59	65	65	59	67	66	59	49	51	64	48	62	58	71	69	65	58	58	60	
Elctrc cnctns	\$k	60	60	60	60	60	60	60	60	60	60	60	60	60	60	60	60	60	60	60	60	60	60	60	60	60	60	60
Hydric system	\$k	7	7	7	7	7	7	7	7	7	7	7	7	7	7	7	7	7	7	7	7	7	7	7	7	7	7	7
Nacelle cover	\$k	36	36	36	36	36	36	36	36	36	36	36	36	36	36	36	36	36	36	36	36	36	36	36	36	36	36	36
Control system	\$k	10	10	10	10	10	10	10	10	10	10	10	10	10	10	10	10	10	10	10	10	10	10	10	10	10	10	10
Tower	\$k	184	189	206	198	163	198	193	172	185	194	179	198	191	164	185	182	223	189	177	187	202	199	241	160	177	161	
Balance of stn	\$k	388	388	397	389	388	393	388	386	388	388	385	389	389	385	384	384	391	384	384	383	386	384	388	382	384	382	
Foundations	\$k	49	48	52	49	48	53	48	46	49	48	45	49	50	45	44	44	46	44	44	43	46	44	48	42	44	42	
Transportation	\$k	51	51	51	51	51	51	51	51	51	51	51	51	51	51	51	51	51	51	51	51	51	51	51	51	51	51	51
Roads, civil wks	\$k	79	79	82	79	79	79	79	79	79	79	79	79	79	79	79	79	82	79	79	79	79	79	79	79	79	79	79
Assmby, installn	\$k	51	51	51	51	51	51	51	51	51	51	51	51	51	51	51	51	51	51	51	51	51	51	51	51	51	51	51
Elect interf/cnct	\$k	127	127	129	127	127	127	127	127	127	127	127	127	127	127	127	127	129	127	127	127	127	127	127	127	127	127	127
Permits, engnrng	\$k	33	33	33	33	33	33	33	33	33	33	33	33	33	33	33	33	33	33	33	33	33	33	33	33	33	33	33
Initial cap cost	\$k	1,393	1,424	1,562	1,433	1,398	1,435	1,387	1,346	1,403	1,349	1,289	1,463	1,396	1,424	1,323	1,329	1,488	1,325	1,322	1,338	1,388	1,341	1,490	1,313	1,333	1,305	
Net ann energy	MWh	4,817	4,817	5,397	4,819	4,817	4,817	4,819	4,817	4,817	4,817	4,818	4,817	4,817	4,817	4,707	4,707	5,318	4,741	4,707	4,707	4,741	4,707	5,318	4,707	4,707	4,707	
Rotor	c/kWh	0.543	0.582	0.677	0.604	0.582	0.576	0.485	0.490	0.547	0.407	0.365	0.625	0.481	0.660	0.438	0.453	0.549	0.459	0.431	0.459	0.510	0.384	0.538	0.462	0.453	0.442	
Drive train	c/kWh	1.234	1.251	1.179	1.225	1.251	1.253	1.257	1.217	1.249	1.253	1.204	1.274	1.285	1.235	1.232	1.237	1.165	1.192	1.255	1.242	1.249	1.293	1.151	1.244	1.255	1.244	
Controls	c/kWh	0.022	0.022	0.020	0.022	0.022	0.022	0.022	0.022	0.022	0.022	0.022	0.022	0.022	0.022	0.023	0.023	0.020	0.023	0.023	0.023	0.023	0.023	0.020	0.023	0.023	0.023	0.023
Tower	c/kWh	0.403	0.415	0.404	0.434	0.358	0.434	0.423	0.377	0.406	0.425	0.391	0.433	0.419	0.360	0.415	0.408	0.443	0.422	0.396	0.419	0.451	0.446	0.479	0.360	0.397	0.362	
Balance of stn	c/kWh	0.852	0.851	0.777	0.852	0.851	0.861	0.851	0.845	0.852	0.850	0.844	0.852	0.854	0.844	0.861	0.861	0.777	0.856	0.861	0.858	0.860	0.861	0.771	0.857	0.862	0.857	
Repl't costs	c/kWh	0.467	0.467	0.417	0.467	0.467	0.467	0.467	0.467	0.467	0.467	0.467	0.467	0.467	0.467	0.478	0.478	0.423	0.475	0.478	0.478	0.478	0.478	0.423	0.478	0.478	0.478	
O&M	c/kWh	0.800	0.800	0.800	0.800	0.800	0.800	0.800	0.800	0.800	0.800	0.800	0.800	0.800	0.800	0.800	0.800	0.800	0.800	0.800	0.800	0.800	0.800	0.800	0.800	0.800	0.800	
Total COE	c/kWh	4.321	4.389	4.273	4.406	4.331	4.414	4.306	4.218	4.343	4.224	4.093	4.474	4.328	4.389	4.247	4.261	4.177	4.226	4.244	4.280	4.366	4.286	4.182	4.223	4.268	4.206	

Appendix B

Details from Task #5 Final Designs

Table B-1. Comparison of Baseline and Final Loads for 3-Bladed Upwind Machines

			750 kW		1.5 MW		3.0 MW	
			Baseline	Final Design	Baseline	Final Design	Baseline	Final Design
			.75A08C01V 04cAdm	.75AA04C01 V00	1.5A08C01V 07cAdm	1.5AA12C05 V00	3.0A09C02 V01adm	3.0AA02C01V 00
Tilt		deg	5.0	5.0	5.0	5.0	5.0	5.0
Coning		deg	0.0	3.0	0.0	3.0	0.0	3.0
Angle of contact		deg	0.0	0.0	0.0	0.0	0.0	0.0
Tip out of pln displt	max	m	1.862	2.468	2.816	3.467	3.467	4.464
	min	m	-1.377	-2.411	-1.711	-3.523	-2.520	-5.934
Tip clearance mrgn			0.210	-0.082	0.138	-0.074	0.322	-0.003
Blade rt flap mt	max abs	kN m	1,363	747	3,298	2,081	8,970	5,369
	equiv fatigue	kN m	465	275	1,237	889	3,956	2,380
Blade rt edge mt	max abs	kN m	335	164	815	497	3,821	1,969
	equiv fatigue	kN m	278	115	847	369	3,578	1,215
Blade 25% flap mt	max abs	kN m	527	335	1,350	1,056	3,917	2,791
	equiv fatigue	kN m	283	156	733	526	2,302	1,369
Blade 25% edge mt	max abs	kN m	175	87	412	248	1,744	1,023
	equiv fatigue	kN m	127	59	382	176	1,590	557
Blade 50% flap mt	max abs	kN m	216	140	553	456	1,622	1,173
	equiv fatigue	kN m	130	66	338	231	1,063	593
Blade 50% edge mt	max abs	kN m	55	33	146	89	599	360
	equiv fatigue	kN m	43	22	126	68	502	206
Blade 75% flap mt	max abs	kN m	53	32	133	108	433	275
	equiv fatigue	kN m	33	16	87	56	272	144
Blade 75% edge mt	max abs	kN m	12	7	33	19	116	69
	equiv fatigue	kN m	8	5	23	13	83	42
Shaft/hub My	max abs	kN m	909	438	2,105	1,360	7,129	3,835
	equiv fatigue	kN m	228	119	583	330	1,656	898
Shaft/hub Mz	max abs	kN m	871	409	2,210	1,274	7,464	3,618
	equiv fatigue	kN m	230	120	579	330	1,655	895
Shaft thrust	max abs	kN	159	128	324	283	797	590
	equiv fatigue	kN	25	16	44	37	89	71
Shaft Mx	max abs	kN m	1,325	484	3,424	1,513	10,820	4,761
	equiv fatigue	kN m	31	33	83	83	235	263
Yaw brg My	max abs	kN m	1,017	475	3,079	1,743	10,707	5,901
	equiv fatigue	kN m	184	93	468	266	1,389	769
Yaw btg Mz	max abs	kN m	685	458	1,966	1,201	4,536	3,179
	equiv fatigue	kN m	182	98	473	279	1,429	801
Tower base Mx	max abs	kN m	12,162	7,478	31,951	22,925	101,040	62,348
	equiv fatigue	kN m	710	526	2,058	1,644	6,944	5,087
Tower base My	max abs	kN m	11,088	7,946	27,390	25,700	95,543	83,851
	equiv fatigue	kN m	2,314	1,095	5,482	3,736	15,129	10,185
First system nat frequ		P		0.68	1.18	0.8		0.87
First blade nat. frequ		P		2.72	3.66	3.38		3.51

**Table B-2. Summary of Costs of Baseline and Final 3-Bladed Machines
at 750 kW, 1.5 MW, and 3.0 MW**

		750 kW		1.5 MW		3.0 MW	
		Baseline	Final Design	Baseline	Final Design	Baseline	Final Design
		.75A08C01V0 4cAdm	.75AA04C01 V00	1.5A08C01V 07cAdm	1.5AA12C05V 00	3.0A09C02V0 1adm	3.0AA01C02 V00
Rotor	\$k	100	66	236	167	654	394
Blades	\$k	63	44	152	112	413	262
Hub	\$k	18	10	48	34	157	90
Pitch mchnsm & bearings	\$k	19	11	36	21	85	42
Drive train, nacelle	\$k	246	225	536	501	1,236	1,125
Low-speed shaft	\$k	7	7	20	22	58	64
Bearings	\$k	4	4	12	12	43	43
Gearbox	\$k	71	66	161	146	375	336
Mech brake, HS cpling, etc	\$k	1	1	3	3	6	6
Generator	\$k	39	39	78	78	156	156
Variable spd electronics	\$k	41	41	81	81	162	162
Yaw drive & bearing	\$k	5	3	12	6	42	18
Main frame	\$k	26	16	66	52	194	144
Electrical connections	\$k	30	30	60	60	120	120
Hydraulic system	\$k	3	3	7	7	14	14
Nacelle cover	\$k	19	15	36	33	67	63
Control, safety system	\$k	10	10	10	10	10	10
Tower	\$k	72	44	179	142	513	370
Balance of station	\$k	223	216	403	397	905	896
Foundations	\$k	41	33	63	57	108	99
Transportation	\$k	27	27	51	51	253	253
Roads, civil works	\$k	45	45	79	79	136	136
Assembly & installation	\$k	24	24	51	51	113	113
Elect interfce/connect	\$k	71	71	127	127	224	224
Permits, engineering	\$k	16	16	33	33	70	70
Initial capital cost (ICC)	\$k	652	561	1,365	1,217	3,318	2,797
ICC per kW	\$/kW	869	748	910	811	1,106	932
Net annual energy	MWh	2,254	2,254	4,817	4,811	10,372	10,364
Rotor	c/kWh	0.470	0.307	0.518	0.365	0.666	0.402
Drive train	c/kWh	1.154	1.056	1.175	1.099	1.258	1.147
Controls	c/kWh	0.047	0.047	0.022	0.022	0.011	0.011
Tower	c/kWh	0.336	0.204	0.394	0.312	0.522	0.377
Balance of station	c/kWh	1.047	1.013	0.884	0.872	0.921	0.913
Repl't costs	c/kWh	0.499	0.499	0.467	0.468	0.434	0.434
O&M	c/kWh	0.800	0.800	0.800	0.800	0.800	0.800
Total COE	c/kWh	4.352	3.926	4.260	3.939	4.612	4.084

Table B-3. Comparison of 1.5-MW Final Loads with Baseline Configurations

			3-Bladed Upwind		2-Bladed Upwind		2-Bladed Downwind	
			Baseline	Final Design	Baseline	Final Design	Baseline	Final Design
			1.5A08C0 1V07cAd m	1.5AA12C05 V00	1.5M03 C01V04 cAdm	1.5AB05C02 V00	1.5Q02C0 3V01cAd m	1.5AC02C01 V00
Tilt		deg	5.0	5.0	6.0	5.0	5.0	0.0
Coning		deg	0.0	3.0	0.0	2.0	2.0	2.0
Angle of contact		deg	0.0	0.0	2.7	2.7	2.0	2.7
Tip out of pln displt	max	m	2.816	3.467	6.926	4.307	6.775	6.294
	min	m	-1.711	-3.523	-4.003	-4.051	-0.429	-1.679
Tip clearance mrgn			0.138	-0.074	-0.533	-0.166	0.041	-0.292
Blade rt flap mt	max abs	kN m	3298	2081	2727	2264	2146	2403
	equiv fatigue	kN m	1237	889	1251	935	1264	1166
Blade rt edge mt	max abs	kN m	815	497	1057	706	1146	802
	equiv fatigue	kN m	847	369	914	418	949	475
Blade 25% flap mt	max abs	kN m	1350	1056	1625	1245	1255	1355
	equiv fatigue	kN m	733	526	772	560	766	670
Blade 25% edg mt	max abs	kN m	412	248	460	365	510	408
	equiv fatigue	kN m	382	176	432	204	448	246
Blade 50% flap mt	max abs	kN m	553	456	670	502	544	539
	equiv fatigue	kN m	338	231	372	252	368	275
Blade 50% edg mt	max abs	kN m	146	89	173	126	190	163
	equiv fatigue	kN m	126	68	150	81	157	102
Blade 75% flap mt	max abs	kN m	133	108	144	104	133	112
	equiv fatigue	kN m	87	56	97	58	95	62
Blade 75% edg mt	max abs	kN m	33	19	32	26	36	31
	equiv fatigue	kN m	23	13	27	16	29	21
Shaft/hub My	max abs	kN m	2105	1360	1417	1109	1562	1544
	equiv fatigue	kN m	583	330	354	310	727	532
Shaft/hub Mz	max abs	kN m	2210	1274	35	52	182	132
	equiv fatigue	kN m	579	330	318	230	442	195
Shaft thrust	max abs	kN	324	283	284	230	254	221
	equiv fatigue	kN	44	37	39	28	39	32
Shaft Mx	max abs	kN m	3424	1513	2758	2010	2520	1760
	equiv fatigue	kN m	83	83	91	110	96	126
Yaw brg My	max abs	kN m	3079	1743	2018	1268	2627	2644
	equiv fatigue	kN m	468	266	225	204	418	579
Yaw btg Mz	max abs	kN m	1966	1201	1080	850	0	313
	equiv fatigue	kN m	473	279	215	212	9	4
Tower base Mx	max abs	kN m	31,951	22,925	14,513	10,214	13,527	14,669
	equiv fatigue	kN m	2058	1644	2815	1150	5021	3373
Tower base My	max abs	kN m	27,390	25,700	24,932	21,563	24,735	21,406
	equiv fatigue	kN m	5482	3736	5927	2609	5687	3091
First syst nat freq		P	1.18	0.803	~1.2	0.78	~1.2	0.822
First blade nat. freq		P	3.66	3.16	3.75	3.70	3.76	3.59

Note: When clearance margins were negative, mass and cost were added to the blade to restore this margin to zero.

Table B-4. Comparison of Final Costs with 1.5-MW Baseline Configurations

Filename		3-Bladed Upwind		2-Bladed Upwind		2-Bladed Downwind	
		Baseline	Final Design	Baseline	Final Design	Baseline	Final Design
		1.5A08C01 V07cAdm	1.5AA12C0 5V00	1.5M03C01V0 4cAdm	1.5AB05C0 2V00	1.5Q02C03V0 4cAdm	1.5AC01C0 2V00
Rotor	\$k	236	167	171	133	168	146
Blades	\$k	152	112	98	70	97	70
Hub	\$k	48	34	57	48	58	60
Pitch mchms & bearings	\$k	36	21	16	15	13	16
Drive train, nacelle	\$k	536	501	547	482	522	518
Low speed shaft	\$k	20	22	21	20	20	20
Bearings	\$k	12	12	13	12	12	12
Gearbox	\$k	161	146	155	145	155	149
Mech brake, HS cpling etc	\$k	3	3	3	3	3	3
Generator	\$k	78	78	98	78	78	78
Variable-speed electronics	\$k	81	81	101	81	81	81
Yaw drive & bearing	\$k	12	6	7	4	6	10
Main frame	\$k	66	52	49	44	62	66
Electrical connections	\$k	60	60	60	60	60	60
Hydraulic system	\$k	7	7	7	7	7	7
Nacelle cover	\$k	36	33	34	28	37	32
Control, safety system	\$k	10	10	10	10	10	10
Tower	\$k	179	142	185	115	177	139
Balance of station	\$k	403	397	396	393	396	393
Foundations	\$k	63	57	57	53	56	53
Transportation	\$k	51	51	51	51	51	51
Roads, civil works	\$k	79	79	79	79	79	79
Assembly & installation	\$k	51	51	51	51	51	51
Elect interfce/connect	\$k	127	127	127	127	127	127
Permits, engineering	\$k	33	33	33	33	33	33
Initial capital cost (ICC)	\$k	1,365	1,217	1,310	1,133	1,272	1,207
Net annual energy	MWh	4,817	4,811	4,707	4,708	4,707	4,708
Rotor	c/kWh	0.518	0.365	0.383	0.298	0.376	0.328
Drive train	c/kWh	1.175	1.099	1.227	1.081	1.170	1.163
Controls	c/kWh	0.022	0.022	0.023	0.023	0.023	0.023
Tower	c/kWh	0.394	0.312	0.415	0.257	0.396	0.312
Balance of stn	c/kWh	0.884	0.872	0.889	0.881	0.889	0.881
Repl't costs	c/kWh	0.467	0.468	0.478	0.478	0.478	0.478
O&M	c/kWh	0.800	0.800	0.800	0.800	0.800	0.800
Total COE	c/kWh	4.260	3.939	4.216	3.818	4.132	3.984

**Table B-5. Governing Load Cases and Margins for
Baseline and Task #5 Final Configurations**

		1.5 MW						750 kW		3.0 MW	
		3-Bladed Upwind		2-Bladed Upwind		2-Bladed Downwind		3-Bladed Upwind		3-Bladed Upwind	
		Baseline	Task 5	Baseline	Task 5						
		1.5A08C 01V07cA dm	1.5AA12 C05V00	1.5M03C 01V04cA dm	1.5AB05 C02V01	1.5Q02C 03V04cA dm	1.5AC01 C01V02	.75A08C 01V04cA dm	.75AA04 C01V00	3.0A09C 02V01Ad m	3.0AA02 C01v00
Blade root My	Governing load	EWM	Displ't	Fatigue	Displ't	Fatigue	Displ't	EWM	Displ't	Fatigue	Displ't
	Next critical margin	Fatigue	EDC	EWM	EWM	EOG	EWS	Fatigue	NTM	EWM	NTM
		52%	33%	10%	10%	39%	44%	18%	14%	1%	50%
Blade 50% My	Governing load	Fatigue	Displ't	Fatigue	Displ't	Fatigue	Displ't	Fatigue	Displ't	Fatigue	Displ't
	Next critical margin	EWM	EDC	EWM	EWSV	EOG	EWSV	EWM	EDC	ECD	NTM
		50%	12%	40%	7%	68%	35%	47%	10%	57%	6%
Hub	Governing load	Fatigue	Fatigue	Fatigue	Fatigue	Fatigue	Fatigue	Fatigue	Fatigue	Fatigue	Fatigue
	Next critical margin	EWM	EDC	EWM	EWM	EOG	EWSV	EWM	NTM	EWM	NTM
		22%	64%	55%	38%	71%	70%	68%	56%	90%	63%
Main- frame	Governing load	Fatigue	Fatigue	Fatigue	Fatigue	Fatigue	Fatigue	Fatigue	Fatigue	Fatigue	Fatigue
	Next critical margin	ECD	NTM	ECD	ECD	EWM	EWSV	ECD	ECD	ECD	ECD
		36%	30%	5%	49%	55%	84%	50%	64%	23%	20%
Tower base	Governing load	Fatigue	Fatigue	Fatigue	Fatigue	Fatigue	Fatigue	Fatigue	Fatigue	Fatigue	Fatigue
	Next critical margin	EWM	NTM	NTM	Estop	EOG	EOG	EWM	EOG	Estop	Estop
		40%	17%	78%	4%	71%	30%	47%	14%	29%	3%

Appendix C

Avon Bearing Costs

Yaw Bearings												
Specifications								Avon Data				
rotor diam	bolt circle diam	maximum moment	maximum thrust	equiv thrust due to mt	thrust capacity	design margin	machine rating	quantity per 50MW	P/N	Unit Cost	Cost/50MW	Weight [kg]
m	m	kN m	kN	kN	kN		kW					
46.6	1.45	1217	494.2	3357	4245	-0.00601	750	67	120B6	\$3,331	\$223,177	355
66	2.14	3773	1201	7052	8866	-0.02941	1500	33	1788B3	\$6,374	\$210,342	770
93	2.548	11826	2919	18565	21746	-0.08648	3000	17	TR15107B	\$29,105	\$494,785	4000
120	4.086	27646	5616	27064	34121	-0.05386	5000	10	TR15168B	\$46,000	\$460,000	6800
Pitch bearings												
46.6	1.005	1440			6523	0.011709	750	200	2544B1	\$4,045	\$809,000	620
66	1.425	4071			10736	-0.16486	1500	100	TR1263B2	\$13,795	\$1,379,500	1850
93	2.000	11514			21976	-0.15173	3000	50	TR2086B1	\$31,754	\$1,587,700	4700
120	3.438	24775			28834	-0.11082	5000	30	TR15142B1		\$0	5700

Avon Bearing costs (f: WindPACT rotor scaling\task 1\bearingcostWtSummaryDM.xls)

Appendix D

Calculation of Fatigue Damage Equivalent Loads

Suppose that the fatigue strength of a material is given by the single relationship

$$S = S_0 N^{-1/m}$$

or

$$N = \left(\frac{S}{S_0} \right)^{-m}$$

where S = load applied

S_0 = a constant

N = number of cycles at load level S

m = a constant

According to Miners cumulative damage rule, the damage, D , done by a number of loads, S_i , applied for n_i cycles respectively, will be

$$\begin{aligned} D &= \sum \frac{n_i}{N_i} \\ &= S_0^{-m} \sum n_i S_i^m \end{aligned}$$

Suppose that the same fatigue damage is done by a single load, S_e , applied for n_e cycles. Then

$$D = \frac{n_e}{N_e} = n_e \left(\frac{S_e}{S_0} \right)^m$$

so that

$$n_e \left(\frac{S_e}{S_0} \right)^m = \left(\frac{1}{S_0} \right)^m \sum n_i S_i^m$$

or

$$S_e = \left[\frac{1}{n_e} \sum n_i S_i^m \right]^{1/m}$$

The last line is an expression for a load level that will cause the same fatigue damage as a combination of loads, S_i , and is known as the equivalent fatigue load. It should be noted that this expression is valid only if the assumption is made of a single relationship between the load and fatigue strength. This corresponds to a single straight line on a log-log graph.

Appendix E

Description of the Blade Pitch Control System

Pitch Control Systems for the WindPACT Rotor Design Study

C. Hansen
Windward Engineering, LLC
March 2, 2001

This document briefly describes the pitch control systems used in the WindPACT Rotor Design Study. All the wind turbines under investigation in this study use full-span, collective pitch control in conjunction with variable-speed generators. Therefore, all the pitch controllers in this study have as their primary goal the control of generator speed. The systems attempt to operate at constant tip speed ratio (fixed pitch) when the wind is below rated. As the wind speed approaches the rated value, the pitch controller attempts to maintain constant rotor speed (“rated speed”).

The generator/power-electronics systems in this study have torque proportional to the square of generator speed below rated, then constant (or very slowly increasing) torque above the rated generator speed. This makes it possible to operate at constant tip speed ratio below rated as long as the blade pitch remains constant. Above rated, the system power output will change only in proportion to rotor speed since the torque remains essentially constant. Hence, power regulation is entirely dependent upon speed regulation.

The pitch control systems are implemented in the form of linear transfer functions in ADAMS and FAST_AD models. The same control subroutines and controller data files are used in both codes to calculate the pitch demand. In ADAMS, this pitch demand is sent to an actuator, which applies a pitching moment to the blade. In FAST_AD the pitching dynamics are not calculated directly. Instead, the actuator is represented as a linear transfer function between pitch demand and actual pitch. The ADAMS actuator and the FAST_AD actuators are selected to have essentially identical characteristics.

Figure 1 shows the control diagram for the basic speed controller. Figure 2 is similar, but tower acceleration is input to the pitch demand controller in an attempt to damp longitudinal vibration of the tower. Both systems use basic PID control with gains denoted in the figures as K_I , K_P , and K_D . When implemented numerically, we use a modified form of the derivative term, $K_D s / (1 + \tau s)$, where τ is a time constant that is small compare with other significant time scales in the system. We implement all the controls in discrete time. The typical time step is 0.025 sec.

Generator speed error is input to the basic controller. The PID controller determines the desired pitch angle, feathering the blade (increasing pitch) when the generator speed is too high. The pitch demand is limited to the range of θ_{\min} to 90° . θ_{\min} is the pitch angle at which optimum rotor aerodynamic performance is achieved when operating at constant tip speed ratio. When the rotor speed is below the desired setpoint, the pitch will remain constant at θ_{\min} . The generator torque characteristics must be matched to the rotor torque in order to actually achieve constant tip speed ratio operation.

The presence of the pitch demand saturation function requires that integrator anti-windup be included in the controller. This is shown as the feedback with gain K_{AW} in the figures. Note that this anti-windup term is fed back to the integrator only. This prevents the integrated speed error from accumulating when the rotor is operating in low winds, below rated speed. We have used a gain of 0.3 rpm/deg in all of our simulations. The results are insensitive to this gain when implemented in this manner.

The rotor characteristics are a strong nonlinear function of wind speed, hence blade pitch. This requires that the PID gains be “scheduled” as a function of blade pitch angle. Each of the PID gains is multiplied by a function, GS , of the form:

$$GS = \left\{ \begin{array}{ll} 1 & \theta < \theta_1 \\ a\theta^p & \theta_1 \leq \theta \leq \theta_2 \\ a\theta_2^p & \theta > \theta_2 \end{array} \right\}$$

where a , p , θ_1 , and θ_2 are constants input by the user. Coefficients a and p must be selected such that $a\theta_1^p = 1$. The exponent p is negative. It should be selected such that the product of the gain schedule value, GS , and the rotor “gain”, $\frac{\partial Q}{\partial \theta}$ (the sensitivity of rotor torque, Q , to blade pitch, θ), is nearly constant for all wind speeds in the operating range.

The pitch actuator in the WindPACT models is a simple second order system:

$$H_a(s) = \frac{\omega_n^2}{s^2 + 2\xi\omega_n s + \omega_n^2}$$

with $\xi = 80\%$ of critical damping and a natural frequency that is a multiple of the rotor speed. In most cases we have used $\omega_n = 4\Omega$, where Ω is the rotor angular velocity.

The turbine drive train is represented as a single torsion spring, k , between the generator inertia, I_g , and rotor inertia, I_r . The generator torque is represented as a linear function of generator speed, with slope = A . The resulting transfer function between rotor torque and generator speed is:

$$H_{DT}(s) = \frac{\frac{k}{I_r}}{I_g s^3 + A s^2 + \left(1 + \frac{I_g}{I_r}\right) k s + \frac{A k}{I_r}}$$

Many of the rotors we are modeling have a tower natural frequency close to 1 cycle per rotor revolution (1P). These systems experience substantial tower motion parallel to the wind direction. The tower motion appears as a cyclic wind speed input to the rotor and causes rotor speed oscillations, which in turn cause pitch oscillations. This motion can be exacerbated by a highly responsive pitch control system. We generally find it necessary to reduce the speed control effectiveness in order to avoid excessive tower fatigue loads. Finding the best balance between tower loads and effective speed control is subjective and largely a matter of trial and error with system simulations.

To alleviate this problem, we have implemented tower acceleration feedback. This is illustrated in Figure 2. The tower dynamics (in the “tower fore-aft motion” box) are represented as a transfer function from rotor thrust to tower-top velocity:

$$H_T(s) = \frac{\frac{s}{k_t}}{\frac{s^2}{\omega_t^2} + \frac{2\xi}{\omega_t} s + 1}$$

Here k_t is the effective stiffness of the tower, ω_t is the natural frequency, and ξ is the structural damping ratio. The rotor thrust is a linear function of the blade pitch (at a given wind speed) with a slope of $\frac{\partial T}{\partial \theta}$, determined from steady-state aerodynamics calculations at the desired wind speed and pitch angle.

The tower acceleration is input to a lag compensator to determine a change in pitch in response to the motion. This compensator is of the form:

$$H_{LC}(s) = \frac{s + \frac{1}{T}}{s + \frac{1}{\alpha T}}$$

where $\alpha > 1$ and T is a time scale related to the period of tower motion.

Two additional derivatives are needed to run a simple linearized model of this system. The sensitivity of rotor thrust to changes in pitch angle, $\frac{\partial T}{\partial \theta}$, was mentioned above. We also need the sensitivity of rotor torque to wind speed (or tower speed), $\frac{\partial Q}{\partial V}$. Using this technique, all of the aerodynamic characteristics of the system are represented by simple constants determined by steady-state simulations. Obviously this approximation neglects unsteady and nonlinear aerodynamic effects, which are known to be important to the system dynamics. As a result, the controllers must be verified and fine-tuned in full system simulations over the entire operating range of the system.

We have found that we can use this feedback to reduce tower loads or to improve speed regulation without increasing tower loads. However, the selection of all the controller parameters remains at least in part a matter of trial and error. We select the constants using simple MATLAB models of these controllers. Then we run a series of turbine simulations in turbulent winds and estimate the fatigue damage at several locations on the turbine. We generally find that we can decrease loads in one area at the expense of increased loads elsewhere. Selection of the best design depends on the lowest cost of energy, obviously not a simple thing to evaluate.

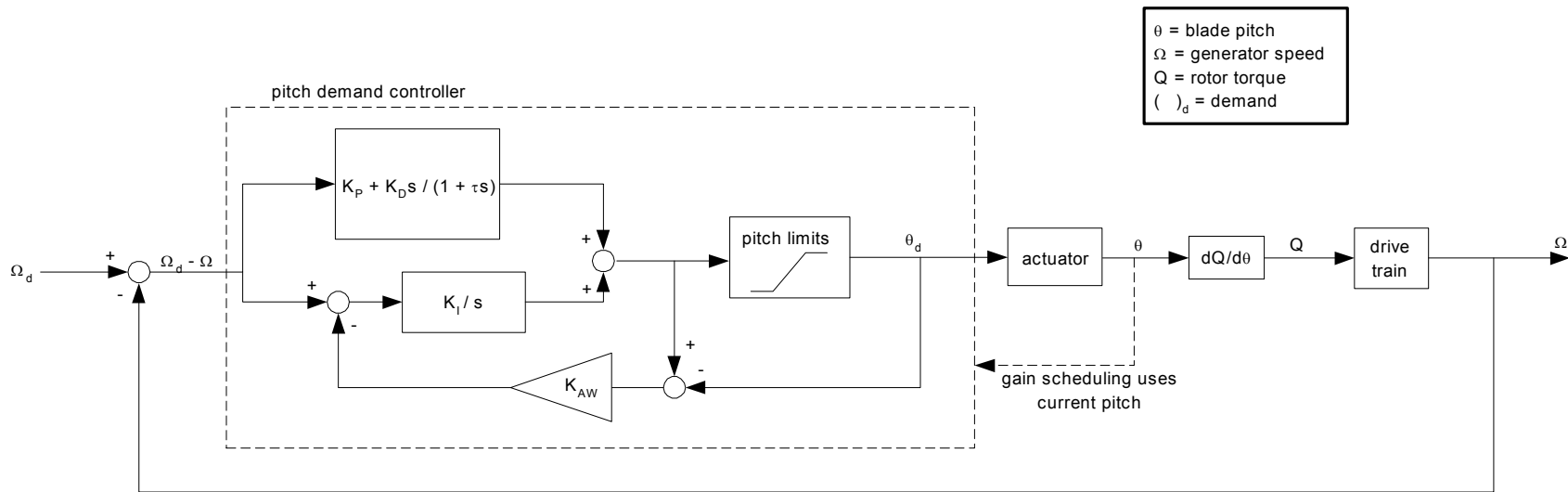


Figure E-1. Basic WindPACT rotor speed control system

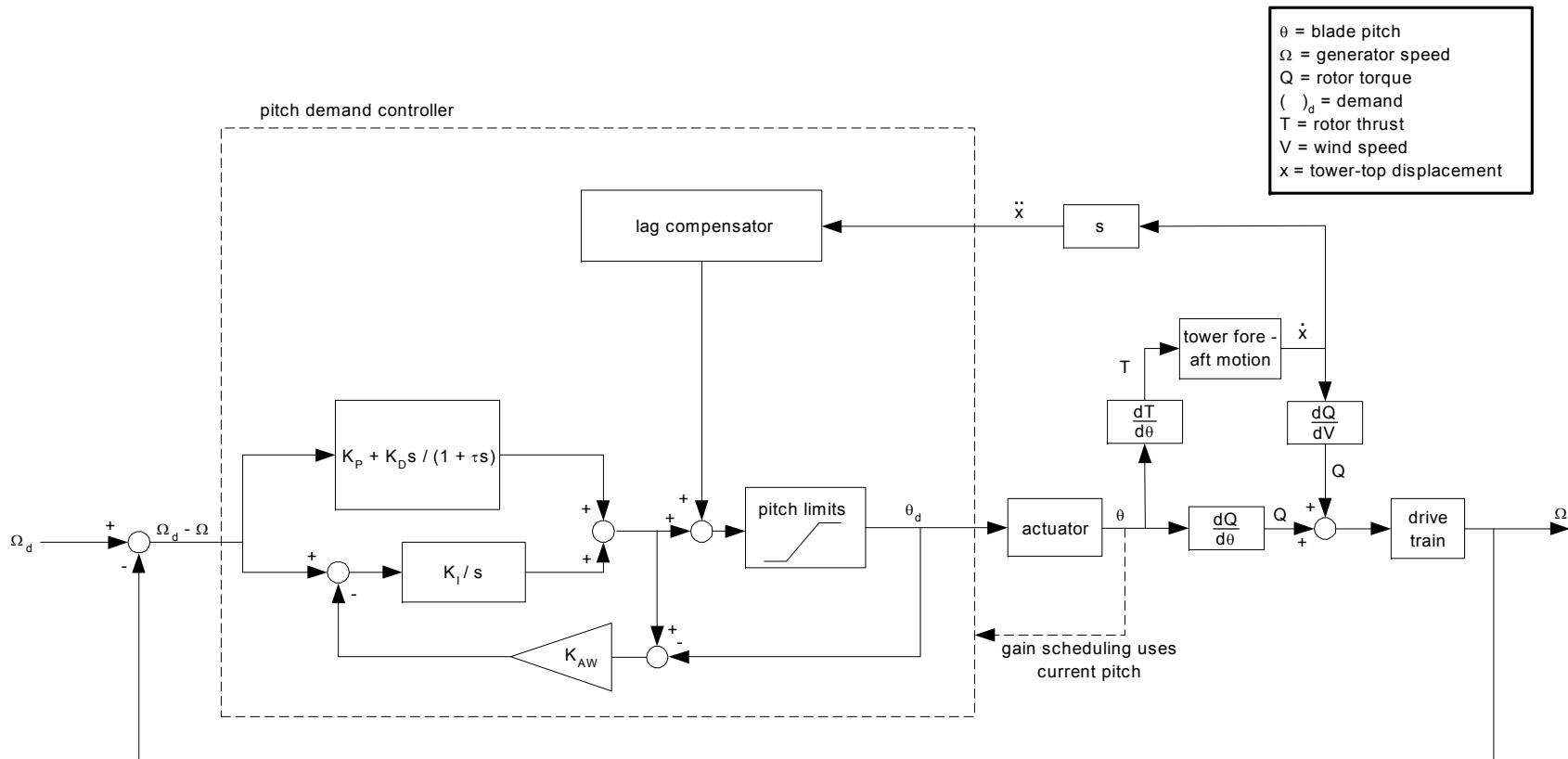


Figure E-2. WindPACT speed control with tower acceleration feedback

REPORT DOCUMENTATION PAGE

Form Approved
OMB No. 0704-0188

The public reporting burden for this collection of information is estimated to average 1 hour per response, including the time for reviewing instructions, searching existing data sources, gathering and maintaining the data needed, and completing and reviewing the collection of information. Send comments regarding this burden estimate or any other aspect of this collection of information, including suggestions for reducing the burden, to Department of Defense, Executive Services and Communications Directorate (0704-0188). Respondents should be aware that notwithstanding any other provision of law, no person shall be subject to any penalty for failing to comply with a collection of information if it does not display a currently valid OMB control number.

PLEASE DO NOT RETURN YOUR FORM TO THE ABOVE ORGANIZATION.

1. REPORT DATE (DD-MM-YYYY) Revised April 2006	2. REPORT TYPE Subcontract Report	3. DATES COVERED (From - To) June 2000 – June 2002	
4. TITLE AND SUBTITLE WindPACT Turbine Rotor Design Study		5a. CONTRACT NUMBER DE-AC36-99-GO10337	
		5b. GRANT NUMBER	
		5c. PROGRAM ELEMENT NUMBER	
6. AUTHOR(S) D.J Malcolm and A.C. Hansen		5d. PROJECT NUMBER NREL/SR-500-32495	
		5e. TASK NUMBER WE001510 and WER11510	
		5f. WORK UNIT NUMBER	
7. PERFORMING ORGANIZATION NAME(S) AND ADDRESS(ES) Global Energy Concepts, 5729 Lakeview Drive NE, #100, Kirkland, WA 98033 Windward Engineering, 4661 Holly Lane, Salt Lake City, UT 84117		8. PERFORMING ORGANIZATION REPORT NUMBER YAT-0-30213-01	
9. SPONSORING/MONITORING AGENCY NAME(S) AND ADDRESS(ES) National Renewable Energy Laboratory 1617 Cole Blvd. Golden, CO 80401-3393		10. SPONSOR/MONITOR'S ACRONYM(S) NREL	
		11. SPONSORING/MONITORING AGENCY REPORT NUMBER NREL/SR-500-32495	
12. DISTRIBUTION AVAILABILITY STATEMENT National Technical Information Service U.S. Department of Commerce 5285 Port Royal Road Springfield, VA 22161			
13. SUPPLEMENTARY NOTES NREL Technical Monitor: A. Laxson			
14. ABSTRACT (Maximum 200 Words) This report presents the results of the turbine rotor study completed by Global Energy Concepts (GEC) as part of the U.S. Department of Energy's WindPACT (Wind Partnership for Advanced Component Technologies) project. The purpose of the WindPACT project is to identify technology improvements that will enable the cost of energy from wind turbines to fall to a target of 3.0 cents/kilowatt-hour in low wind speed sites. The study focused on different rotor configurations and the effect of scale on those rotors.			
15. SUBJECT TERMS wind turbine rotor; wind energy; WindPACT; Global Energy Concepts			
16. SECURITY CLASSIFICATION OF:			17. LIMITATION OF ABSTRACT UL
a. REPORT Unclassified	b. ABSTRACT Unclassified	c. THIS PAGE Unclassified	
			18. NUMBER OF PAGES
			19a. NAME OF RESPONSIBLE PERSON
			19b. TELEPHONE NUMBER (Include area code)